Polytetrafluoroethylene Nanofibres Fabricated by the Island-in-the-Sea Method

SUBMITTED IN PARTIAL FULFILLMENT OF THE REQUIREMENTS OF THE DEGREE OF DOCTOR OF PHILOSOPHY

September 2016

Zhifei Zhang

School of Engineering and Materials Science

Queen Mary University of London

Mile End Road, London, E1 4NS

Declaration

I, Zhifei Zhang, confirm that the research included within this thesis is my own work or that where it has been carried out in collaboration with, or supported by others, that this is duly acknowledged below and my contribution indicated. Previously published material is also acknowledged below.

I attest that I have exercised reasonable care to ensure that the work is original, and does not to the best of my knowledge break any UK law, infringe any third party's copyright or other Intellectual Property Right, or contain any confidential material.

I accept that the College has the right to use plagiarism detection software to check the electronic version of the thesis.

I confirm that this thesis has not been previously submitted for the award of a degree by this or any other university.

Signature:

Date:

Abstract

Polytetrafluoroethylene (PTFE) has some unique properties such as high hydrophobicity and high resistance to elevated temperatures, chemicals and solvents, which make it of interest for numerous fibre and textile applications. However, PTFE normally has a very high viscosity and poor flowability in the melt due to its ultra-high molecular weight, meaning that it cannot be readily melt-spun into textile fibres. In addition, PTFE is insoluble in all common organic solvents, prohibiting its use in common solution spinning methods such as dry, wet or electrospinning.

Here we aim to develop an easy and environmentally friendly alternative for the production of PTFE nanofibres, using a modified island-in-the-sea spinning process. For this, first a dispersion of PTFE homopolymer, PVA and water was compounded to create a blend of PTFE particles in PVA solution using different methods, including casting, single-step extrusion and two-step-compounding and extrusion. After solid-state drawing of this blend and removal of the PVA, we were able to collect PTFE nanofibres with finest diameters of around 50nm and lengths up to 15µm. The effects of blend composition, morphology and drawing on PTFE fibre formation and properties were studied and discussed. Furthermore, some other material modification systems, including plasticized PVA, or the use ethylene glycol as a solvent, was studied with the aim of scaling up the fabrication of PTFE nanofibres by spinning the PTFE/PVA blend fibres directly for a twin-screw extruder.

Acknowledgement

I would like to express my gratitude to many people who so generously contributed to the work presented in this dissertation. First, certainly my supervisors, Profs. Cees Bastiaansen and TonPeijs, for their tremendous academic support, experienced advice and incredible patience. Also, many thanks to some of the scientists at Nanoforce Technology, including Dr. Olivier Picot and Dr. Wei Tu. Thanks for the guidance on equipment and discussions and suggestions, especially Wei, you truly helped me a lot, particularly on twin-screw extrusion. I also appreciate the help from other labs, like Mr. Russell Bailey from Nanovision, Dr.Alice Williams from the SEMS 233 lab, and many other people for their academic support. Meanwhile, thanks for the scholarship from QMUL and the China Scholarship Council (CSC). Finally, but by no means least, thanks go to my parents and all my friends for their support.

List of abbreviations and acronyms

PTFE: Polytetrafluoroethylene

PVA: Polyvinyl alcohol

EG: Ethylene glycol

PFOS: Perfluorooctanesulfonates

SEM: Scanning electron microscopy

EDS:Energy-dispersive X-ray spectroscopy

DSC:Differential scanning calorimetry

XRD: X-ray diffraction

FTIR: Fourier transform infrared spectroscopy

Table of contents

List of figures

List of tables

Chapter 1

General Introduction

1.1. Background

Thermoplastic fibres based on polymers such as polyesters and polyamides have great mechanical properties and dimensional stability. They are widely utilised in many fields of life and society, including textiles for clothing and home interior applications, car interiors and many other technical applications. Since the requirements of textile and fibre applications are very wide, the existing polymer fibres may not fulfil some of these requirements in terms of physical properties. Even if some strikingly new polymer fibres could be designed to match the demands, the low efficiency and productivity would still potentially lead to problems. The development of multifunctional polymer fibres based on existing polymers is a high priority in the textile industry. There are many examples and cases of composite fibres herein. For instance, one component may cover mechanical properties such as strength and toughness, while some other component increases functional properties such as electrical conductivity or abrasion resistance. There are many examples of composite fibres, and several procedures and technologies have been developed to achieve the required structures and properties of such fibres.

In recent years, ultrafine nanofibres has also been of great interest. Such ultra-fine fibres can be used in many applications, for examples, membranes, filters, artificial leather, biomedical applications and functional textiles exhibiting new feelings and senses by using the soft touch and delicateness unavailable from general fibres. In addition, the compact inter-fibre gaps are used to provide high-density woven fabrics usable as sports clothing requiring wind-breaking capability and water-repelling capability. The ultrafine fibres go into fine grooves and provide large specific surface areas, while the very fine inter-fibres voids can catch dirt. Therefore, ultrafine fibres can exhibit a high absorbability and dust collectability. Their properties are used for industrial material applications such as wiping cloths and precision polishing cloths for precision apparatuses, etc.

In our study, PTFE is the material of choice to make ultra-fine fibres or nanofibres. PTFE has many excellent properties that make it attractive for many textile applications. However, the technology to create PTFE nanofibres is basically absent due to its insolubility and high viscosity in the melt. Although there are some new methods reported in the literature, they are also accompanied with some major disadvantages. Those factors about PTFE, including properties, application, tradition and new methods, are all reviewed in the next part of this chapter.

1.2. General introduction to PTFE

Polytetrafluoroethylene (PTFE) is a synthetic polymer, and usually has ultra-high molecular weight. The IUPAC name of PTFE is poly(1, 1, 2, 2-tetrafluoroethene), and its molecular formula is $(C_2F_4)_n$.

PTFE is synthesised through the free-radical polymerization from tetrafluoroethylene, the process equation is:

$$n\ F_2C{=}CF_2 \rightarrow -[F_2C{-}CF_2]-_n$$

During the process, there is special apparatus used in the polymerization in order to avoid tetrafluoroethylene to decompose to tetrafluoromethane and carbon. Persulfate is used to initiate this process, in which

$$[O_3SO\text{-}OSO_3]^{2-} \rightleftharpoons 2\ SO_4\bullet^-$$

Therefore, the resulting polymer is terminated with sulphate ester groups, and the polymer would be given the -OH end group after hydrolysation. [1]

Because PTFE cannot be dissolved in most types of solvents, the polymerization is conducted as an emulsion in water with surfactants, such as PFOS(perfluorooctanesulfonic), with the PTFE particles usually being stored as a PTFE/water suspension.

1.3 History of PTFE

In 1938, Roy Plunkett accidentally discovered PTFE while he intended to make a new chlorofluorocarbon refrigerant when he was working in New Jersey for Kinetic Chemicals. During the process, he noticed that the tetrafluoroethylene(TFE) gas stopped flowing into a pressure bottle before getting the signal that indicated that the TFE bottle was empty. He had to separate the weighing bottle to figure out where the extra weight came from. Then he noticed that the inside of the container was covered with a slippery waxy white material.

Through analysis, he knew that at this high pressure, the iron of the container could act as a catalyst, causing the polymerization and converting tetrafluoroethylene into poly(tetrafluoroethylene) (PTFE). This new polymer was patented in 1941 and registered as Teflon® trademark in 1945 by Kinetic Chemicals. [2][3]

DuPont, as a partner of Kinetic Chemicals with General Motors, is the biggest PTFE manufacturer, and was already producing over 900 tonnes of Teflon per year by 1948 in Parkersburg, West Virginia. [4]In the famous Manhattan Project, PTFE was used to coat valves and seal the pipes that held highly reactive uranium hexafluoride at the vast K-25 uranium enrichment plant in Oak Ridge, Tennessee. [5]

For the people in the street, PTFE is best known as the Teflon coating of non-stick frying pans and other cookware. This can be back-dated to 1954, when a French engineer named Marc Grégoire created the first non-stick frying pan by coating a pan with Teflon resin under the brand name of Tefal. [6] This kind of non-stick frying pan was marketed in 1961 as “The Happy Pan”®, the first US-made Teflon coated frying pan by Marion Trozzolo in the United States. [7]

There is another interesting discovery related to PTFE. Usually, radiation will cause chain scission of PTFE, allowing it to be reground and reused more easily. Therefore, people had been using irradiation at ambient conditions to break down PTFE for recycling for many years. [8] However, in the 1990s, scientists discovered that PTFE could be cross-linked above its melting point in a non-oxygen environment by electron beam irradiation. [9] Many

properties of PTFE are significantly improved after cross-linking, for example, high-temperature mechanical properties, radiation stability and so on.

1.4 Properties and applications of PTFE

PTFE is a white solid thermoplastic polymer at room temperature, which has a density of around 2200kg/m^3 and a melting temperature of 327^{o}C. [10] PTFE maintains good mechanical properties, including strength, toughness and self-lubrication, in cryogenic environments up to temperatures as low as −265 °C. [11]

One of the unique and excellent properties of PTFE is its low friction. PTFE has the third-lowest coefficient of friction of any known solid material, which is between 0.05 and 0.10. [10] The other two are respectively BAM (Aluminium magnesium boride, $AlMgB_{14}$) (coefficient of friction of 0.02) and diamond-like carbon (coefficient of friction of 0.05). The coefficient of friction of PTFE is so low that even geckos cannot stick to it. [12] Therefore, there are applications that use PTFE coatings on some surfaces to prevent insects from climbing up. For example, PTFE is used on the wall of formicaries to keep ants in a container. Meanwhile, due to the low coefficient of friction of PTFE, it is also used in industry for parts of sliding actions, including plain bearings, gears, and slide plate and so on. In these kinds of applications, PTFE has significantly better performance than polyamides Nylon® and Acetal®. In addition, PTFE has low resistance against flowing liquids and this property is applied in fuel and hydraulic lines. The flow of these fluids reduces at colder temperatures and at high altitudes. PTFE coatings of the interior surfaces of fuel and hydraulic lines improve this flow at high altitude situation. [13]

PTFE has excellent dielectric properties, which is responsible for its major applications, consuming about 50% of it. In these kinds of applications, PTFE is used for wiring in aerospace and computer applications, including hook-up wire, coaxial cables and so on. The dielectric constant property is also very low at high radio frequencies. Therefore, PTFE is also a very useful material for cable insulators and connector assemblies, and printed circuit boards used at microwave frequencies. Although polyethylene (PE) is also used in these kinds of applications, PTFE is a wise choice as a high-performance substitute of PE because of its high melting temperature.

PTFE has great chemically inert properties, which results from the fluorine atoms surrounding the carbon backbone like a protective sheath with very strong carbon-fluorine bonds. Therefore, PTFE is used for bushings and bearings that require no lubricant and as the liner of equipment that is used for the storage and transportation of strong acids and organic solvents. [14] Moreover, its high corrosion resistance property makes PTFE of interest for many laboratory applications, for example, containers, magnetic stirrers, tubing for highly corrosive chemicals such as hydrofluoric acid and containers for storing fluoroantimonic acid.

Another excellent property of PTFE is its superhydrophobicity. The coating of the non-stick frying pan utilises this property, while high heat resistance is also key. One of the largest applications of PTFE coatings is in a membrane called Gore-Tex®. Gore-Tex® is a material structure incorporating a fluoropolymer membrane with micro-pores in the middle of the layers that allow air to pass through but prevent water passage. The structure is shown below in Figure 1.1.

One of the biggest applications of PTFE in Gore-Tex® is the roof of the Hubert Humphrey Metrodome in Minneapolis, USA, which is using 81,000m^2 of the materials in a double-layered white dome made with fibreglass with a PTFE coating.

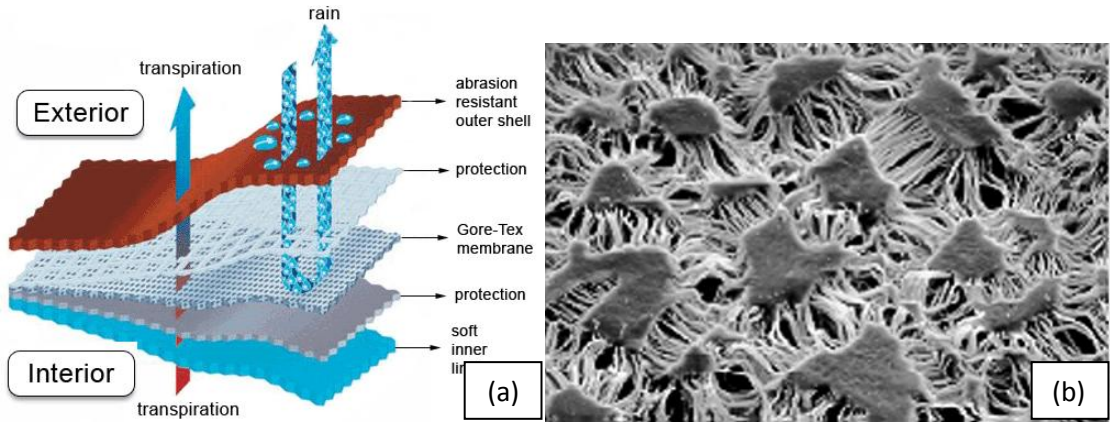

Figure 1.1: (a) Schematic of Gore-Tex® multi-layer structure; (b) Gore-Tex® membrane under an electron microscope.

1.5 Applications of PTFE fibres

From the properties of PTFE introduced above, it is clear that PTFE fibres have many useful properties for a wide variety of industrial applications and articles. For examples, its chemically inert property makes PTFE fibres interesting for filters for trapping splashes and mists of highly aggressive liquids, and as protective agents and special clothing. Because of its heat resistant properties, textile materials and articles made from PTFE fibres are used in environments with a high oxygen concentration. Due to its biologically stable and bio-inert properties, those articles can be used as prostheses for internal organs, blood vessels and heart valves, suture materials, and instruments for filtration of biological media and so on.

For example, PTFE grafts could be used for peripheral vascular disease to bypass the stenotic arteries when there is no suitable autologous vein graft available.

1.6 Methods to produce PTFE fibre

1.6.1 Traditional methods

Because PTFE is insoluble, and also has a very high viscosity (up to 10^6 - 10^9 Pa·s) with almost no fluidity in the melt, the process of making PTFE fibres involves great difficulties compared to other polymeric materials. However, PTFE can become processable above the melting temperature, and particles from a water suspension can fuse together above it too. Hence, people usually use sintering as the basic method to fabricate PTFE solid parts, fibres and films. [1][4] [5-7] [10-14] [3-32]

The basic method to fabricate PTFE fibres and yarns is by wet spinning of PTFE suspensions. Usually, the dispersion solution contains 50-60wt% PTFE particles, which is mixed with 7-8wt.% viscose, usually α-cellulose, and surfactants at a ratio of surfactant: α-cellulose of 1:10. Usually a surfactant based on low molecular weight PTFE (brand number 7090) is used for lubricating. After wet spinning, the fibres are washed in hot water and dried. The following step is a thermal treatment, which is typically performed at a temperature between 375 and 390^{o}C for about 13-18sec. In this step, PTFE particles are sintered into a fibre and meanwhile, the decomposition of cellulose occurs. Next, these PTFE fibres are drawn at a temperature between 330 and 350^{o}C to a draw ratio of about 4.5-5.5. Because of the decomposition of α-cellulose, the product of PTFE fibres has a dark brown or black colour. Therefore, afterwards the PTFE fibres are whitened with oxidants or prolonged

treatments at 290 – 300°C in air for 20-24 hrs to eliminate the carbon residues that comes from the decomposition of α-cellulose.

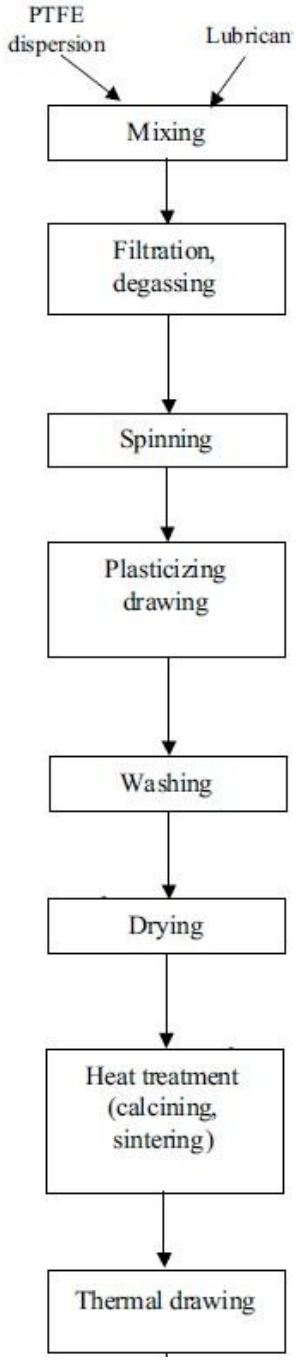

Figure 1.2: Schematic representation of the method of fabricating PTFE fibres from suspension [21].

The second method of fabrication of PTFE fibres is to sinter the PTFE dispersion at 340-350^{o}C under a pressure of 15-20MPa into blocks followed with additional annealing for 18-20 hrs at 340-350^{o}C to completely remove pores and make them monolithic. Then the PTFE blocks are processed into fibres or continuous thin ribbons with a thickness of 50-100µm. These fibres or ribbons are then cut into thin strips and drawn at 300-325^{o}C to draw ratios of 4-5.

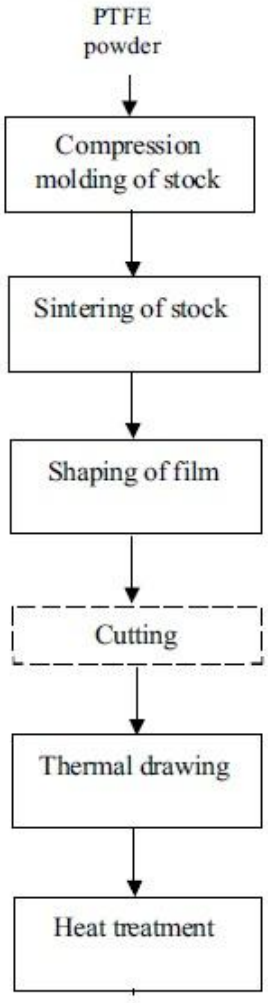

Figure 1.3 : Schematic representation of method of fabricating PTFE fibres by sintering [21].

The other method to manufacture PTFE fibres is by making it from paste. First, PTFE powder is mixed with lubricant and then extruded into the shape of ribbon. The lubricant is removed from the blend by evaporation at a temperature around 250^{o}C, and ribbons are cut into strips and hot drawing is performed. Furthermore, a thermal treatment at a temperature of approximately 360^{o}C is performed for final sintering.

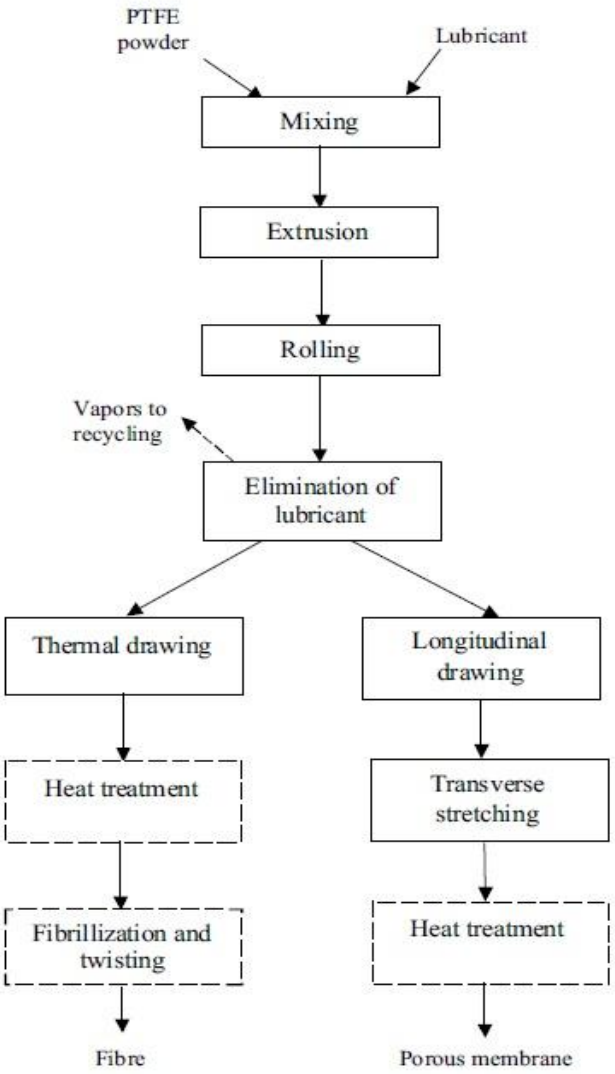

Figure 1.4: Schematic representation of method of fabricating PTFE fibres from paste [21].

Table 1.1 shows some fundamental properties of PTFE fibres and yarns fabricated through the three methods described above, including linear density, strength, elongation at break and shrinkage. We can see that the PTFE fibres fabricated through paste extrusion with lubricants have the highest strength but lowest elongation at break.

Table 1.1: Properties of PTFE fibres and yarns fabricated through the three methods mentions above [21].

Polymer (copolymer)	Spinning method	Density, g/cm^3	Linear density, tex		Strength, cN/tex	Elongation at break, %	Shrinkage, %	Maximum temperature of use, °C
			yarn	fibre				
PTFE	From dispersions with polymer thickener	2.15-2.2	11-150	0.2-1.0	10-18	20-40	2-6 at 180 °C	260
PTFE	Extrusion of pastes with lubricant	2.15-2.2	40-100	–	20-35	10-30	2-5 at 180 °C	260
PTFE	Shaping of stock	2.15-2.2	1000-2000	–	6-12	20-40	2-5 at 180 °C	260

1.6.2 Recent methods

Goessi etal. [28] developed a method based on blending of high and low molar weight PTFE grades to create a melt-processable PTFE. After blending, these new bimodal grades of PTFE, with weight-average molar masses (Mw) between 500 and 1000 kg/mol, were found to be melt-processable and to exhibit tough mechanical behaviour. Furthermore, they demonstrated that PTFE with a narrow monomodal molar weight distribution (Mw= 50-300 kg/mol) comprising 0.04-0.5 mol.% perfluoro(propyl vinyl ether) (PPVE) can enhance the delicate balance between processability and properties. [28]

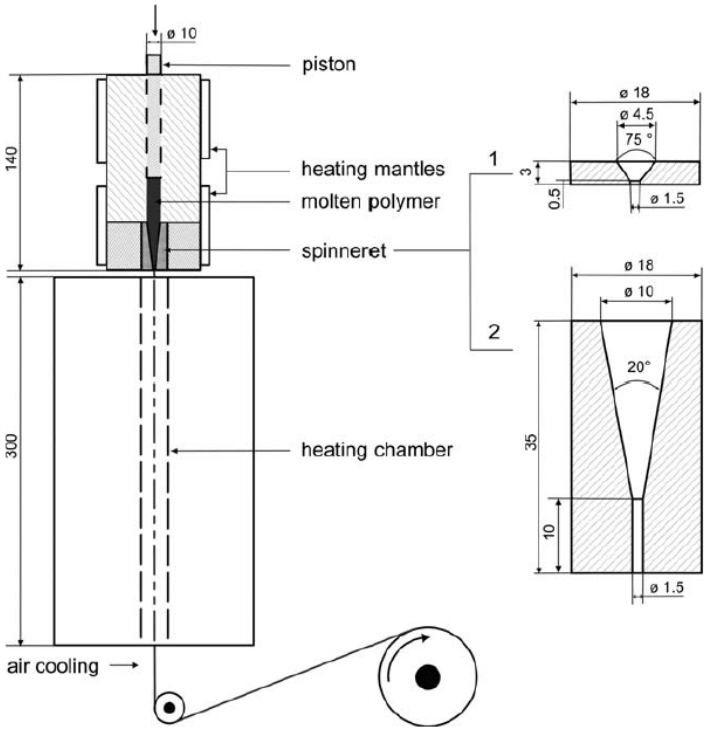

Figure 1.5:Schematic of the melt-spinning setup used for the processing of the bimodal PTFE blend, consisting of a piston extruder, an (optional) heater and a take-up device. Also shown are the shapes of the two spinnerets employed. Dimensions in mm. [28]

In this method, the extrusion rate needed to be 22 mm/min or lower, and the diameter of the extrudate would always be the same as that of the orifice because of the low coefficient of friction of PTFE that results in low friction between melt and extruder wall. Under optimal spinning condition and PTFE molecular weights, fine PTFE monofilaments could be spun with a draw-down ratio of up to 2750. Furthermore, the fibres, which were spun at maximum draw-down exhibited excellent mechanical properties, respectively, tensile strength of up to 258 MPa and Young's modulus up to 1972 MPa.

Endo and Kanamoto[29] successfully applied a two-stage drawing technique to make PTFE fibres by super-drawing of PTFE virgin powder. First, they compression-moulded the virgin powder into film below the melting temperature (T_m = 335°C), then initially solid-state coextruded it to an extrusion drawratio (EDR) between 6 and 20 at 325°C. In a second-stage pin drawing process these samples were drawn ata temperature (T_d) range of 300-370°C. The schematic of the pin-drawing process is shown in Figure 1.6.

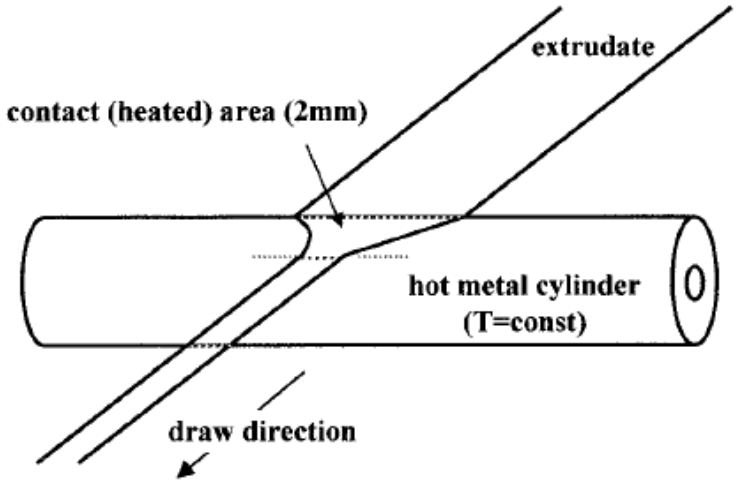

Figure 1.6:Schematic representation of the pin-drawing process [29].

At T_d=300°C, the total maximum draw ratio could reach 60. When the drawing temperature (T_d) is between 340 and 360°C, with the increasing of T_d, the maximum draw ratio would rapidly increase to 100-160. The maximum tensile modulus and strength achieved in this work were respectively 102 ± 5 and 1.4 ± 0.2 GPa at 24 °C. Meanwhile, the best-drawn fibres had high crystallinity and chain orientation, respectively up to 87% and 0.997, and the crystallite size is large as well, reaching 160 nm.

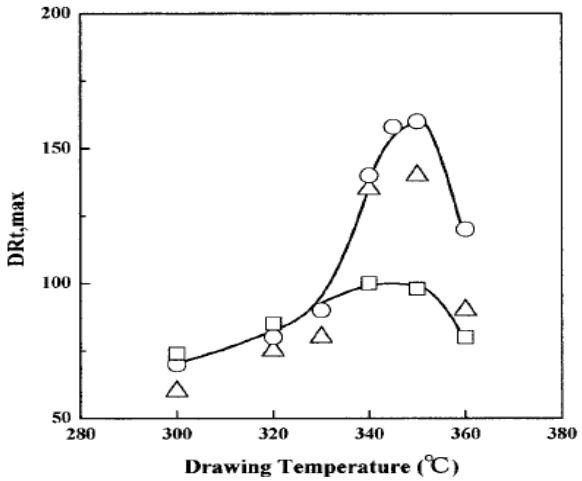

Figure 1.7: Maximum achieved draw ratio versus drawing temperature for the second-stage pin draw of PTFE extrudates with an initial EDR of 6 (△), 12(○) and 20 (□) [29].

The highest draw ratio of 160, was achieved when the initial draw ratio was 12 at a drawing temperature of around 350 °C.

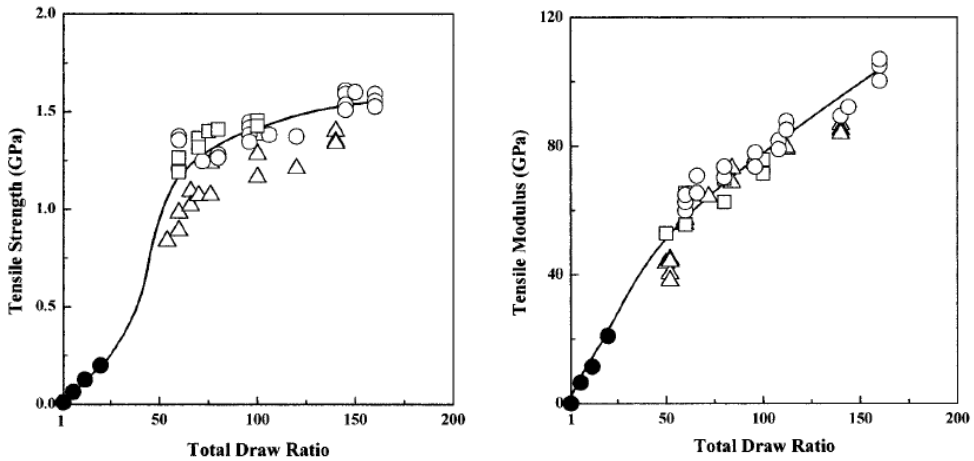

Figure 1.8:Tensile strength (left) and modulus (right) at 24 °C versus draw ratio for solid-state co-extrusion and second-stage pin drawing. The double drawn products were prepared from different initial EDRs of 6, 12, and 20 (same symbols as in Figure above) [29].

Using the method shown in Figure1.8, the strength and modulus increased in the same way as a function of draw ratio. The maximum tensile strength was 1.4 GPa, which was achieved at EDR = 12 and a pin draw ratio of 160, and under the same conditions the modulus reached its highest value of approximately 100 GPa.

Takagi et al. [30] developed a method that prepared PTFE fibres with superior mechanical properties directly from emulsion by a novel manufacturing process. Extremely high shear flow was applied at a high temperature PTFE emulsion making it into a paste, and then extruding this paste into a thick strand consisting of aggregated PTFE particles. Die-drawing was used to reduce the diameter of the fibres and increasing its mechanical properties. The die-drawing was carried out in water at 90 ^{o}C and by pulling stepwise through five increasing sizes of plastic conical dies. Then the die-drawn strand was dried and pulled through a metal conical die, which was heated to a temperature ranging between 250 ^{o}C to 380 ^{o}C.

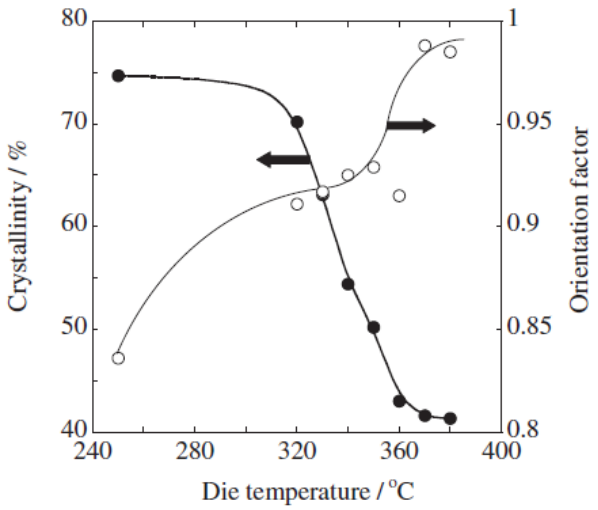

Figure 1.9: Crystallinityand orientation factor of PTFE fibres die-drawn at various temperatures. [30]

Thermal properties were evaluated by DSC under N_2atmosphere and the degree of crystallinity was calculated from the area under the melting peak. Meanwhile, wide-angle X-ray diffraction (WAXD) patterns were also obtained and used to reveal the orientation factor of the PTFE fibres. As shown in Figure 1.9 the orientation factor increased monotonically from 240 °C to 340 °C and then remained constant between 340 °C and 360 °C. The orientation factor increased rapidly between 370 °C to 380 °C. On the other hand, the degree of crystallinity remained constant from 240 °C to 320 °C, then sharply dropped to around 40 % from 320 °C to 360 °C and then stayed constant.

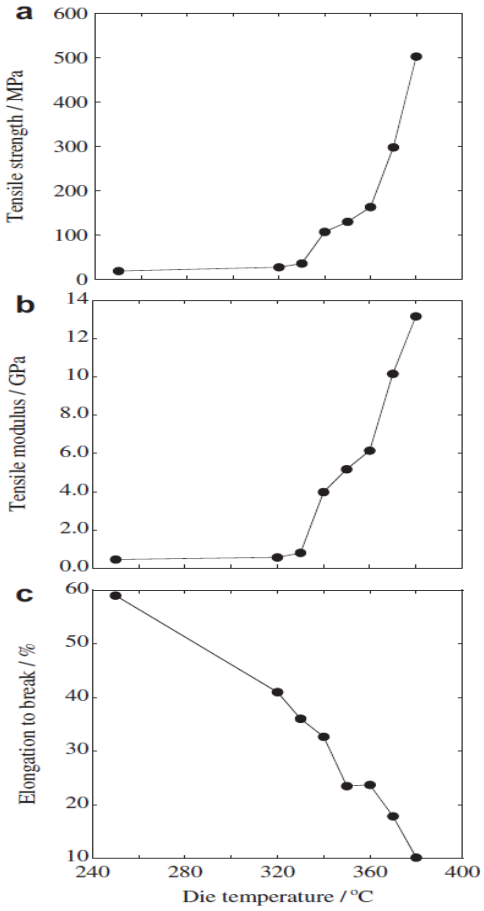

Figure 1.10: The mechanical properties of PTFE fibres die-drawn at various temperatures. (a) tensile strength, (b) tensile modulus, and (c) elongation to break. [30]

Figure1.10 shows that the mechanical property of the PTFE strand remains low until the temperature of die-drawing was raised to 250^{o}C, but this improvement is rather small until a temperature of 330^{o}C is reached, at which the tensile strength and modulus start to increase dramatically, reaching 502MPa and 13GPa respectively. However, as opposed to the tensile strength and modulus, the elongation to break drops with increasing die-drawing temperature, decreasing from 60 % at 240^{o}C to 10 % at 380^{o}C.

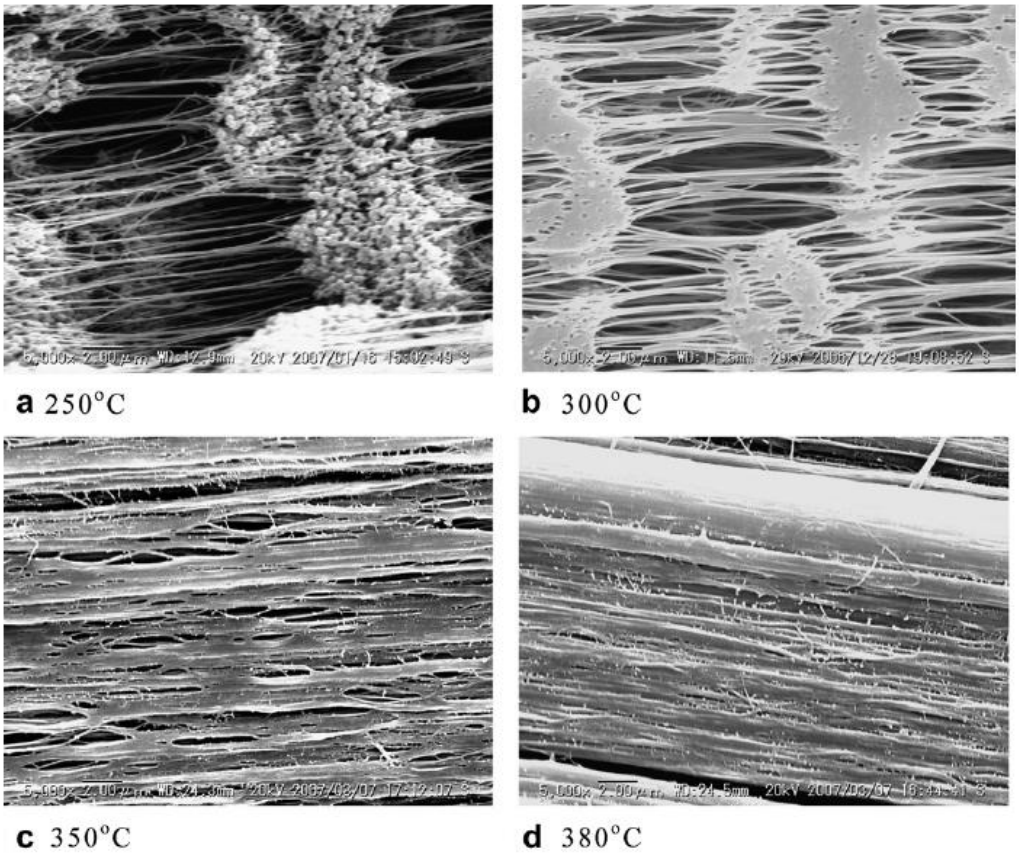

Figure 1.11: SEM images of the inner structure of the PTFE fibres die-drawn at (a) 250 ^{o}C, (b) 300 ^{o}C, (c) 350 ^{o}C and (d) 380 ^{o}C. [30]

SEM micrographs showed the morphology of the PTFE fibres after die-drawing at many sets of different temperatures. As shown, at a temperature of 250^{o}C there are still many

particles that are not fully stretched, while some of them are stretched and drawn into fibres. At a temperature of 300^{o}C, the unstretched particles started to fuse together. The situation became better when the temperature was increased to 350^{o}C and 380^{o}C, when most of the PTFE particles fused into a fibrillar structure.SEM revealed that the inner structure of the PTFE fibreswasthe main reason for the changein tensile strength with drawing temperature, as PTFE particles started to fuse and form fibrous and oriented structuresabove 300^{o}C.

Borkar et al. developed an interesting method called jet blowing to make PTFE fibres. [31] In their technique, they placed high molecular weight PTFE into a tube with a high-pressure jet of gases such as nitrogen or argon as a plasticiser. PTFE could be extensionally stretched to several millimetre long fibres in the tube with the plasticization of hot and high-pressure gases to facilitate fibre formation below the melting temperature of PTFE. In fact, jet blowing is very different from extrusion, because the fibres processed within the nozzle were multiple fibres, of which the diameters are much smaller than that of the nozzle. In addition, because there is no extruder involved in jet blowing, no true mixing or blending effect exists in this method. Moreover, the molecular weight of PTFE used here is lower than in extrusion as a low melt viscosity of PTFE is required for this jet process.

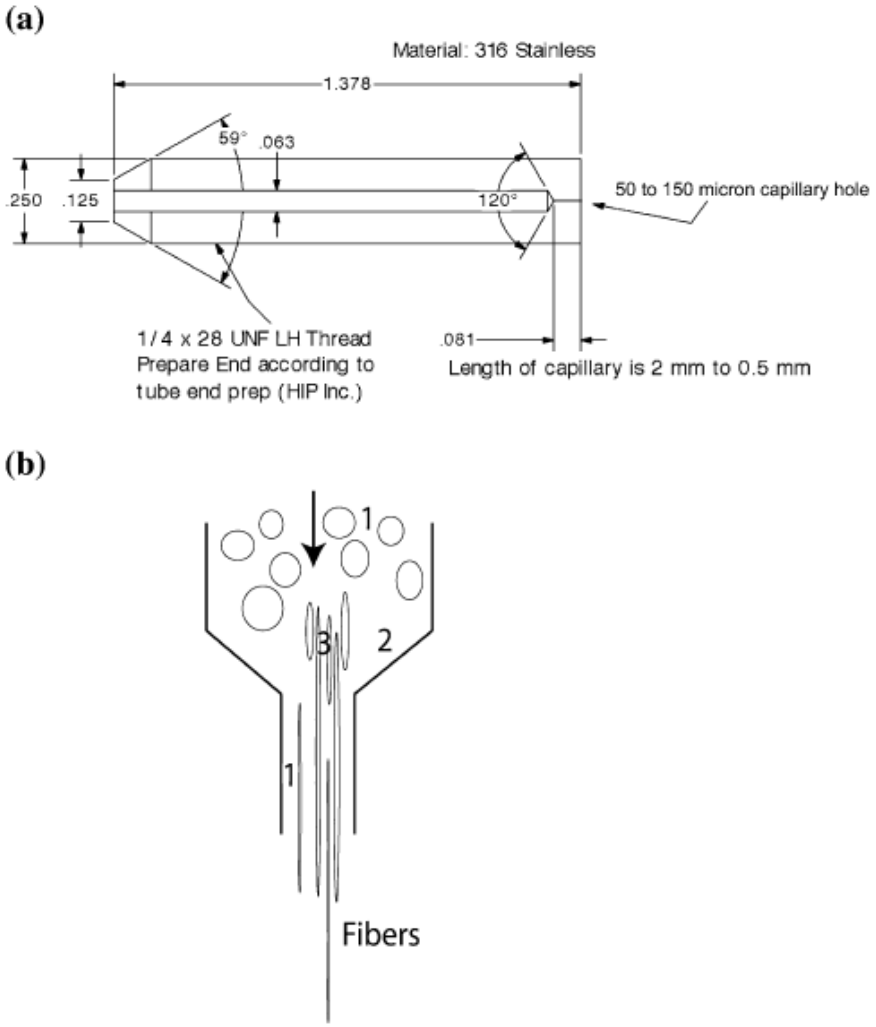

Figure 1.12:(a) Engineering drawing of the nozzle used for jet blowing. (b) Schematic representation of the jetblowing process high-pressure gas at an elevated temperature forces particles of PTFE starting materials through an approximately25:1 axisymmetric contraction. Numbers indicate regions of principally shear flow (1), a vertical region (2), and an extensional flow region just upstream of the contraction (3), where fibre formation likely occurs. [31]

In their article, the authors mainly discuss the PTFE7A and PTFE601Afibre formation processed using jet blowing. Through their results, the PTFE7A showed better fibre

formation than PTFE 601A (PTFE 601A remains a particle-like structure until the jet blowing temperature was raised up to 360 ^{o}C, and fibres obtained under these processing conditions exhibited very short lengths).Here we show some SEM pictures of the best morphologies for PTFE fibres formation from this PTFE 7A grade.

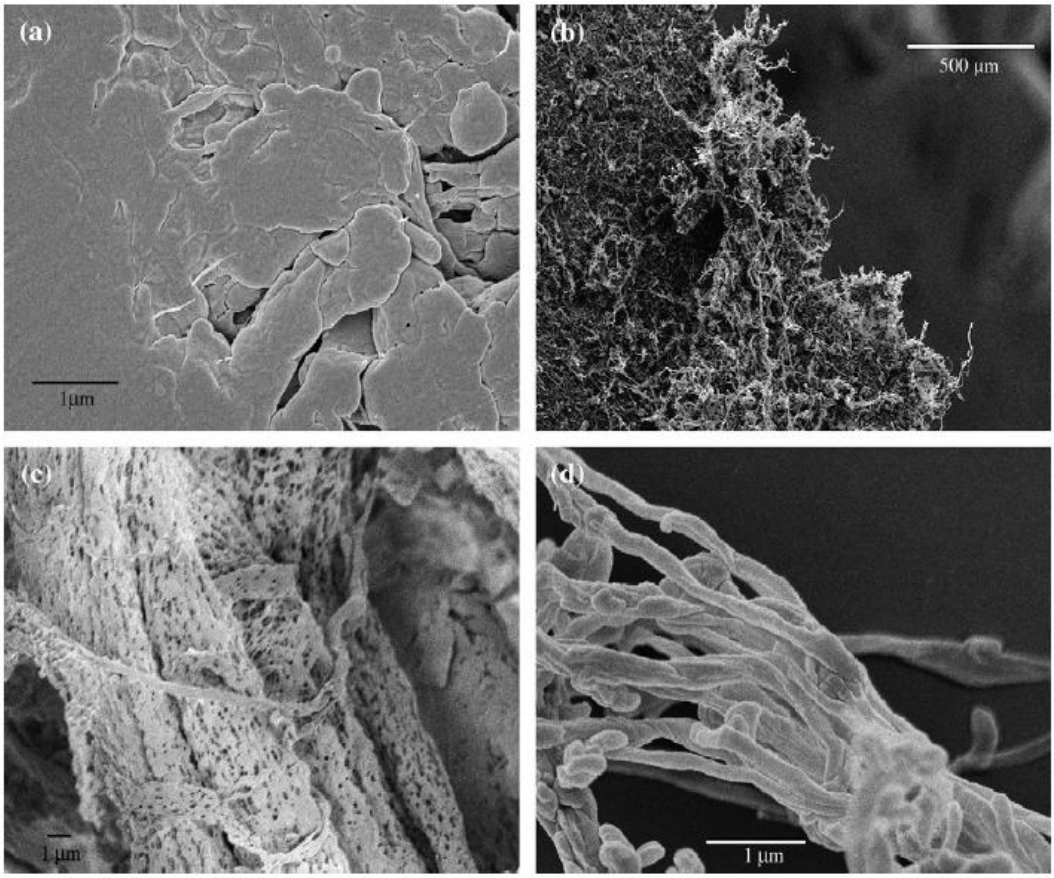

Figure 1.13:SEM images of (a) virgin PTFE 7A, (b) the edge of a fibre mat of PTFE 7A, (c) PTFE 7A jet blown at 310 ^{o}C exhibiting nanopores and (d) a PTFE 7A fibres jet blown at 330 ^{o}C composed of nanofibrils. [31]

In summary, the methods developed by Goessi et al.[28] and Endo and Kananmot[29] could produce PTFE fibres with tensile strength's and Young's moduli of 258MPa and 1972MPa, and 1.4GPa and 102GPa, respectively. The PTFE fibres produced with Goessi et al. have the

advantage of convenience of processing, while the PTFE fibres produced by Endo and Kanamoto have much better mechanical properties. However, both these methods could only produce PTFE fibres with diameters at the micron-scale. The method of paste extrusion from Takagi et al. [30] could also achieve a good tensile strength and modulus, respectively, reaching 502MPa and 13GPa, but here the fibres are in the nanometre scale. However, this method shows poor fibre formation. SEM images show that fibres are not clearly individual fibres but resemble more a fused fibre mat. Similar to paste extrusion, the method of jet blowing from Borkar et al. [31] could also produce PTFE nanofibres. Assuming that one has the special equipment for jet blowing, this method is a rather convenient one to produce PTFE nanofibres. However, it also has the disadvantage of poor fibre formation in that fibres fuse into mats (see Figure 1.13).

1.7 Introduction to Island-in-the-Sea spinning

From the previous introduction about the fabrication of PTFE fibres, it can be concluded that, although people have conquered some of the difficulties of producing PTFE fibres, the technologies for fabricating PTFE nanofibres is still underdeveloped. This will be the subject of this thesis, in which the island-in-the-sea fibre technology, with some modification, will be utilised to fabricate PTFE nanofibres.

Bicomponent fibres are designed to meet requirements of two materials into one single fibre by hosting two components along the fibre length. Formation of typical melt spun bicomponent fibres or filaments involve extruding two polymers from a single spinneret with a desired cross-sectional arrangement. Bicomponent fibres are classified according to the distribution of each component within the cross-sectional area. Typical cross-section

configurations include side-by-side, core/sheath(c/s), island-in-the-sea, alternating segments or segmented-pie, citrus and tipped. [32]

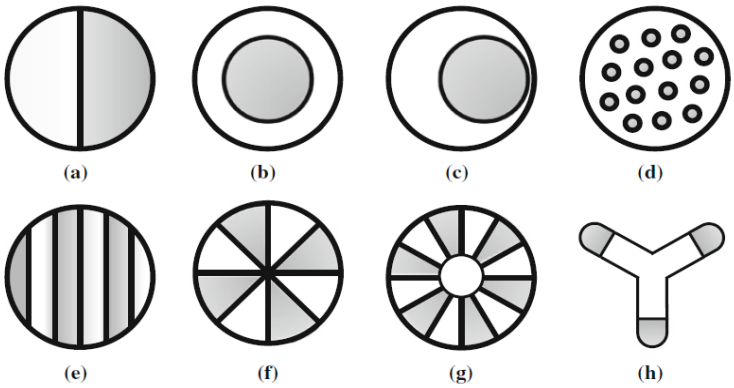

Figure 1.14:Type of bicomponent fibre cross-sections: (a) side-by-side, (b) sheath-core with concentric and (c) eccentric configurations, (d) islands-in-the-sea, (e) alternating segments with stripes and (f) pies, (g) citrus, and (h) tipped trilobal. [33]

Islands-in-the-sea is one type of bicomponent fibre whereby many fibrils of one polymer are dispersed in the matrix of another polymer. The fibrils are known as islands and the matrix is the sea. [33]

Island-in-sea type fibre spinning is a method among those technologies, which can produce numerous ultra-fine fibres distributed in the polymer matrix component. The technology relates to an island-in-sea type composite or blends fibre, particularly to an islands-in-sea type blend fibre that having a very large number of island parts from which a fine fibre group having a very large number of filaments can be easily obtained by dissolving and removing the sea part. [34]

1.7.1 Requirements and parameters involved in the island-in-sea method

To produce the islands-in-the-sea type composite or blend fibres, the polymers should match the requirement below. First, the polymer used for island parts should have respectively low melt viscosity and poor solubility in some specified solutions. Secondly, the polymer used for the sea parts should have a higher melt viscosity than the former polymer, and should be easy to dissolve in solvents, which cannot dissolve the former polymer. Moreover, the melt viscosity relation between sea part and island parts is important for the dispersion morphology and the ratio of sea part to island part. When the interval between adjacent island parts is reduced, and the mass of sea parts is lower than the required amount mentioned above, the sea part would flow through the flow paths between the islands within the melt spinning spinneret of the composite fibre at a high speed where the melt viscosity of the sea part is low.

In the following section, the requirements of solubility, viscosity, quantity and some other parameters are introduced in more detail.

(1) Solubility

The principle of selecting polymers to form the islands-in-the-sea type composite or blend fibre is that the solubility of the island part is lower than that of the sea part. The ratio of thedissolution rate of sea part to that of the island parts has to be above 200. If the dissolution rate cannot reach this requirement, the island parts of the composite fibre, which are present in the surface layer of the fibre, will be partly dissolved while the sea part of the fibre has not been dissolved completely. Inhomogeneous thickness of the island parts

and deterioration of the strength of island parts are the result because of solvent corrosion. Fibre fluff is consequently produced, resulting in a low quality product. Thus, any polymer can be used in the blend fibre for the sea part as long as it satisfies the requirement of the ratio of dissolution rate mentioned above.

Although any polymer can be used as the sea part polymer as long as the above ratio is preferably satisfied, polymers such as polyester, polyamide, polystyrene and polyethylene that have great fibre forming capability are particularly preferred. Appropriate examples of an aqueous alkali solution-easily soluble polymer include polylactic acid, ultrahigh molecular weight polyethylele oxide, polyethylene glycol-copolymerized polyester and polyester copolymer in which a polyethylene glycol compound and 5-sodium sulfoisophthalate are copolymerized. Moreover, Nylon® polyamide 6 is soluble in formic acid, and a polystyrene-polyethylene copolymer is very soluble in organic solvents such as toluene. [35]

Normally, 5-Sodium sulfoisophthalate is used to improve the hydrophilicity and melt viscosity, and polyethylene glycol is used to improve the hydrophilicity of the polymer blend for the purpose of making the alkali easy soluble. Furthermore, the polyethylene glycol has a function of lowering the melting point; it can therefore be used to protect the sea part polymer, like in the case of PVA, because it decomposes before melting.

(2) Melt viscosity

In the process of melt spinning, the melt viscosity of the polymer used as sea part should be higher than that of polymer used for the island parts. Otherwise, the island parts may fuse together, creating a fibre structure that has not an island-in-the-sea morphology.

Generally, the ratio of melt viscosity of the sea part to that of the island part should range between 1.1 to 2.0. The island parts will fuse together when the ratio is below 1.1, and the stability of the melt spinning process will be reduced when this ratio is higher than 2.0.

(3) Productivity with proportion and quantities of island parts and sea part

During the process of dissolving and removing the sea part to produce the required fine fibres, the productivity will increase if the numberor volume fraction of island parts increases. The number of fibres obtained from a blend fibre with large numbers of island parts will increase, while the hardness, surface smoothness and lustre can also improve in the case of ultra-fine fibres [34] [35] [36]. Therefore, it is important that the number of island parts reaches 100 or more, while it would be even better if this number were above 500. Otherwise, a multifilament bundle composed of individual fine fibres cannot be obtained even if the sea part is dissolved completely and removed properly. However, if the number of island parts far exceeds 500, the spinneret would be very costly, while the working precision of the spinneret would reduce as well. Therefore, in general, the number of island part should preferably be kept between 500-1000.

In order to obtain a better fibre morphology, the mass ratio of the polymer sea part to that of the island part is important. If the percentage of sea part is too high, the thickness of the sea part amongst the island parts will be quite large, which is not easily to remove. On the contrary, if the proportion of sea part is below 5 %, the island parts will probably fuse together due to the small amount of sea in between.

(4) Diameter of island parts and distance between islands

The thickness of each island (or fibre) part should be between 10 to 1000 nm, but a range of 100 to 700 nm is often preferred [34]. A thickness below 10 nm is not optimal because neither the physical properties nor the fibre structure is stable at such a low thickness. On the other hand, if the thickness exceeds 1000 nm the softness and specific advantages of ultra-fine fibres are lost. Moreover, a more uniform thickness of each island part in the cross-section of the islands-in-the-sea composite fibres results in a better quality and durability of the multifilament bundle composed of fine fibres after dissolution and removal of the sea part polymer.

1.7.2 Challenges in the island-in-sea method

There are many methods and procedures of producing island-in-the-sea structured composite fibres [34] [35] [36]. However, the ratio of island parts to sea parts is still difficult to increase. When we make some improvement to increase the island proportion, we would have to face the following problems: the relationship between the island parts and sea part would be reversed, that is, the formal island-parts will form a continuous structure and convert into the sea part, similar to the sea part. Even if the quantity of island parts can be increased, it is difficult to adjust the location and number of island parts, and this might cause the non-uniform composite structure of the fibres. The uniformity of the island phases is inadequate because it is blended. Furthermore, the fibre consists of aggregate fibres formed from fine fibrils each having a finite length in the longitudinal axis direction of the fibre.

1.8 Introduction to PVA

Polyvinyl alcohol (PVA, PVOH or PVAl) is a linear water-soluble synthetic polymer, which is actually not prepared by polymerization of the corresponding monomer, vinyl alcohol, because of its unstability. Instead PVA is converted from polyvinylacetate with the polymerization of vinyl acetate, and the conversion is usually conducted by base-catalysed transesterification with ethanol, in which other precursor polymers could also be used, such as chloroacetate etc. [37]

$$[CH_2CH(OAc)]_n + C_2H_5OH \rightarrow [CH_2CH(OH)]_n + C_2H_5OAc$$

Usually the hydrolysis degree is between 80 % and 99 %. When PVA is crosslinked, it forms a hydrogel, and it will be nearly fully hydrolyzed. Speaking of which, the PVA hydrogels are formed by the crosslinking of the linear polymers, leading to a polymer (gel) – fluid (solvent) with tunable properties. Fluid can easily move through the matrix when the polymer content is low, which makes the material soft and flexible; while with increasing polymer content the material gets stiffer.

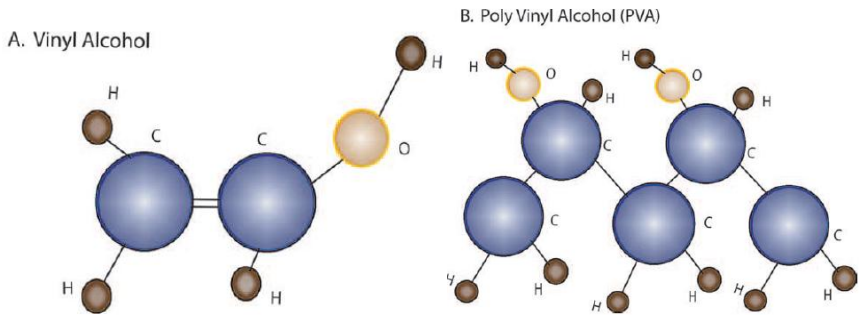

Figure 1.15:Molecular structure of (A) Vinyl alcohol and (B) Polyvinyl alcohol. [37]

PVA is hydrophilic and highly soluble in water but is resistant to most organic solvents due to the hydroxyl groups. However, when the degree of hydroxylation and polymerization of PVA increases, the solubility in polar solvents drops. As we mentioned above, when gelation of PVA occurs, it results in molecular crosslinking that increases the hydroxylation and causes the lower solubility and higher strength of PVA. In our study, the gelation effect is important. During the process of spinning, physical gelation after spinning upon cooling down provides the filaments with enough strength for transportation to a drawing oven for solid-state drawing. Physical gelation only occurs with specific solvents like ethylene glycol (and not with water). It is also possible to get liquid-liquid demixing, which should be suppressed by rapid quenching. Subsequently, the PVA is removed by dissolution in the final stage of the manufacturing process to separate the PTFE nanofibers. In our study, the spinnability of PTFE/PVA is mostly related to the PVA, which is the matrix. Therefore, in order to guarantee a good solution at elevated temperature, the extrusion speed, residence time and temperature, all have to be considered to make sure to have a spinnable PTFE suspension in PVA solution.

The melting temperature of PVA is around 230^{o}C but it starts to decompose at 180 – 190 ^{o}C, and decomposes rapidly above 200^{o}C, undergoing pyrolysis at even higher temperatures. PVA has some excellent properties, including film formation, emulsifying properties, adhesive properties, a high resistance to oil, grease and other organic solvents, great solubility to water, environmentally friendly, biodegradability etc. It also has a high tensile strength and flexibility, which can be significantly affected by humidity due to the hydrophilic nature of PVA, as well as high oxygen and aroma barrier properties, all of which make it attractive for many applications. There are many application fields for PVA, for

example in textiles, industries of paper-related products, films for packaging, CO_2 barrier films in PET bottles, films for water transfer printing, as surfactant for the formation of polymer encapsulated nanobeads, protective chemical-resistant gloves, support materials in 3D printing and so on. Many applications are also related to its excellent barrier properties and the health and safety properties. FDA has approved PVA to be in close contact with food for applications in food packaging. Furthermore, because of its biocompatible, non-toxic, non-carcinogenic, swelling properties and bio-adhesive characteristics, [38] PVA is also used in medical devices.

1.9 Introduction to fabrication methods for PVA fibres

Because the melting temperature of PVA is quite close to or above its decomposition temperature, PVA cannot be processed as most other polymers through melt spinning. Instead, there are many other methods for the fabrication of PVA fibres.

One of the methods is gel spinning. In gel spinning, the filaments pass through the air first and then a liquid bath, in where the filaments are cooled. Gel spinning is a method of materials processing, which is usually used to fabricate fibres of high strength or some other properties. Different from melt spinning or solution spinning, the polymer is in solution during spinning and physical gelation occurs via crystallization upon cooling down. [39]

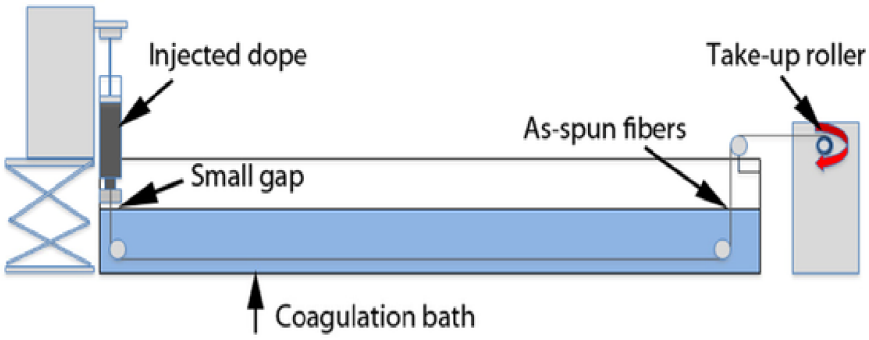

Figure 1.16: Illustration of gel spinning [40].

In the study of Cha et al. [40], they used dimethyl sulfoxide (DMSO) and water to prepare the PVA solution. The best solvent they found for the spinning and coagulation was a DMSO: H_2O = 80:20 (w/w) mixture and methanol, giving the PVA fibres the best drawability. Then the as-spun PVA fibres were stretched in a hot two-stage drawing process to reach their maximum drawability, strength and Young's modulus. The concentration of PVA in the solution was 6wt.%, and the coagulating temperature of methanol was -20°C. The temperatures of the two-stage drawing were respectively 160°C and 200°C. With the condition shown above, a maximum draw ratio of PVA fibres could be reached of 45, leading to a high tensile strength of 2.8GPa, and Young's modulus of 64GPa.

There are quite some studies devoted to the electrospinning of PVA fibres, more precise PVA nanofibers, mainly for membrane applications.

Electrospinning is a fibre fabrication method that draws charged threads from polymer solution or melt with an electrical field. The diameter of fibres produced with this method can be as low as tens of nanometres [41]. A great advantage of electrospinning is that the production is simple and there are no coagulation baths or high temperatures required in this method.

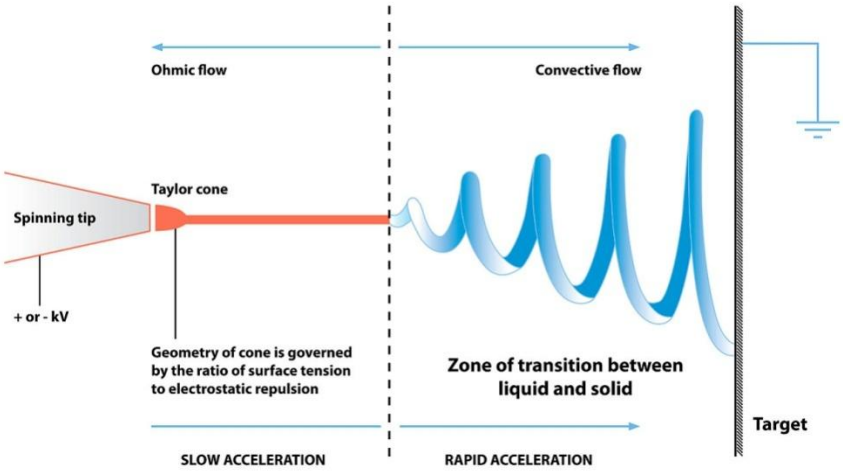

Figure 1.17: Schematic of electrospinning [41].

For instance, in the study of Yang et al., a PVA solution at 80 ^{o}C was prepared by stirring for about 2 hrs to get a PVA solution with a concentration between 5 – 10wt.%. After the solution is cooled down, some sulphuric acid was added to control the pH value between 2 and 3 for the cross-linking reaction with maleic anhydride as a cross-linker to fabricate slightly soluble nanofibre membranes. The cross-link reaction formula is as:

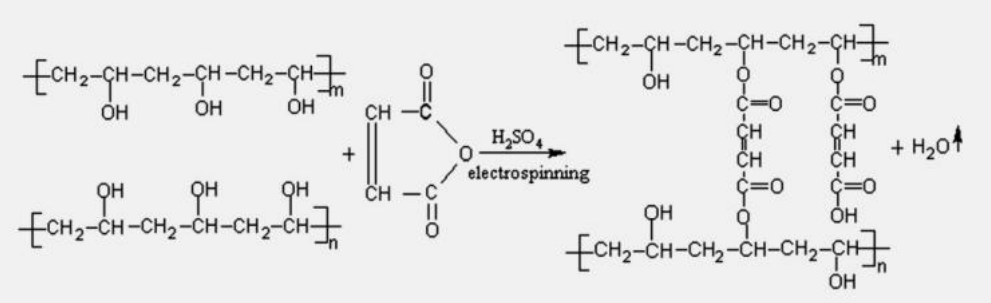

This was followed by a simple electrospinning process, at a voltage of 20 kV and a tip-to-collector distance of 20 cm. [41]

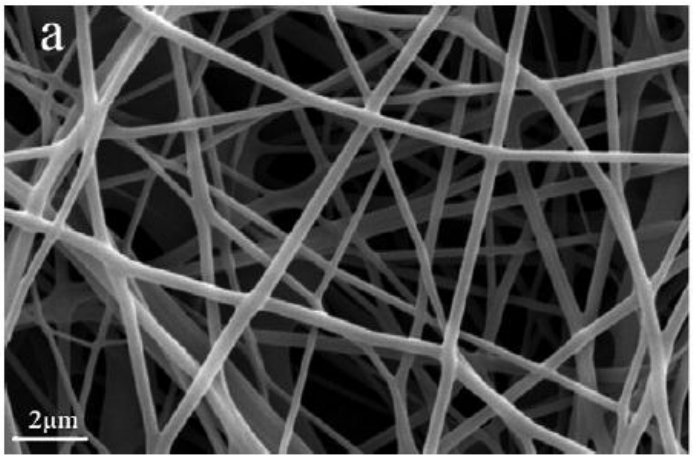

Figure 1.18: SEM image of electrospun PVA nanofibre membrane [41].

Solution spinning is the most common method for PVA fibres fabrication. In the solution spinning of PVA, ethylene glycol is typically used as a solvent and solutions are usually spun at around 160 ^{o}C. After spinning PVA fibres, the ethylene glycol is removed from the fibres by extraction in methanol. In the solution (gel) spinning method by of Schellekens and Bastiaansen [42], the concentration of PVA in ethylene glycol is shown below in Table 1.2.

Table 1.2: Polyvinyl alcohol grades used in the study by Schellekens and Bastiaansen [42].

Grade	DP_w [−]	M_w [kg/mol]	c^* [% w/w]
PVAL: e	1300	57	27
f	3400	149	15
g	13,000	572	6
h	29,000	1270	4

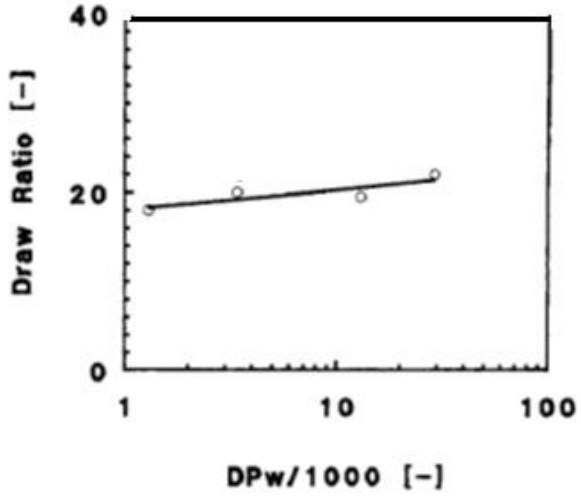

Figure1.19: Maximum attainable draw ratios of polyvinyl alcohol fibres (drawing temperature is 190 °C). [42]

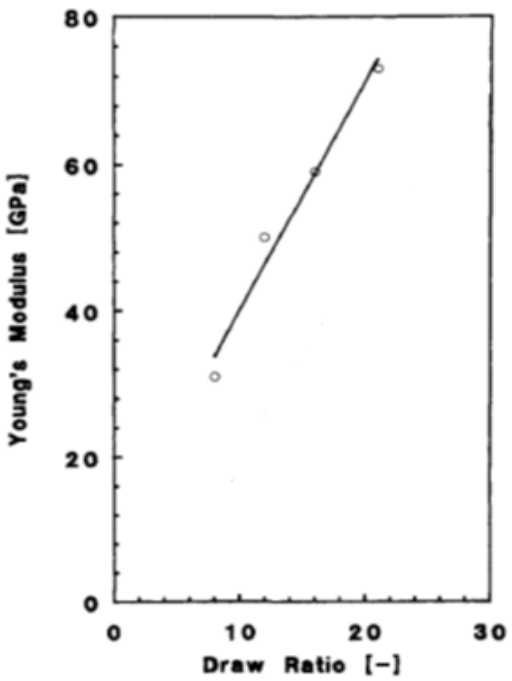

Figure 1.20: Young's modulus of polyvinyl alcohol fibres as a function of draw ratio. [42]

Their study shows that draw ratio is fairly independent of molecular weight, while the Young's modulus of the polyvinyl alcohol fibres increases rapidly with increasing draw ratio. Consequently, polyvinyl alcohol fibres with a high Young's modulus were obtained despite the low maximum attainable draw ratio. This is because in the polyvinyl alcohol crystal lattice, hydrogen bonds exist, which resist shear deformation and intermolecular chain slippage. Consequently, the unfolding of lamellae during solid-state drawing is restricted, which results in a low, and molecular weight independent, maximum attainable draw ratio. However, the limited maximum attainable draw ratio of polyvinyl alcohol fibres does not result in poor mechanical properties after drawing. [42]

Meanwhile, researchers are not giving up on the possibility of processing PVA fibres through melting spinning methods. That is because of the disadvantages of wet spinning and the

large amount of energy and time required in the process of dissolution, drying and solvent recovery. Compared with wet spinning, melt spinning technologies have plenty of advantages for the manufacture of some types of products, including fibres, films, injection-moulded articles, etc. Melt spinning is simple, costs less energy, takes less time and has a relatively high efficiency. Therefore, there are many researchers attracted to develop a better way to manufacture PVA by melt processing. In pursuing such a thermal process, it is essential to be aware of the thermal processing window for PVA. There are two ways to increase the thermal processing window of PVA. First, decreasing the melting temperature (T_m), and secondly, increasing the decomposition temperature (T_d) of PVA. [43] People usually use the method of blending [44] [45] [46], chemical modification [47-52] and the addition of plasticisers and stabilisers [53-59] to achieve a workable thermal processing window for PVA.

In terms of blending, Nishino et al. [44] developed a way to significantly improve the thermal stability of PVA without decreasing the melting temperature using poly(GEMA). They utilised the strong intermolecular hydrogen bonds between hydroxyl groups of PVA and carbonyl groups of poly(GEMA) to stabilize the PVA at high temperatures to improve the thermal processability.

Meanwhile, changing the chemical structure of PVA by grafting and post-reaction can also improve the thermal processability of PVA. However, changing the chemical structure is far too complex, while not always desirable as some excellent chemical and physical properties of PVA would possibly be lost during a process of grafting and post-reaction. More importantly, the maximum attainable strength and modulus always reduces significantly.

Generally, the most common way of improving the thermal processability of PVA is through the usage of plasticisers, which can effectively decrease the melting temperature and viscosity of PVA. Water is a solvent and also can be considered as a very good plasticiser for PVA [60], because it is very common and environmentally friendly, and can be easily extracted as well. However, the control of processing conditions is stricter due to its low boiling temperature, which limits the industrialisation of this method. Although having said that, the potential could be enormous for this method.

The normal process for spinning PVA is with water as a solvent. However, physical gelation via crystallization does not occur and consequently the maximum attainable draw ratio (<5), modulus and strength are relatively low.

There are many additives used as plasticisers for PVA. For example, Wang et al. used a kind of compound as a plasticiser, which contains amino groups (Ac). [43][53][54] This kind of compound, Monoethanolamine for instance, in combination with water, could form hydrogen bonds with PVA, decreasing the melting temperature of PVA while increasing the decomposition temperature. Other kinds of widely used plasticiser are organic compounds containing hydroxyl groups, including ethylene glycol, glycerol, low molecular weight poly(ethylene glycol) and so on. These plasticisershave an advantage over water due to their higher boiling temperatures, but the complex further post-spinning treatment, extraction process etc. prevents this method from achieving full commercial/industrial success.

In our study, we tried different methods to fabricate PTFE/PVA blends, including solution casting, single-step extrusion, and two-steps compounding and extrusion. Based on the best

results of these three methods, for instance, mechanical properties, fibres formation etc., we developed a method that was able to spin PTFE/PVA blend fibres, which after removal of the PVA resulted in ultrafine PTFE fibres. First, through lab scale experiments in a mini-extruder, material and processing parameters were investigated and optimized. Subsequently, we transferred the work to a larger pilot scale spinning line using a twin-screw extruder. The three methods of processing the blends, together with the two methods of spinning and drawing are presented in the further parts of the thesis.

1.10 Objective of the thesis

The objective of this thesis is to develop a method to produce PTFE nanofibres. From the literature review related to production methods for PTFE nanofibres, it can be concluded that the technology for producing PTFE nanofibres is basically non-existent. In this thesis, the method of island-in-sea is studied and modified for producing PTFE nanofibres, in which PVA is used as the matrix (sea) phase because its high solubility to water. However, the properties of these two materials would bring some difficulties because PTFE has a ultra-high viscosity in melt and PVA has a melting temperature that is higher than its decomposition temperature, which makes both polymers not melt processable or intractable. Here we therefore used a slightly modified method based on a PTFE suspension in a PVA/water solution, which will be described in more detail in the following chapters. The blend morphology and mechanical properties of the blend PTFE/PVA fibres produced using different procedures are tested and advantages and disadvantages of each method are discussed to select the best method for compounding and fibre formation. Optimized processing parameters, including temperature, component ratio etc, were also investigated and confirmed. After drawing and extraction, the obtained PTFE nanofibres were studied.

Finally, using some optimized process parameters, this lab-scale study was transferred to a semi-industrial scale twin-screw extrusion process to prove its practicality for industry.

Chapter 2

Ultra-fine PTFE fibres from PTFE/PVA blend tapes prepared by solution casting

2.1 Introduction and objective

This chapter reports on a proof-of-principle study of a modified island-in-the-sea method for the fabrication of PTFE nanofibres using PTFE/PVA as a system. As mentioned in Chapter 1, PTFE cannot be dissolved in most organic solvents, and cannot be processed in the melt either due to its high viscosity in the melt state. PVA is water soluble and therefore an interesting candidate for the sea part. The melting temperature of PVA is higher than its decomposition temperature. Therefore, the most common method to process PVA is via solution processing. For this, first PTFE particles in water suspension will be mixed with a PVA/water solution. After casting and evaporation of water, a film should be obtained consisting of PTFE islands in a PVA sea of matrix. After solid-stated drawing of this film, a highly fibrillar morphology of ultrafine PTFE fibres in an oriented PVA matrix should be obtained from which the PTFE nanofibres can be extracted by dissolving the PVA matrix. Some essential material and processing parameters will be studied and optimized, including blend composition, drawing conditions etc.

2.2 Experimental

2.2.1 Materials

Poly(vinyl alcohol) (PVA), 98-99 % hydrolyzed, with a typical weight average molecular weight Mw of 95.000 - 124.000 g/mol was purchased from Sigma-Aldrich Co Ltd.

Poly(tetrafluoroethylene) (PTFE) was used in the form of a Teflon® (PTFE TE-3893 N) aqueous dispersion from Dupont de Nemours Int'l S.A. containing 60wt.% PTFE particles in water with a diameter of 210 ± 50 nm. This PTFE resin has a crystalline melting temperature of 337°C and cannot be processed by solvent or melt techniques but is instead typically processed as a dispersion for making coated or impregnated fibre or wire products. Received as a milky white dispersion in water with a viscosity at room temperature of approximately 25mPa·s, it also contains approximately 6% (by weight of PTFE) of a non-ionic wetting agent and stabiliser. Isotropic PTFE in its final form has a tensile strength of 24MPa, and a strain at break of 400 % according to the product information. [70]

2.2.2Processing and characterization

2.2.2.1 PTFE/PVA blend preparation

PVA was dissolved in water by magnetic stirring in an oil bath at a temperature of 80^{o}C for 6hrs to prepare a PVA solution (10wt.%). This PVA solution was then mixed with the PTFE suspension at a weight ratio of PTFE: PVA= 1:9, 2:8, 3:7, 4:6, 5:5 (i.e. the volume of PTFE in the PTFE/PVA mixtures are respectively 5.7 vol.%, 12vol.%, 19vol.%, 26vol.% and 35vol.%). Magnetic stirring was used to make the solution/suspension uniform at 80^{o}C for 0.5 h. A drop of every set of mixture was placed onto a glass slide and uniformly coated by spin-

coating (Spincoat G3P-8) at room temperature. Finally, the specimens were dried by evaporating the water to obtain a thin film with a thickness of 100 µm.

Each set of mixtures was placed in an evaporation dish and dried to obtain a thick film (about 500 µm) of the mixtures. From this PTFE/PVA films, strips were cut with dimensions of 50mm x 10 mm and marked with a pen at every 5mm for determination of the draw ratio after solid-state drawing.

The thin film coated glass slides were observed with an optical microscope (Olympus BX 60 with Digital Imaging) between cross-polarizers.

2.2.2.2 Drawing temperature

The thick PTFE/PVA blend films were drawn at elevated temperature. Ultra-drawing was performed at100^{o}C, 130^{o}C, and 150^{o}C using an Instron 5566 universal tensile tester equipped with an oven at 5 mm/min to see which temperature is most suitable for the drawing of the PTFE/PVA blend films. Because the PVA in the blend film is easily oxidised, we could see some discolouration of the blend film at a drawing temperature of 130^{o}C, and this discolouration became more significant at 150^{o}C (light yellow appearance). Further hot drawing tests were performed to identify the optimal drawing conditions for the blend films of different compositions (100^{o}C, 130^{o}C and 150^{o}C). Specimens with different PTFE content (0vol.%, 5.7vol.%, 12vol.%, 19vol.%, 26vol.% and 35vol.%) were drawn in a universal tensile tester (Instron 5566) equipped with 1kN load cell, and the oven temperature set at 130^{o}C and 150^{o}C in air atmosphere. During tensile deformation, we observed some unstable

drawing at these temperatures. The details are discussed in the results and discussion section.

2.2.2.3Solid-state drawing

Solid-state drawing was performed by placing the PTFE/PVA film on a hot plate at 100^{o}C for 5min and then drawing it using pliers by hand. Mechanical properties of the drawn blend tapes with approximate dimensions of 50 x 5 x 0.2mm^{3} were tested using a universal tensile tester (Instron 5566) equipped with a 1kN load cell at a test speed of 5 mm/min.

2.2.2.4 SEM

Specimens were immersed into liquid nitrogen for approximately 2 min and then broken perpendicular to the drawing direction with two clamps holding each sides. All specimens were coated with gold. High vacuum FEG source scanning electron microscope (SEM) (FEI Inspector-F) was used to observe the microstructure of the PTFE/PVA blends.

2.3 Results and discussions

2.3.1 PVA/PTFE dispersion morphology by optical microscopy

From the photographs of the solution cast films (Figure 2.1), we can see that when the PTFE content exceeds 70 wt.%, the PTFE becomes the continuous phase, but with poor film forming properties as a result of major inhomogeneities. Based on this, in further experiments, the compositions of the PTFE/PVA blends were set at PTFE: PVA = 1:9, 2:8, 3:7, 4:6 and 5:5 w/w. Higher PTFE contents were found to be not homogeneous. The pure PVA film was transparent or slightly translucent due to the semi-crystalline character of PVA. The

films with a PTFE/PVA weight ratio below 5:5 all scatter light to a certain degree and this light scattering increased with increasing PTFE content.

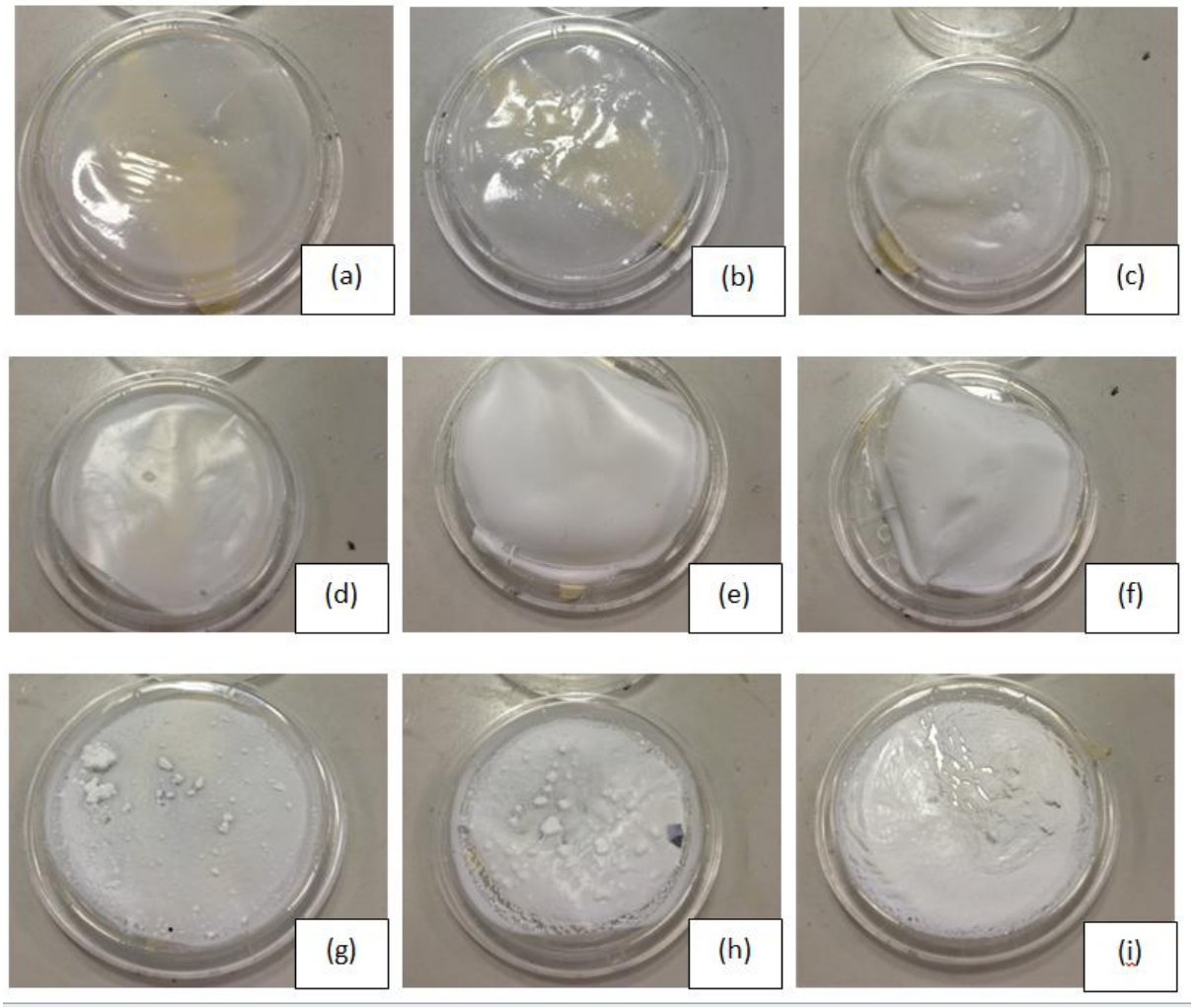

Figure 2.1: Photographic images of cast PTFE/PVA blends with weight ratios of (a) 1:9; (b) 2:8; (c) 3:7; (d) 4:6; (e) 5:5; (f) 6:4; (g) 7:3; (h) 8:2; (i) 9:1.

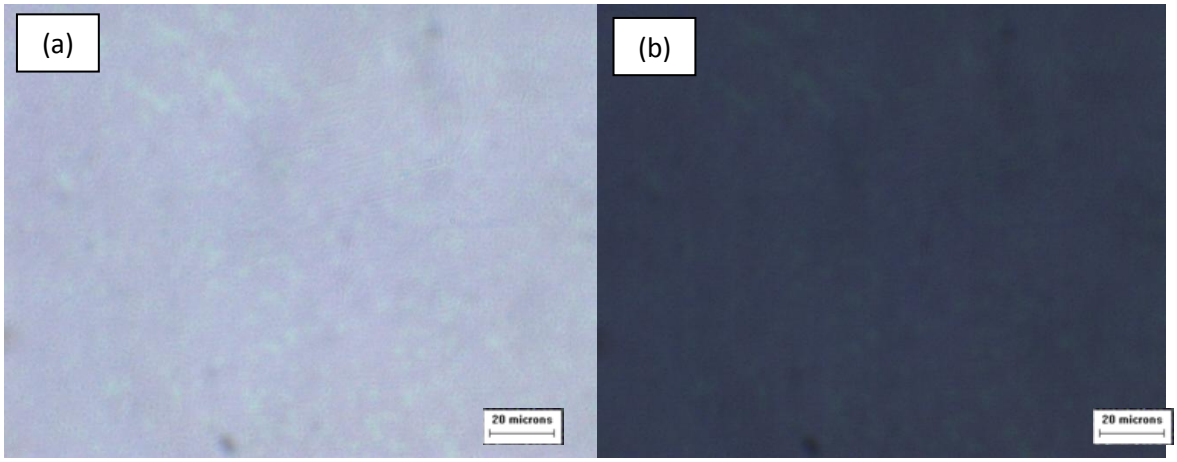

Figure 2.2: Optical microscopy images of (a) pure PVA in bright field (b) PVA between crossed polarizers.

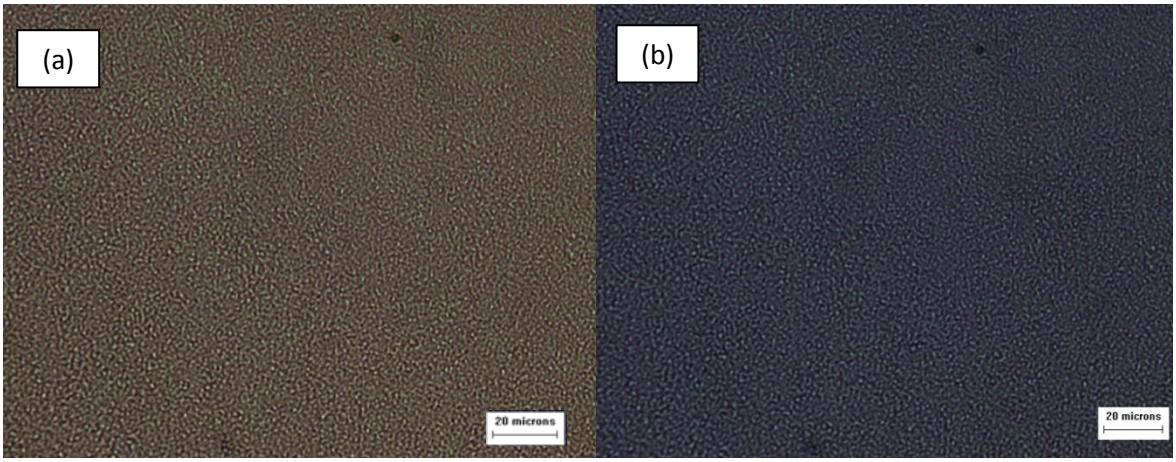

Figure 2.3: Optical microscopy images of (a) pure PTFE in bright field (b) PTFE between crossed polarizers.

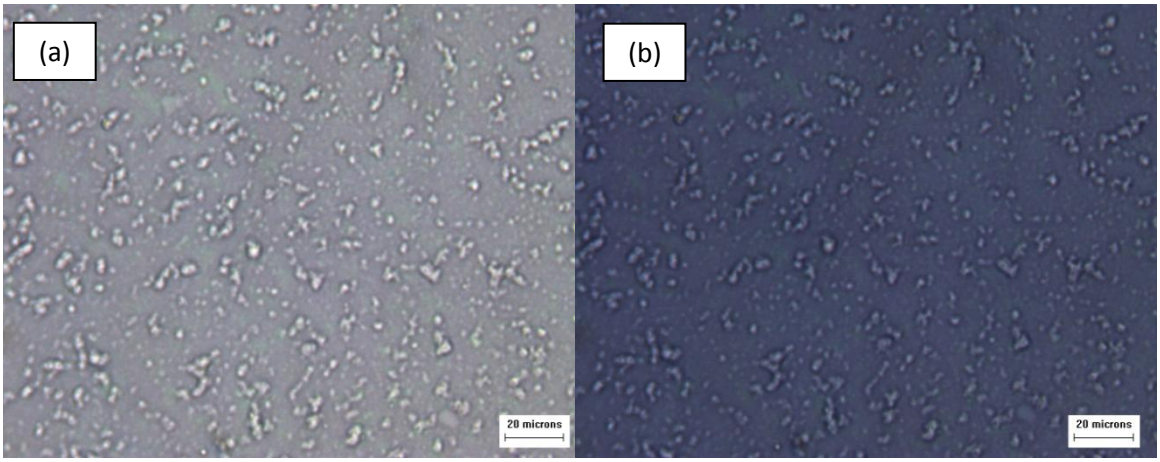

Figure 2.4: Optical microscopy images of blend PTFE: PVA = 1:9 (PTFE = 5.7 vol.%) (a) in bright field (b) between crossed polarizers.

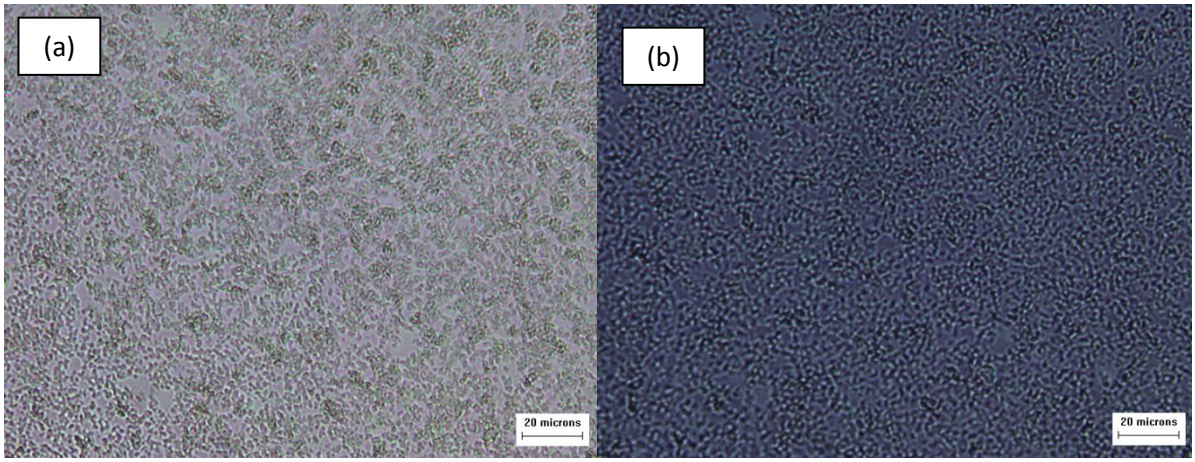

Figure 2.5: Optical microscopy images of blend PTFE: PVA = 2:8 (PTFE = 12 vol.%) (a) in bright field (b) between crossed polarizers.

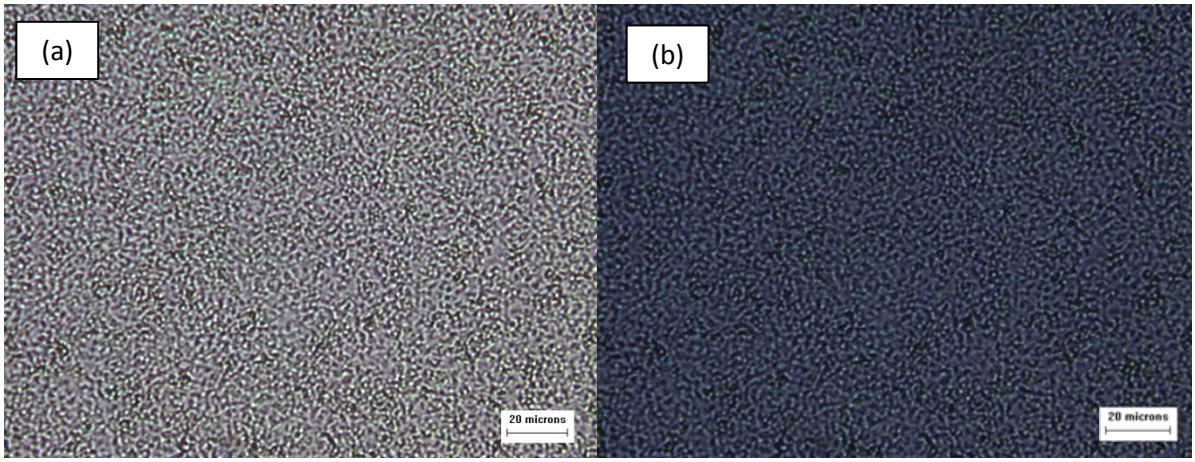

Figure 2.6: Optical microscope images of blend PTFE: PVA= 3:7 (PTFE = 19 vol.%) (a) in bright field (b) between crossed polarizers.

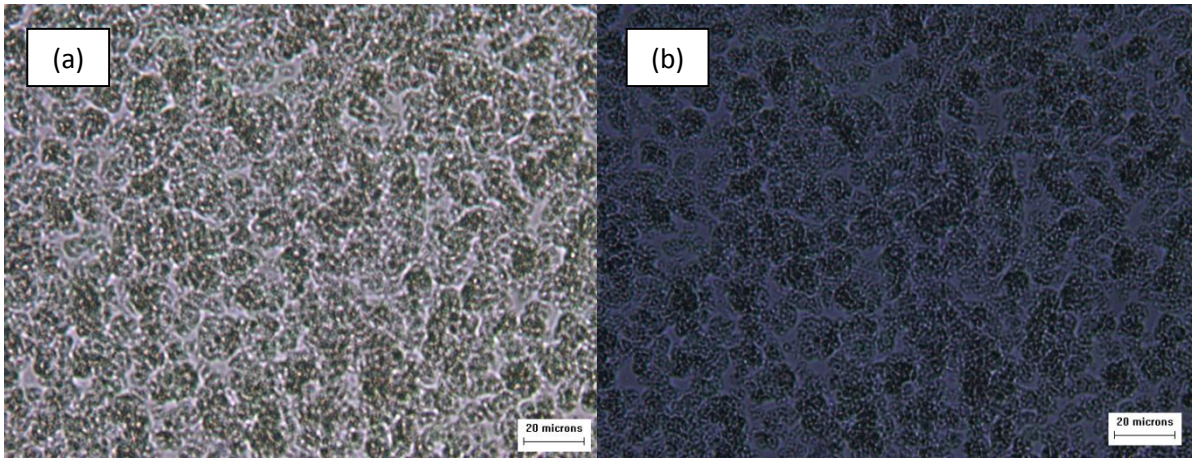

Figure 2.7: Optical microscopy images of blend PTFE: PVA =4:6 (PTFE = 26 vol.%) (a) in bright field (b) between crossed polarizers.

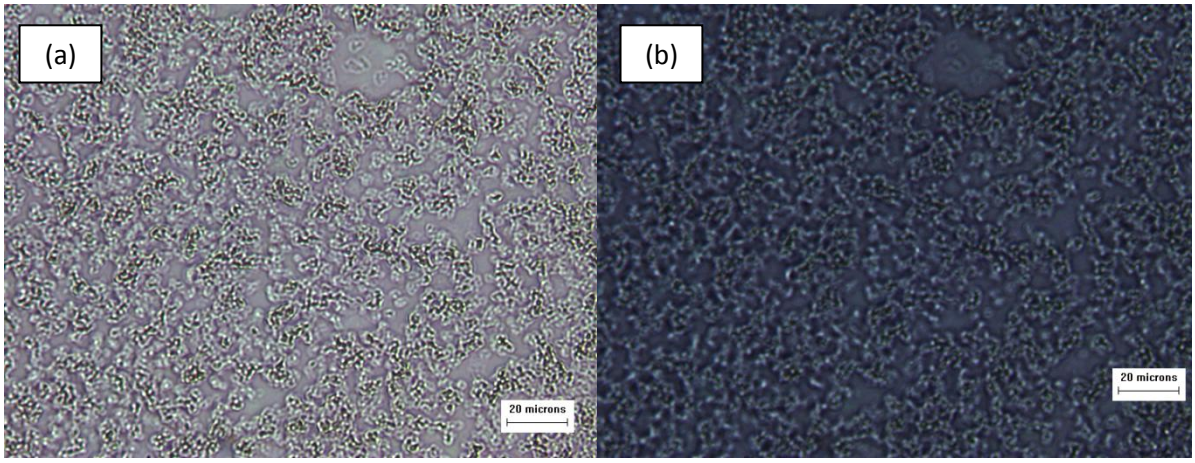

Figure 2.8: Optical microscopy images of blend PTFE: PVA =5:5 (PTFE = 35 vol.%) (a) in bright field (b) between crossed polarizers.

In Figure 2.2 and 2.3, we can see that the morphology of pure PVA film is uniform, while the morphology of PTFE is that of well-dispersed uniform small particles. The morphologies in Figure 2.5 and 2.6 are similar to that of the neat polymer ones, indicating a well dispersed mixture on the micron scale in blends with 12 vol.% and 19 vol.% PTFE. Either higher or lower concentrations lead to non-uniform dispersions.

2.3.2 PTFE/PVA dispersion morphology by SEM

The dispersion of PTFE particles in the cast films look homogeneous macroscopically but is still rather poor on a micron-scale. According to the previous optical microscopy pictures, the blends with a PTFE content of 12vol.% and 19vol.% have a better dispersion morphology than the other blends. Therefore, in subsequent studies and discussions, similar to Figure 2.9, SEM images of only blends with 19vol.% PTFE will be used to describe and illustrate the

dispersion morphology and subsequent fibre formation, although samples with other PTFE contents were also tested.

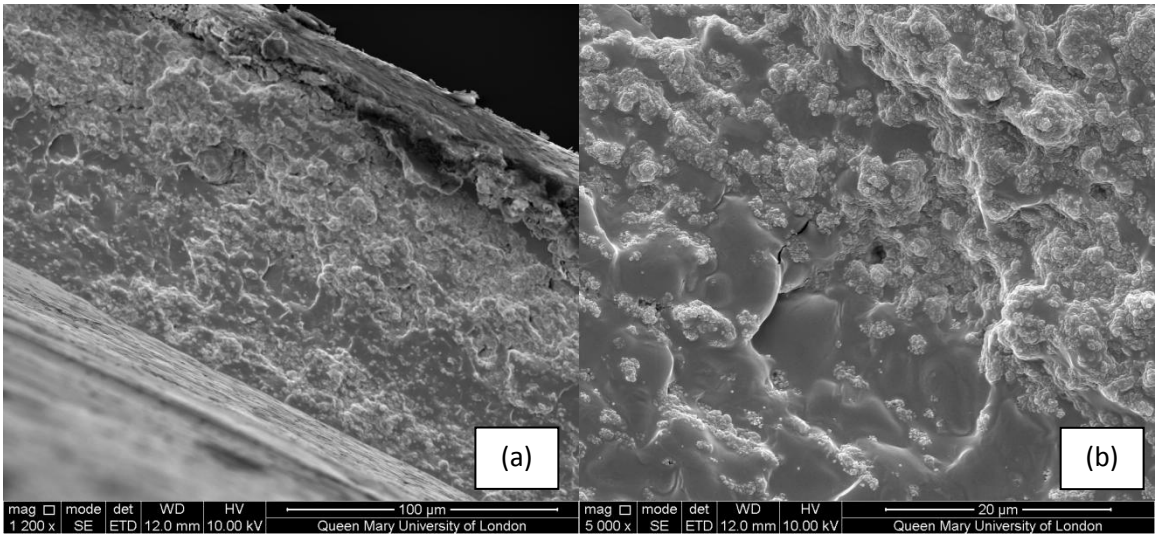

Figure 2.9: SEM images of cast films observed from the cold fractured surface of a blend tape with 19 vol.% PTFE, (a) magnification 1200x; (b) 5000x.

2.3.3 Drawing behaviour and mechanical properties

In Figure 2.10, 2.11 and 2.12 the draw ratio, tensile stress and modulus of undrawn blend tapes with different compositions at 100^{o}C, 130^{o}C and 150^{o}C are compared.

In Figure 2.10, some of the draw ratios at 150^{o}C are higher than those obtained at 130^{o}C, but the average draw ratios are not reproducible. This unstable drawing probably originates from the oxidation and decomposition of the PVA. The phenomenon of discolouration, in which films turn into yellow/light-brown, is indicative of oxidation and decomposition. On the other hand, the draw ratios of samples drawn at 130^{o}C are much more reproducible

than the ones at 150^{o}C, especially when the content of PTFE is 19vol.%, 27vol.% and 35vol.%. Therefore it is concluded that 130^{o}C is a more suitable drawing temperature than 150^{o}C.

Meanwhile, by comparing the maximum draw ratios between 100^{o}C and 130^{o}C, we could see that the samples achieved a higher draw ratio at 130^{o}C than at 100^{o}C. However, there is a drop in draw ratio for samples of 12vol.% and 19vol.% as shown in Figure 2.10b, indicating that drawing is more sensitive to the PTFE content at higher temperature, and apparently drawing of samples with a high PTFE content is not stable at 130 ^{o}C, which might be caused by possible oxidization and degradation at these temperatures.

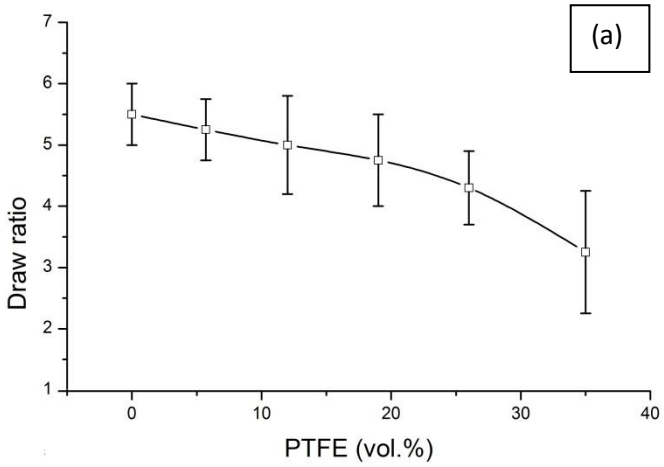

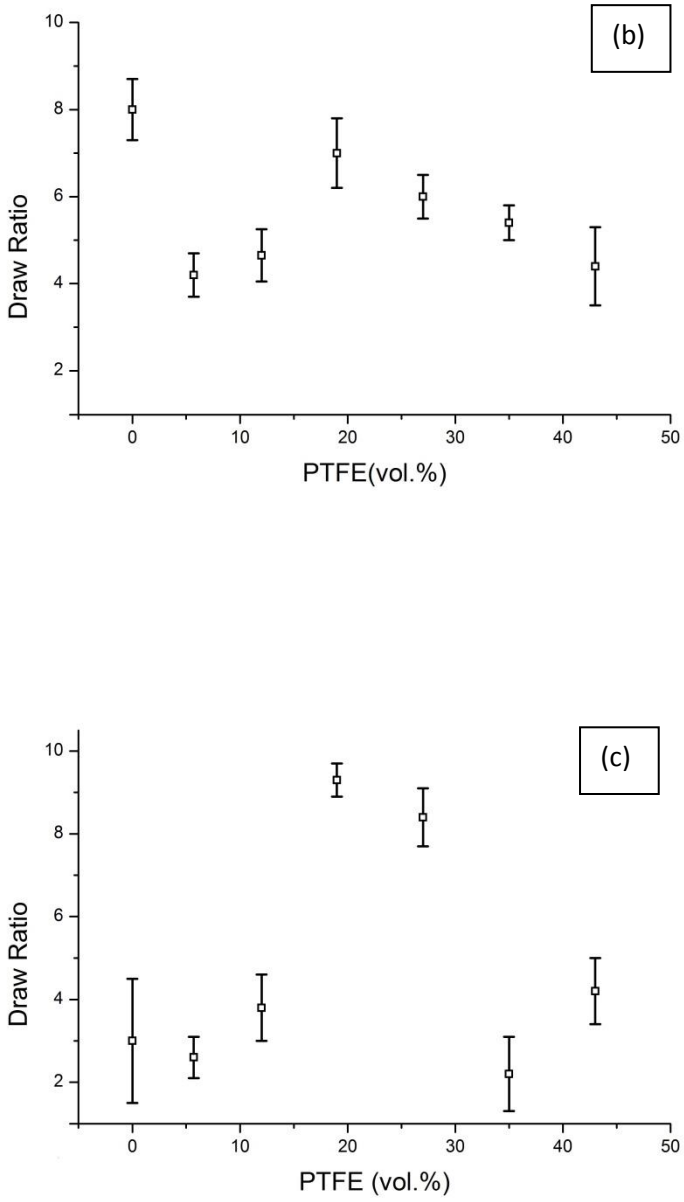

Figure 2.10: Maximum draw ratio of cast PTFE/PVA film as a function of PTFE content drawn at (a) 100 ^{o}C, (b) 130 ^{o}C and (c) 150 ^{o}C.

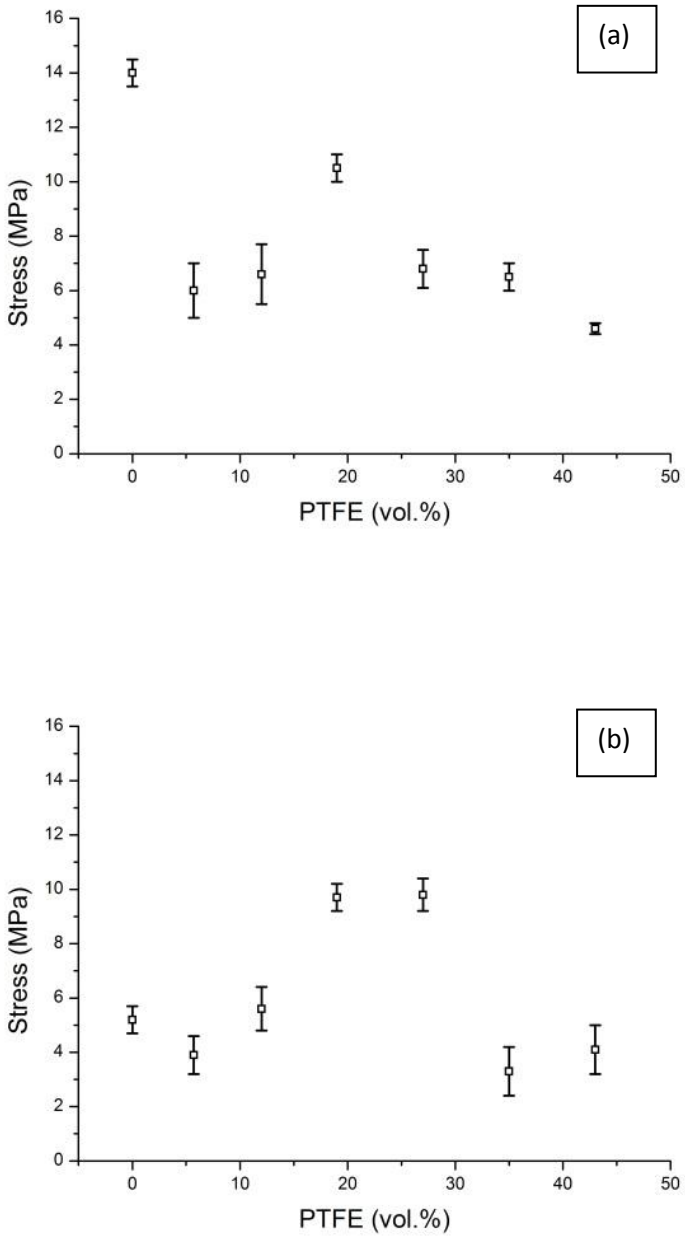

Figure 2.11: Tensile strength of cast PTFE/PVA films as a function of PTFE content drawn at (a) 130 ^{o}C and (b) 150 ^{o}C.

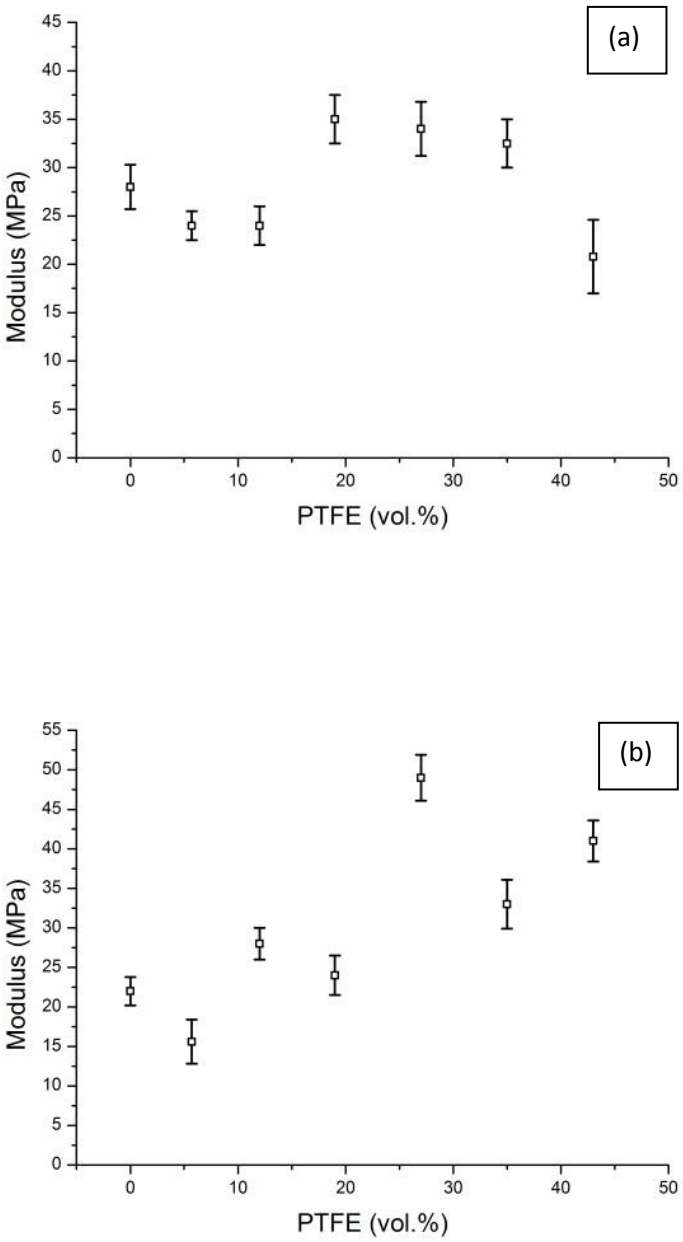

Figure 2.12: Young's modulus of cast PTFE/PVA films as a function of PTFE content drawn at (a) 130 ^{o}C and (b) 150 ^{o}C.

By comparing the tensile stresses of samples drawn at 130^{o}C and 150^{o}C in Figure 2.11, we can also see that the tensile stress of samples drawn at 130^{o}C is generally around 6MPa except for the sample with 19vol.% PTFE which is slightly higher. However, for the samples

drawn at 150^{o}C, the tensile stresses are less constant and vary from 2MPa to 11MPa. Similar to the tensile strength, the Young's modulus of those samples shows a similar pattern (Figure 2.11). As we can see, the modulus decreases steadily with increasing PTFE content at a drawing temperature of 130^{o}C while the trend for modulus at 150^{o}C is less clear.

Therefore, from the draw ratio, tensile strength and Young's modulus, we can see that drawing stability decreases with increasing drawing temperature from 130^{o}C to 150^{o}C, while the change of tape colour indicates a possible oxidation and decomposition of PVA.

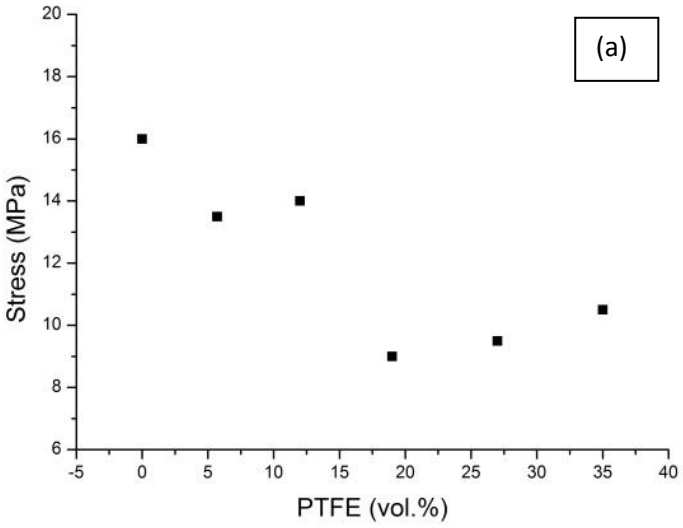

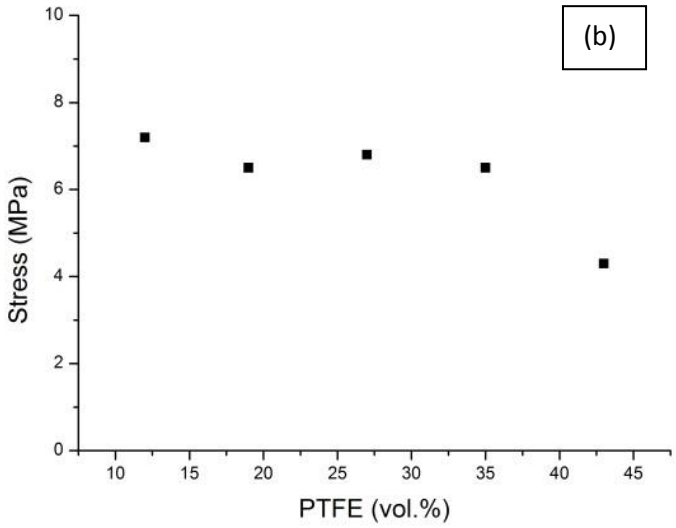

Figure 2.13: Tensile strength of drawn PTFE/PVA tape of λ = 4as a function of PTFE content at (a) 100 °C and (b) 130 °C.

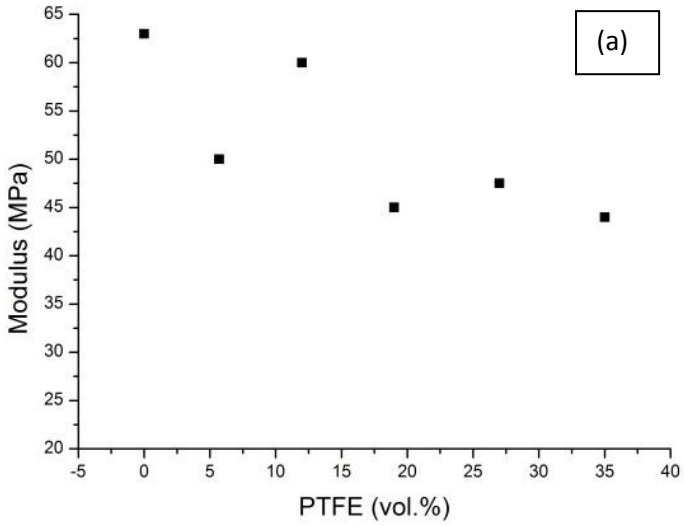

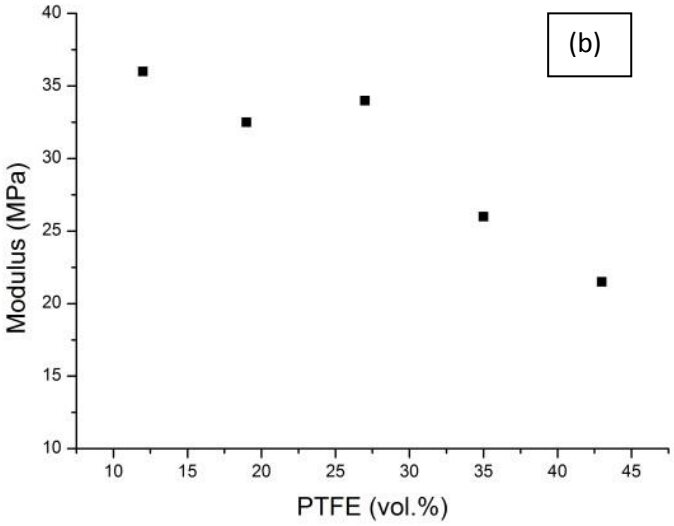

Figure 2.14: Young's modulus of drawn PTFE/PVA tape of λ = 4as a function of PTFE content at (a) 100 °C and (b) 130 °C.

Furthermore, by comparing the tensile properties for samples that were drawn at 100°C and 130°C to a draw ratio λ = 4, we can see that the strength (Figure 2.13) and Young's modulus (Figure 2.14) for both sets of samples drops with increasing PTFE content. However, the values of both tensile stress and modulus are higher at 100°C than 130°C. This is because mobility of the molecular chains is higher at 130°C, meaning relaxation of the orientated chains during drawing. Therefore, we would choose 100°C as the drawing temperature in further experiments.

2.3.4 Morphology of PTFE/PVA tapes after drawing by optical microscopy

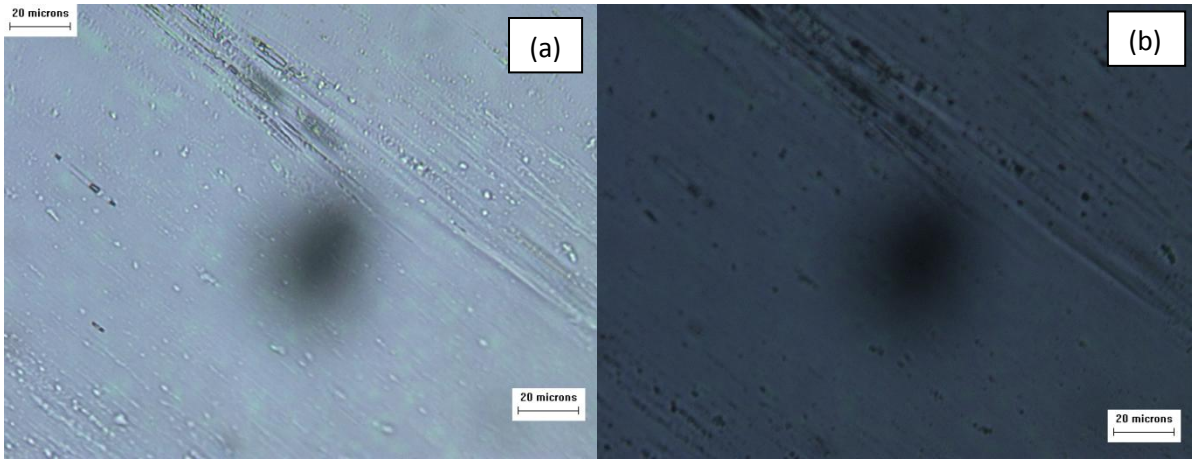

Figure 2.15: Optical microscopy images of drawn PVA tapes (a) in bright field (b) between crossed polarizers.

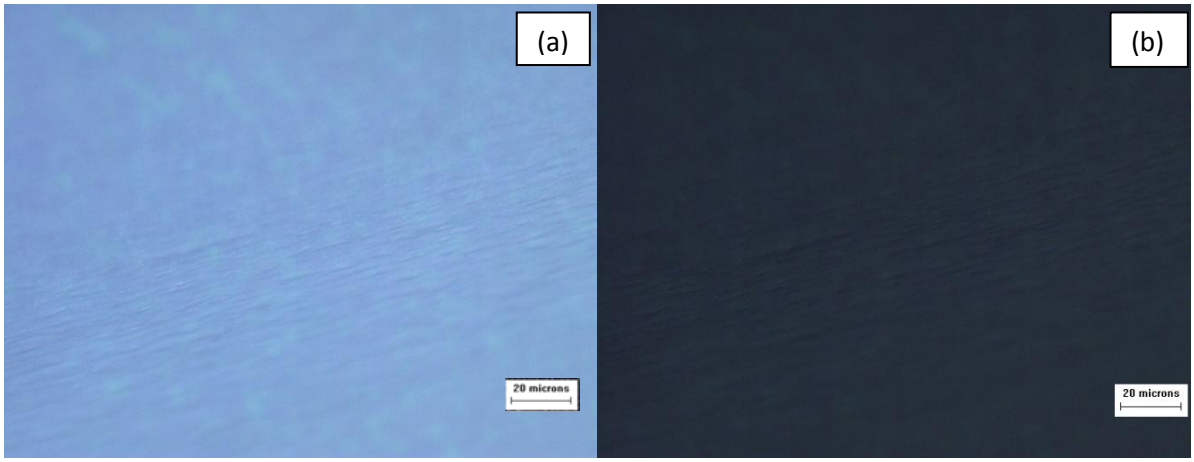

Figure 2.16: Optical microscopy images of drawn blend tapes of PTFE:PVA = 1:9 (a) in bright field (b) between crossed polarizers.

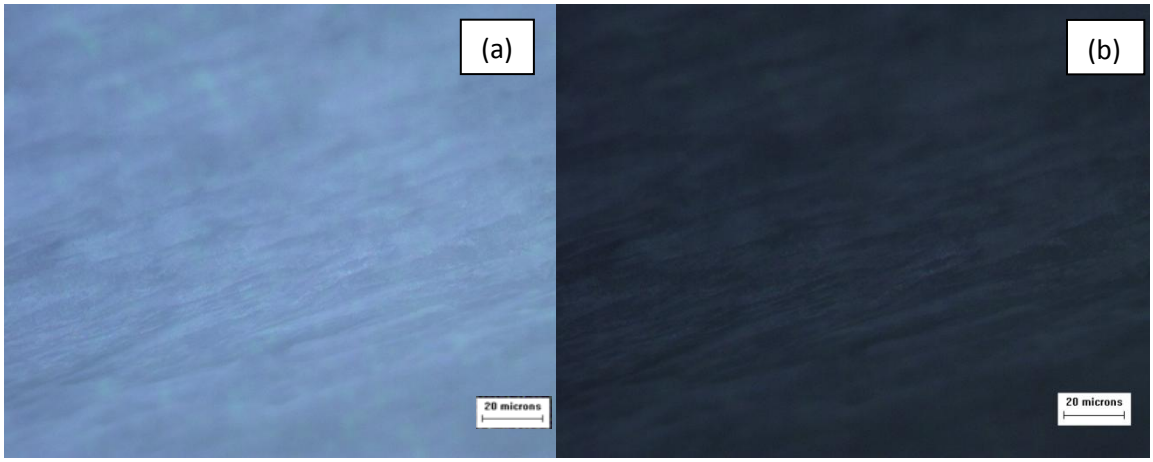

Figure 2.17: Optical microscopy images of drawn blend tapes of PTFE: PVA = 2:8 (a) in bright field (b) between crossed polarizers.

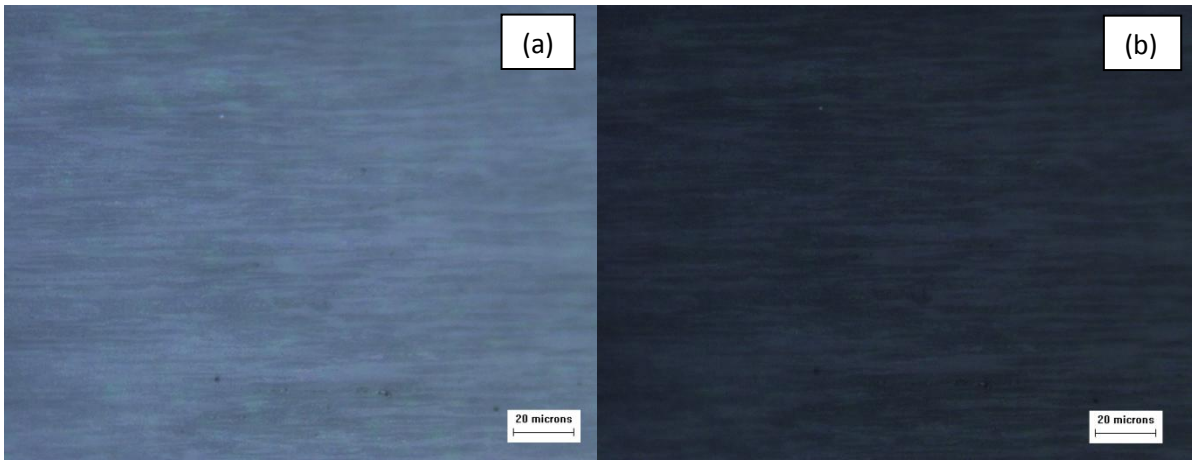

Figure 2.18: Optical microscopy images of drawn blend tapes of PTFE: PVA = 3:7 (a) in bright field (b) between crossed polarizers.

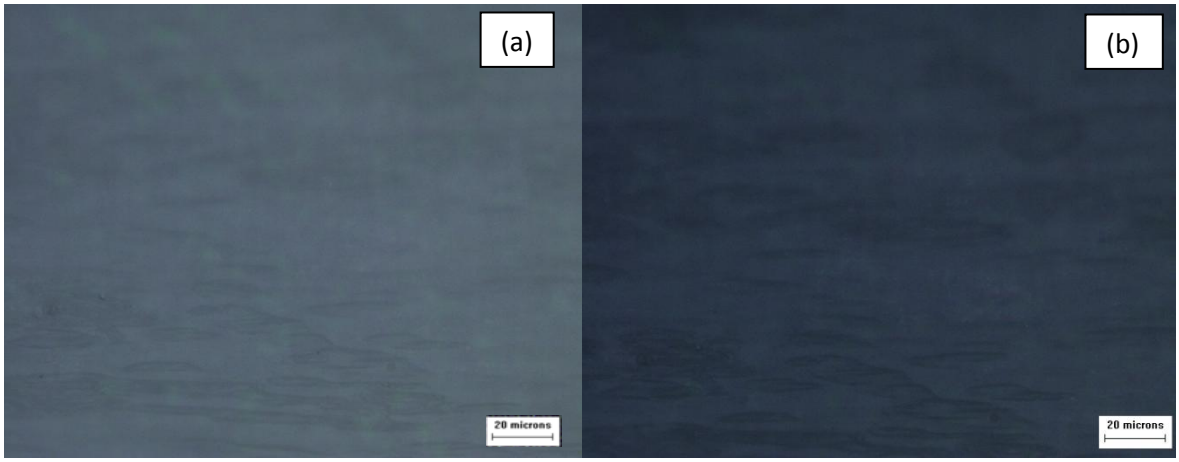

Figure 2.19: Optical microscopy images of drawn blend tapes of PTFE: PVA = 4:6 (a) in bright field (b) between crossed polarizers.

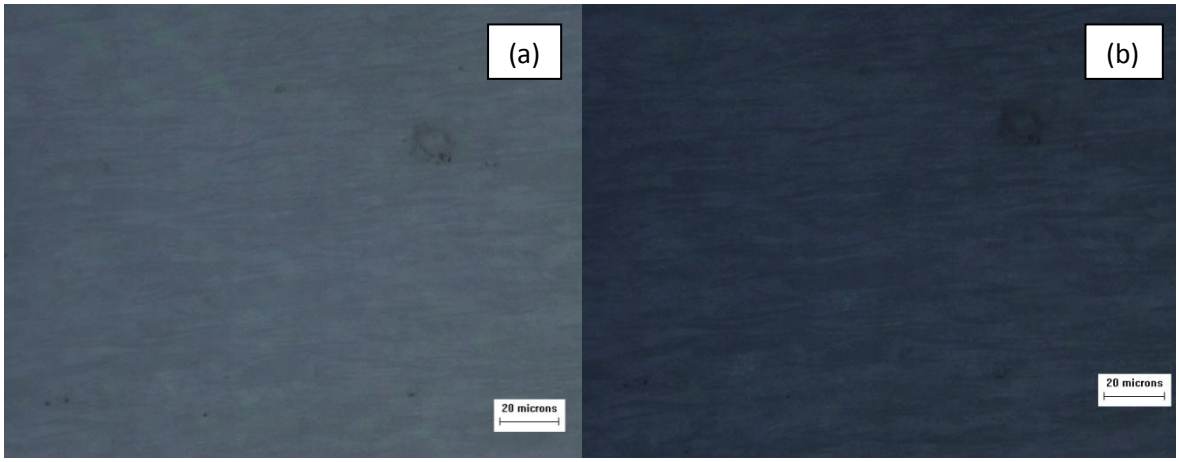

Figure 2.20: Optical microscope images of drawn blend tapes of PTFE: PVA= 5:5 (a) in bright field (b) between crossed polarizers.

From the optical microscopy images in Figures 2.15-2.20, and by comparing them with Figures 2.2-2.8, we can see significant orientation along the drawing direction, which confirms that pure PVA and PTFE/PVA blend films were orientated after drawing in the solid

state. The actual molecular orientation and crystallinity of these tapes were evaluated through XRD and will be discussed later.

2.3.5 Fibre formation after drawing by SEM

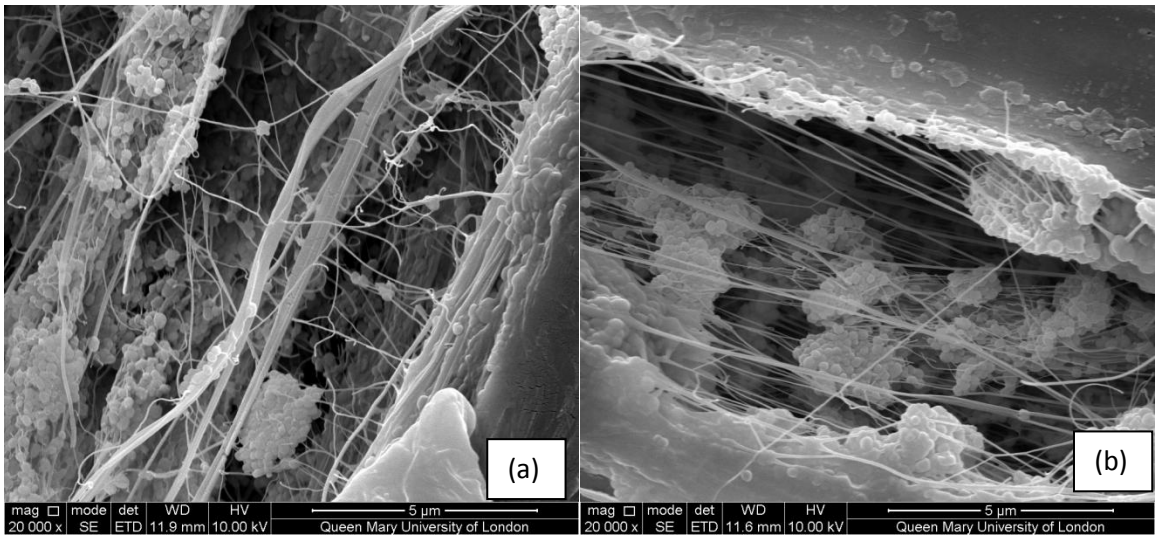

Figure 2.21: SEM images of drawn PTFE/PVA blend tapes showing (a) many large fibre bundles, and (b) single fibres and small fibre bundles.

From Figure 2.21 we can see that fibres are formed in the blend after drawing but we can also identify many large agglomerates of undrawn PTFE particles with sizes up to 2-3 µm. Fibre formation occurs through drawing of PTFE particles. Further confirmation of these PTFE fibres will be shown through EDS and FTIR later.

Although partly successful, from these initial drawing studies we can already identify some problems. First, in Figure 2.21(a) we can see many fibres bundles rather than single fibres, formed from PTFE particle agglomerates. Meanwhile, in Figure 2.21(b) we can see that although some single nanofibres are present many PTFE agglomerated particles exist that

remain undrawn. This commonly existed in all samples produced through casting, no matter what composition, indicating that the casting method could not provide a good enough dispersion in the PTFE/PVA blend. Moreover, the adhesion between PVA and PTFE is much weaker than that between fused PTFE particles themselves, causing a large number of PTFE particles and agglomerates to remain undrawn.

2.3.6 Maximum attainable draw ratio and tensile properties

We can see that the average maximum draw ratio of the cast blend films drawn at 100^{o}C (see Figure 2.10a) decreases with increasing PTFE content. Initially draw ratio is reduce lineraly with PTFE content up to 19vol.% PTFE, while a more significant reduction in draw ratio is observed at PTFE contents of 26vol.% and 35vol.%. This indicates that the dispersion of PTFE particles becomes less uniform at these high PTFE loadings, which is in agreement with the morphological studies of Figure 2.1-2.7 and 2.8.

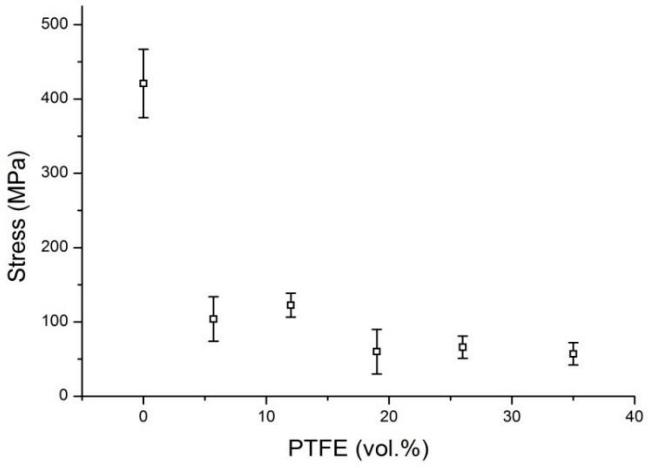

Figure 2.22: Tensile strength of cast PVA and PTFE/PVA blend tapes drawn to λ = 4 as a function of PTFE content drawn at 100°C.

Tensile tests were performed on PTFE/PVA tapes drawn to a fixed draw ratio of 4. The cross-sectional area of the tapes was calculated from their linear density by:

$$A = \frac{m}{(\rho_{PTFE}.V_{PTFE}+\rho_{PVA}.V_{PVA}).l} \qquad \text{Equation 2.1}$$

Where, *A* is the cross-sectional area of the tape, *m* is the weight of tape, ρ_{PTFE}*(2.2g/cm^3)*is the density of PTFE, $\rho_{PVA}$is the density of PVA, V_{PTFE} is the volume fraction of PTFE, V_{PVA}(1.2g/cm^3)is the volume fraction of PVA, and *l* is the length of the drawn tape.

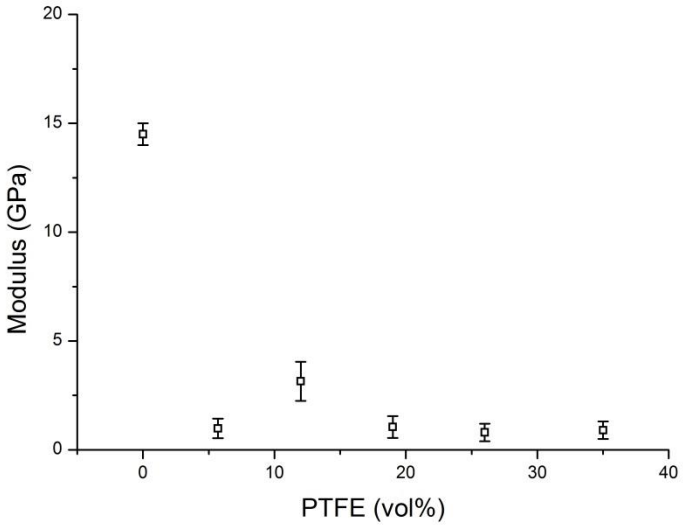

Figure 2.23: Young's modulus of cast PVA and PTFE/PVA blend tapes drawn to λ = 4 as a function of PTFE content drawn at 100°C.

Figure 2.22 and 2.23 shows the tensile strength and Young's modulus of solution cast PVA and PTFE/PVA blend tapes drawn to a draw ratio of λ=4. Blend tapes have much lower properties than pure PVA, while the values of both stress and modulus decrease at a rate

significantly faster as predicted by the standard 'rule of mixtures'. The theoretical modulus is calculated through Equation 2.2 and Equation 2.3 as shown below.

Theoretical predictions of the Young's modulus of the blend fibres were performed using the rule of mixture (ROM)[61,62]which is the simplest and intuitive method for the estimation of the effective mechanical properties interms of its constitutes.

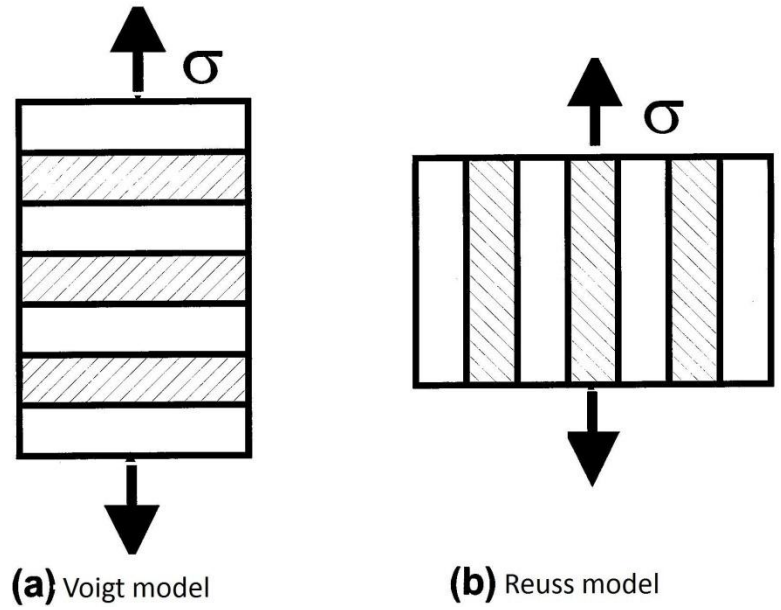

Figure 2.24 Schematic diagram showing (a) Voigt model and (b) Reuss model [61].

The parallel (Voigt) model, also known as the 'rule of mixtures' or 'iso-strain' model is based on the equal strain assumption, while the series (Reuss) model [63], also known as the 'inverse rule of mixtures' or 'iso-stress' model, is based on the equal stress assumption. Since the Voigt model represents the upper bound and the Reuss model represents the lower bound of the mechanical properties [64], the results of the Voigt model are always

higher than that of the Reuss model, with actual mechanical properties of particulate filled composites or blends often positioned between these two limits.

$$E_{b11} = V_{PTFE} \, . \, E_{PTFE} + V_{PVA} \, . E_{PVA}$$ Equation 2.2

$$E_{b22} = (\frac{V_{PTFE}}{E_{PTFE}} + \frac{V_{PVA}}{E_{PVA}})^{-1}$$ Equation2.3

Where $E_{b11}$is the theoretical upper bound Young's modulus of the PTFE/PVA blends, and E_{b22} is the theoretical lower bound modulus of the blend tapes. V_{PTFE} is the volume fraction of PTFE and V_{PVA} is the volume fraction of PVA. The value of E_{PVA} used in the calculations is the experimental result of the modulus of pure drawn PVA with a draw ratio λ=4 (14GPa). Modulus data for drawn PTFE was taken from literature and estimated as 500MPa [28].

Figure 2.25 shows the Young's modulus of the drawn cast PTFE/PVA tapes with a draw ratio λ=4 together with predictions using the parallel (Voigt) and series (Reuss) model. The experimental data lays very close to the properties predicted by the Reuss model. This is presumably because of weak adhesion and poor stress transfer between the PVA and the PTFE fibres, or an indication of poor dispersion of PTFE in the cast blends. Since the data lays well below the Voigt predictions it also indicates that the blend morphology consists of a discontinuous PTFE fibre phase in a continuous PVA matrix phase. However, there is also still some data that falls below the prediction by the Reuss model. This might be caused by the poor adhesion and stress transfer between the PVA and PTFE phase, together with poor dispersion, leading to void formation during drawing.

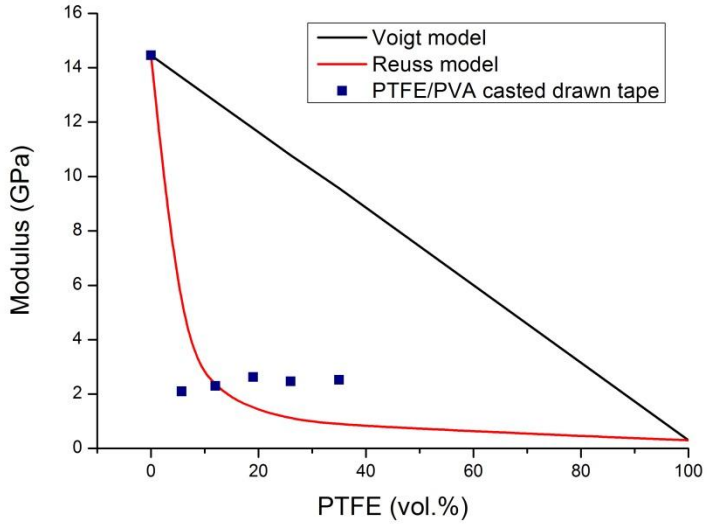

Figure 2.25: Young's modulus of cast PTFE/PVA tapes with λ=4 as a function of PTFE content (before removal of PVA) together with theoretical predictions using upper-bound parallel (Voigt) model and lower-bound series (Reuss) model.

2.4 Conclusions

According to optical microscopy pictures, SEM images and tensile tests results, we believe that we have achieved a 'proof-of-principle' methodology for the fabrication of PTFE nanofibres from PTFE/PVA blends using a modified island-in-the-sea method. Processing parameters of the island-in-the-sea fibre formation method were evaluated, including drawing temperature and PTFE content in the blend.

However, this study also revealed that the initial dispersion state of the PTFE particles in the PVA is highly important. The poor state of dispersion of PTFE particles in the PVA in these solution cast blends greatly affected further PTFE nanofibre formation and production, as well as the tensile properties of the drawn PTFE/PVA blends. Apparently, the shear forces

provided by magnetic stirring are not high enough to disperse the PTFE particles uniformly in the PVA/water solution. Because of the viscosity of the PVA solution, the PTFE particles agglomerate during the weak mixing. This poor state of dispersion not only causes the formation of PTFE fibre bundles rather than individual PTFE nanofibres but also is responsible for plenty of undrawn PTFE particles and agglomerates. Therefore, in the next chapter, we will alter the mixing method by using a micro-extruder, while still processing and drawing the as-mixed blends using the optimal parameters identified in this chapter including PTFE content, drawing temperature and so on.

Chapter 3

Ultrafine PTFE fibres from PTFE/PVA tapes prepared by extrusion compounding

3.1 Introduction and objective

In the previous chapter, we have shown that simple magnetic stirring and casting was not capable to create blends with well-dispersed PTFE particles in PVA solution. In this chapter, we will try to improve the dispersion of PTFE particles in the PVA/water system by using a more efficient mixing method, being extrusion compounding. In order to study the entire process of fabrication systematically, including the variation of many parameters, these trials were performed in a small-scale mini-extruder. The properties and morphologies of these blends, the fibre formation upon drawing of these blends as well as their phase behaviour before and after drawing were studied. In addition to this, the drawing behaviour of the blends, tensile properties, and method of matrix extraction and final nanofibres identification was studied and discussed.

3.2Experimental

3.2.1 Materials

All materials including, grades of poly(vinyl alcohol) (PVA) and poly(tetrafluoroethylene) (PTFE) were the same as in Chapter 2.

3.2.2Processing and characterization

3.2.2.1 PTFE/PVA blends preparation by extrusion

PVA powder and water were pre-mixed as a suspension and was fed into a mini-extruder machine (DSM X'plore 15) (see photograph below) while stirring with PVA concentrations of 10wt.%, 15wt.%, 20wt.%, 25wt.%, 30wt.%, 35wt.% and 40 wt.% respectively.

Photograph 3.1: DSM X'plore mini-extruder with recirculation system.

These experiments should reveal the minimum water content necessary for processing. Through this set of experiments, we confirmed that the system with 25wt.% PVA could still be processed and this was therefore selected for further extrusion trials.

PVA powder and PTFE suspension were pre-mixed in a beaker at a weight ratioofPTFE:PVA= 1:9, 2:8, 3:7, 4:6, 5:5 (PTFE content in PTFE/PVA were respectively 5.7vol.%, 12vol.%, 19vol.%, 26vol.% and 35vol.%). Then extra water was added to make sure the concentration of PVA in water is around 25wt.%.

Processing parameters were also investigated. Temperatures were set at 70^{o}C, 80^{o}C and 90^{o}C, while extrusion speeds evaluated were 50rpm, 100rpm and 150rpm, combined with residence times of 5min, 10min and 15min. Cross matching of these 3 sets of parameters results in 27 sets of process parameters. Because water is easy to evaporate at such high temperatures close to its boiling temperature, optimal parameters were directly observed from the processing situation due to system sensitivity and a narrow processing window.

After the initial experiments, we selected as optimal processing parameters for temperature as 80^{o}C, 85^{o}C and 90^{o}C for the extrusion zones (top to bottom) of the mini-extruder, an extrusion speed of 50rpm and a residence time of 5min. All the following sets of experiments would use these parameters, and compositions were similar as mentioned above.

3.2.2.2 Compression moulding

(a) Hot pressing of PVA

Aluminum foil with a thickness of 1mmwas used to make a simple mould for hot-pressing the PVA and PTFE/PVA blends into films. In order to make the neat PVA films, a little water was added to the PVA powder until the powder had fully absorbed the water. The temperature of the hot press (Dr.Collin P300E) was set as 90^{o}C. The pressure was held for 10min, and released a few times, then final compaction for 3min, followed by cooling down with the pressure held at around 50MPa. Pressure was released when the temperature was around room temperature. Films were removed from the mould and placed into an oven at 80^{o}C for 2 hrs until the remaining water in the PVA had fully evaporated.

(b) Hot pressing of extrusion compounded PTFE/PVA blend

PTFE/PVA blend strands were dried in an oven at 70 ^{o}C for 2 hrs to completely remove the water. After drying, the strands were cut into a short pellets with a length of 50 mm.

Samples were hot-pressed at temperatures of 100^{o}C, 110^{o}C, 120^{o}C, 130^{o}C, 140^{o}C and 150^{o}C. From this, 140^{o}C was confirmed to be the optimal temperature for compression moulding of the PTFE/PVA blend. This temperature would therefore be applied throughout all further compression moulding experiments. Rectangular specimens of 10mm x 50mm were cut from these hot-pressed films for further drawing experiments.

3.2.2.3 Drawing

The rectangular film specimens were marked at every 5mm with a marking pen. Specimenswere placed on a hot plate with a temperature of 100^{o}C and then were drawn by hand using pliers with rubber inserts. Samples were physically pushed onto the hot plate while drawing. Drawing was stopped when it became too difficult to further draw by hand. The specimens were kept under tension until they were cooled down to room temperature. By measuring, the distance between the marked lines the draw ratio could be determined. Meanwhile, some specimens with varying PTFE content were drawn to a fixed draw ratio of λ=4 along with a ruler placed on the hot stage parallel with the drawing direction of the sample to measure the extension.

3.2.2.4 Tensile testing

After removal of both clamping ends from the tapes, the remaining drawn middle section of the tapes was used for tensile testing. These drawn sections were weighted using a microbalance. Using the length of the tape, we can now calculate the cross sectional area of the drawn tape using Equation 2.1 (see Chapter 2). A universal tensile tester (Instron 5566) equipped with a 1kN load cell was used to test the tensile properties of the tapes at a test speed of 5 mm/min. Approximately 5 specimens of each sets of samples were tested.

3.2.2.5 DSC

The melting temperature (T_m) was measured using Differential Scanning Calorimetry (DSC) (Mettler-Toledo 822e) and involved a temperature scan from room temperature to 400°C at a rate of 5°C/min, then holding for 30min, followed by cooling to -50°C at 5°C/min. This

procedure was repeated again to have two heating curve, which could also confirm the decomposition of PVA. However, because of the degradation of PVA, only the first heating scan was used for analysis.

3.2.2.6 SEM

Procedures for SEM was the same as described in the previous chapter. For analysing the PTFE particles, one drop of PTFE suspension was diluted into a glass bottle with about 50ml water, and stirred with a magnetic stirrer for about 10min to make sure that all PTFE particles had been uniformly dispersed in the water. A drop of this diluted PTFE suspension was then placed onto an aluminium foil and dried. Again, this powder was coated with gold and observed with SEM to measure the size of the particles.

3.2.2.7 Matrix extraction

Here a drawn PTFE/PVA blend tape was placed into a bottle of water with a magnetic stirring bar, and heated to 80^{o}C using an oil bath on a hot magnetic stirring plate for 5hrs. A vacuum filter system was used to extract the PTFE nanofibres from the suspension with 0.1µm pore size filter paper (MF-Millipore Membrane Filter, VCWP09025, mixed cellulose esters, Hydrophilic, 0.1um, 90mm). The paper with PTFE fibres was rinsed a few times with water after finishing the filtration to remove possible remaining PVA on the PTFE nanofibres or filter paper. Next, the filter paper with the PTFE fibres was dried at room temperature overnight to remove the remaining water.

3.2.2.8 SEM, EDS and FTIR of PTFE fibres

For this a piece of filter paper with PTFE nanofibres on top was cut from the whole filter and coated with gold for SEM investigations (FEI Inspect-F, High vacuum FEG source scanning electron microscope). Clean filter paper was observed as well for comparison. Energy Dispersive Spectroscopy (EDS) was used together with SEM to identify the individual PTFE fibres. Meanwhile, another piece of the filter paper with PTFE nanofibres was cut for FTIR tests. Clean filter paper, pure PVA tape and pure PTFE was again analysed by FTIR as a reference. Fourier transform infrared (FTIR) spectra of various samples were measured using a Bruker Tensor 27 spectrometer. Attenuated total reflectance (ATR) mode was used for the IR measurements. The spectra were obtained by collecting 64 scans at a $4cm^{-1}$ resolution from $500cm^{-1}$ to $4000cm^{-1}$. OPUS software was used for data collection and analysis such as peak picking.

3.3Results and discussions

3.3.1 Dispersion morphology of PTFE/PVA blends by SEM

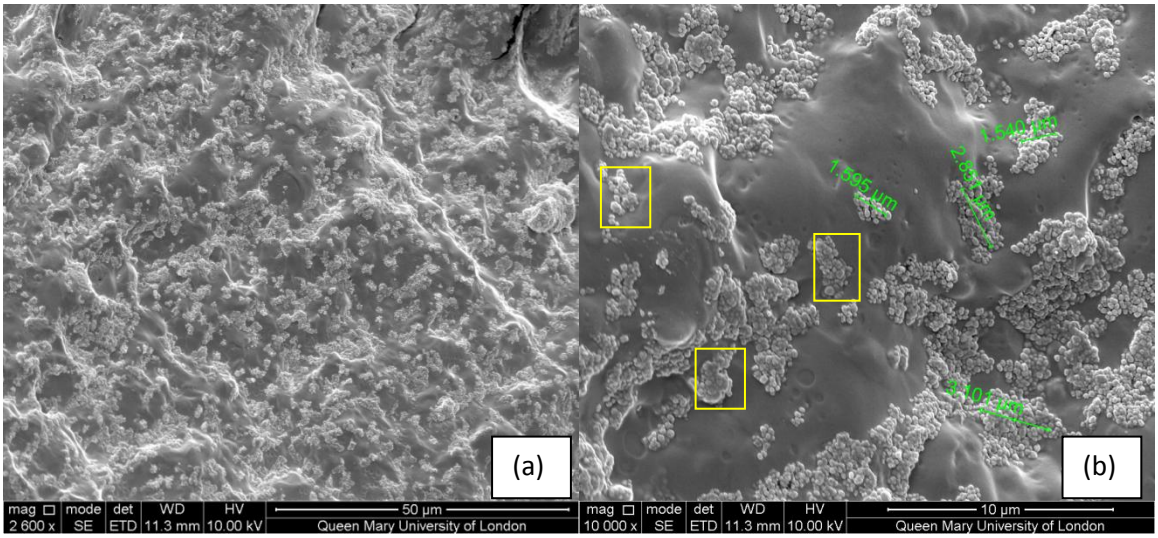

Figure 3.1: SEM images of cold fracture surfaces of compression moulded film (PTFE 19vol.%): (a) mag 2600x; (b) mag 10 000x.

Comparing the dispersion of PTFE particles in the blend with that of cast PTFE/PVA blends in Figure 2.9, we can see that the dispersion situation is significantly improved and that the dispersion is much more homogeneous at low magnification (2600x) (Figure 3.1a) while the number of PTFE particles in the agglomerates is also decreases (Figure 3.1b). Some of the agglomerates are marked in Figure 3.1b as examples. This shows that the dispersion situation of the PTFE in the blend has been improved with the extrusion compounding method, although the agglomeration problem still exists.

3.3.2 Phase behaviour of PTFE/PVA blends by DSC

SEM investigation identified a relatively homogeneous dispersion of PTFE particles in PVA matrix. However, in order to distinguish if these two phases are fully phase separated, with the dispersive phase being neat PTFE and the matrix phase being neat PVA, the phase behaviour of the PTFE/PVA blend was studied with DSC. Figure 3.2 shows the melting temperatures of PVA and PTFE as a function of PTFE content for the extruded and hot-pressed films. For all composition, two melting peaks are clearly observed. A phase diagram for the PTFE/PVA system can be constructed from these melting temperatures as shown in Figure 3.2. In Figure 3.2, there are two melting temperatures present for PTFE and PVA for all blends. Meanwhile, we can also see that the melting temperatures of each material remain the same with increasing PTFE content, suggesting that the composition does not affect the melting temperatures of each individual component. Since the melting temperatures of each component are not affected by blend composition, the crystal structures of PVA and PTFE are unaffected by each other. Therefore, it can be concluded that the PVA and PTFE phases are fully separated, meaning that the dispersive phase (i.e. the islands) consists of pure PTFE.

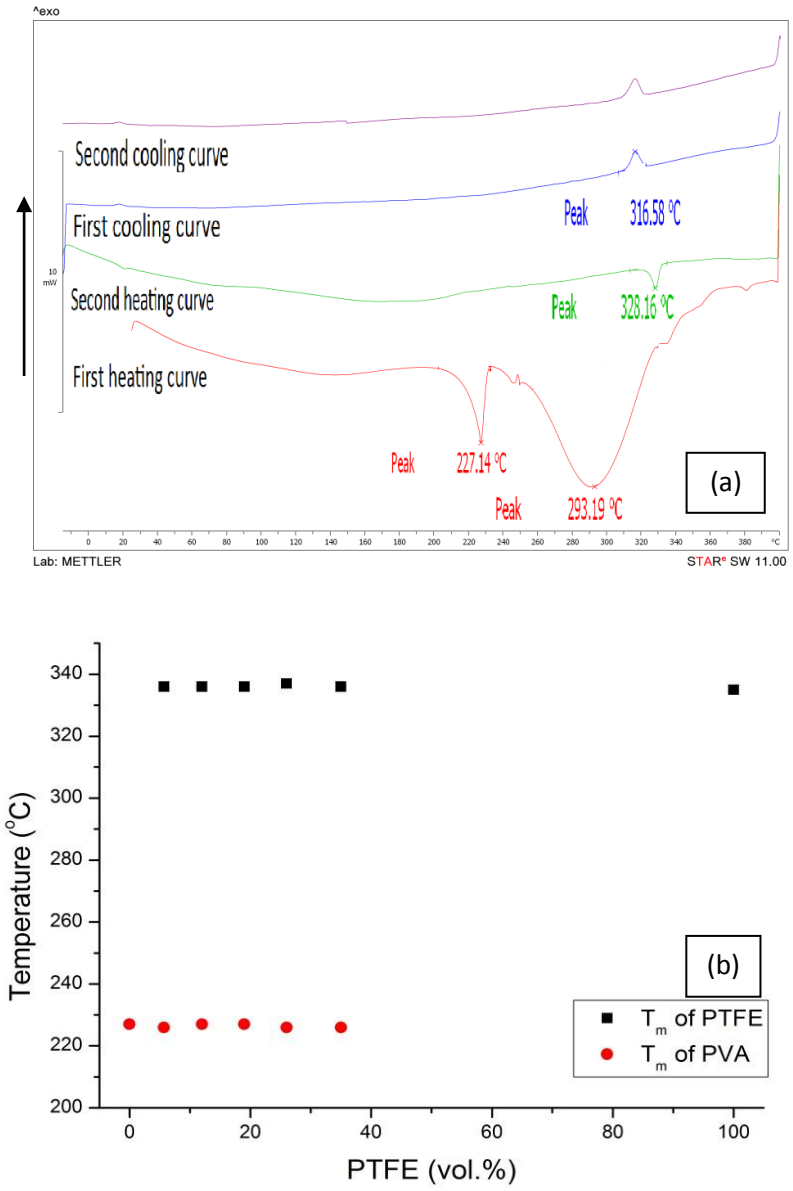

Figure 3.2:(a) DSC curve of blend sample with 19 vol.% PTFE as an example to show thermal behaviour; (b)Phase diagram of extruded and hot-pressed PTFE/PVA films, melting temperature of PTFE and PVA as function of content of PTFE, indicating an immiscible blend.

3.3.3 Drawing behaviour of PTFE/PVA blends

Drawing of the hot-pressed PTFE/PVA films was performed by hand on a hotplate in the solid-state at 100 °C in the air well below the melting temperature of PVA and PTFE.

Since PVA is the continuous phase and PTFE the dispersed phase in these blends, the drawability of the PTFE/PVA blends is clearly more related to the drawability of the PVA, although the state of dispersion of the PTFE particles is expected to affect the drawability of these blends. Figure 3.3 shows that the average maximumdraw ratio of the blends remains relatively the same, while it slightly decreases at high PTFE contents. Above 20vol.% PTFE, the drawability significantly drops. Compared with the drawing behaviour of cast PTFE/PVA blend tapes as shown in Figure 2.22, we can see that the reduction in average maximum draw ratio is much smaller for the extrusion compounded system than for the casting system. This again suggests that the dispersion of PTFE particles in the extrusion compounded system is better than for the solution cast system due to the much higher shear forces involved.

Furthermore, the fact that the blends systems can also be drawn to a similar draw ratio is not all that straightforward since weak interfacial interactions between PTFE and PVA may lead to the debonding of the PTFE particle during the stretching, potentially creating stress concentrations and early fracture. However, because of the small PTFE particle size (~200nm) and the homogeneous dispersion, such stress concentrations are expected to be low, leading to a stable drawing process without premature failure.

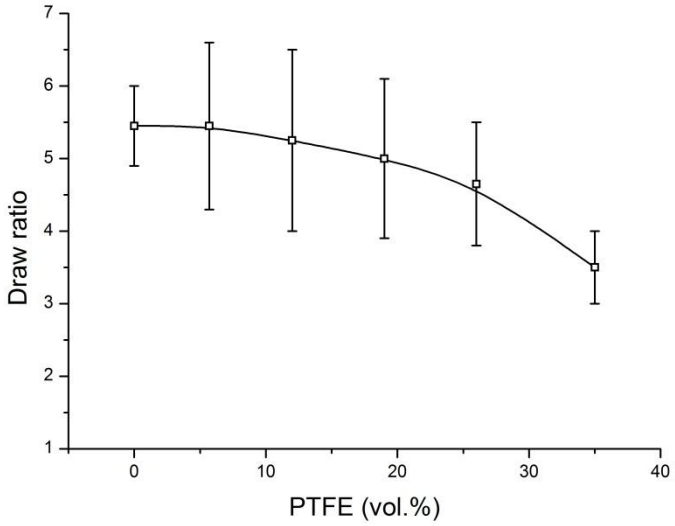

Figure 3.3: Maximum draw ratios of PTFE/PVA blends as a function of PTFE content.

3.3.4 Fibre formation after drawing

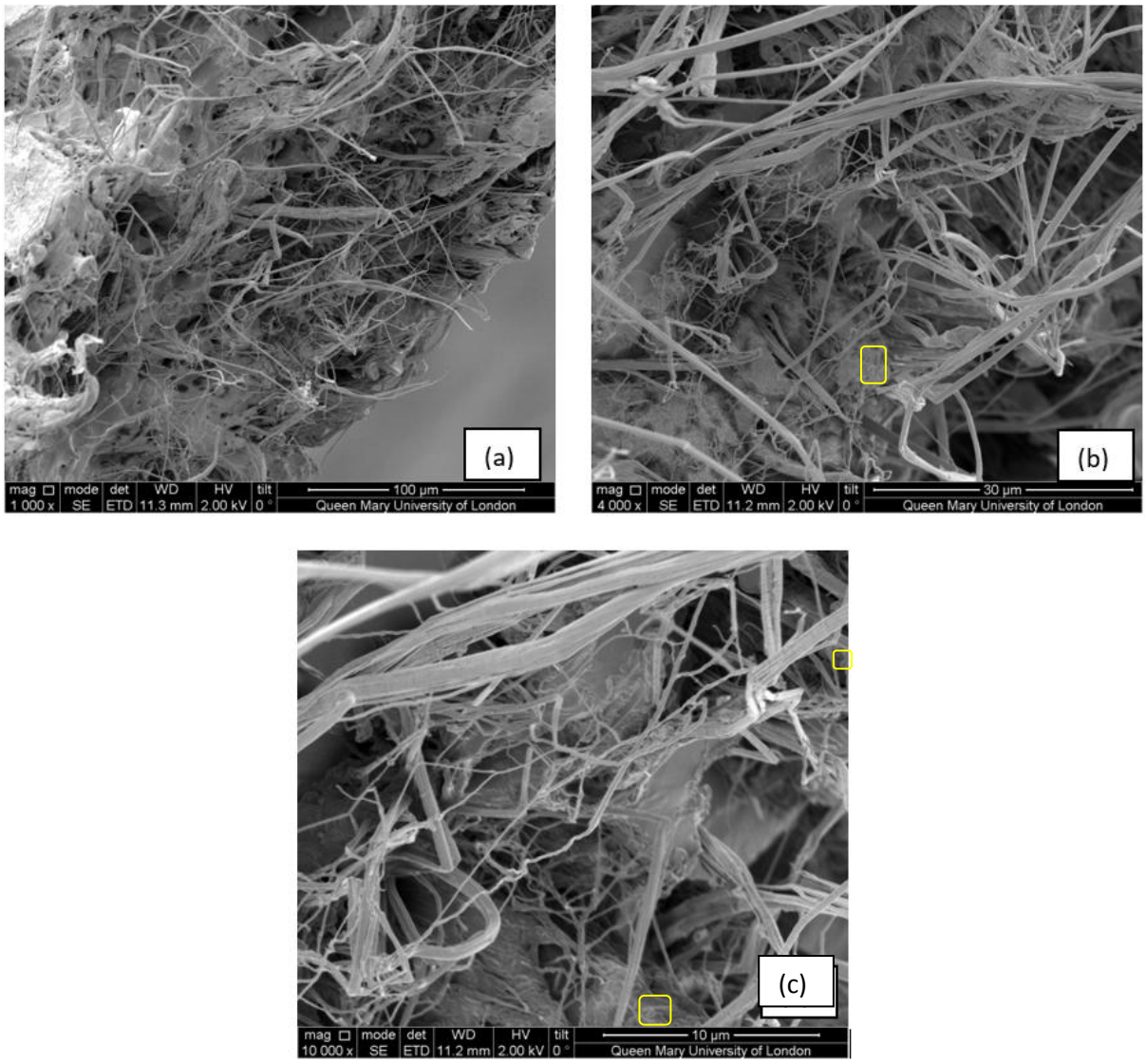

Figure 3.4: SEM images of drawn PTFE/PVA blend tape (a) mag 1000x; (b) mag 4000x and (c) mag 10000x.

Meanwhile, in the SEM pictures in Figure 3.4 of drawn PTFE/PVA blends, we can observe a much stronger fibrillar structure with very few undrawn PTFE particles remaining (The area of undrawn particles is circled in Figure 3.4, although only very few of these areas were present). This is because, when dispersion of PTFE is improved, the size of the agglomerates

decreases. Instead of being unattached to PVA, more PTFE single particles are attached to PVA and can be drawn. On the other hand, when the size of the PTFE agglomerates decreases, the stress distribution in the blend is more uniform with less stress concentrations from large PTFE agglomerates in the blends as in the case of solution casting. Therefore, along with improved dispersion of PTFE particles in the blend, the number of undrawn PTFE particles significantly decreases. In solution cast samples, on the other hand, many PTFE particles remained undrawn. Furthermore, we can also see many long fibres, many of which could reach tens of micrometres. We will discuss the length and diameter of the fibres at a later stage. However, we could not confirm the exact composition of these fibres at this point and we have to assume them as a combination of PTFE and PVA. Further confirmation on the composition will be made later through DSC, EDS and FTIR Experiments.

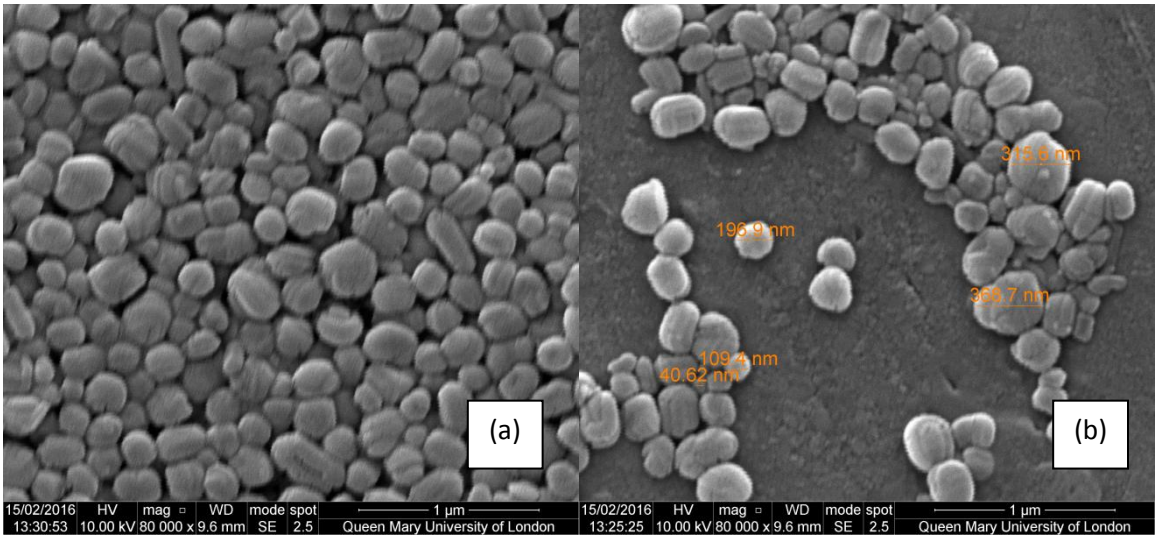

Figure 3.5: SEM images of PTFE particles and their sizes.

From the SEM images of pure PTFE particles (Figure 3.5), we can see that the diameters of the PTFE particles are between 200-300nm, which is rather uniform and matches the data of the DuPont datasheet. However, in the right picture, we can see that there are also many

small particles of PTFE. Some of these particles are even smaller than 50nm, and the amount of smaller particles seems to be around 10%. This is an important factor, which affects the diameter distribution of the PTFE nanofibres after drawing.

Figure 3.6 shows that some fibres are in fact nanofibre bundles that consist of individual PTFE nanofibres rather than single microfibres (Figure 3.6a), while also ultrafine single nanofibres with diameters of around 50nm and lengths up to 5µm are present (see Figure 3.6b).

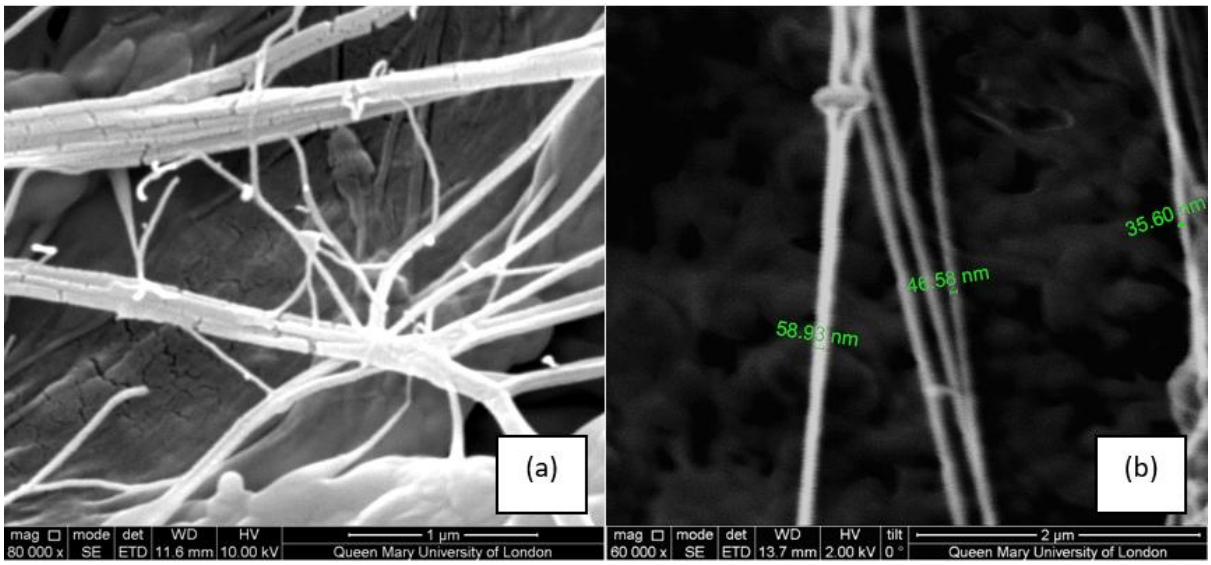

Figure 3.6: SEM images of (a) PTFE nanofibre bundles, and (b) individual PTFE nanofibre present in drawn PTFE/PVA tape (19 vol.% PTFE).

By giving the PTFE particle an average diameter range and assuming that the volume of PTFE does not change during the solid-state drawing process, we can estimate the diameter of PTFE fibres after stretching using;

$$\frac{4}{3}\pi {r_0}^3 = \pi {r_d}^2 \cdot l,$$

$$\text{with} \quad l = 2r_0 \cdot \lambda \quad \text{giving} \quad r_d = \sqrt{\frac{2}{3\lambda}} \cdot r_0 \qquad \text{Equation 3.1}$$

Where, r_0 is the radius of the PTFE particle before drawing, l is the fibre length, λ is draw ratio, r_d is the radius of the fibre after drawing. Assuming an average particle diameter of 210nm (r_0=105nm) and a draw ratio of five (λ=5), we can estimate the radius of the final PTFE nanofibres when drawn from single PTFE particle at 38nm (which means a fibre diameter of 76nm) and a length at around 1µm. This predicted fibre diameter is of the same order as those observed in Figure 3.6b (35-60nm). Deviation might be down to statistical variability in initial particle size, which according to the manufacturer and our SEM observation, can be as low as 50nm. Conversely, some particles are expected to be as large as 500nm or even form aggregates, which can lead to significantly larger fibres or bundle diameters as well. Based on particle size variability from 50 to 500nm we may expect fibre diameters ranging from 20nm to 350nm and lengths up to 2.5µm. Also, the length of PTFE fibres drawn from agglomerations of PTFE particles would be longer than expected, and the length would be even longer when the particles aggregate in line with the drawing direction. In Figure 3.4 we could see that there are some fibres with lengths up to tens of micrometres. This is even more clearly shown in Figure 3.7(and later in Figure 3.11) where we can see single fibres with lengths of up to 10µm. The relation between final fibre length and particle aggregation is schematically depicted in Figure 3.8.

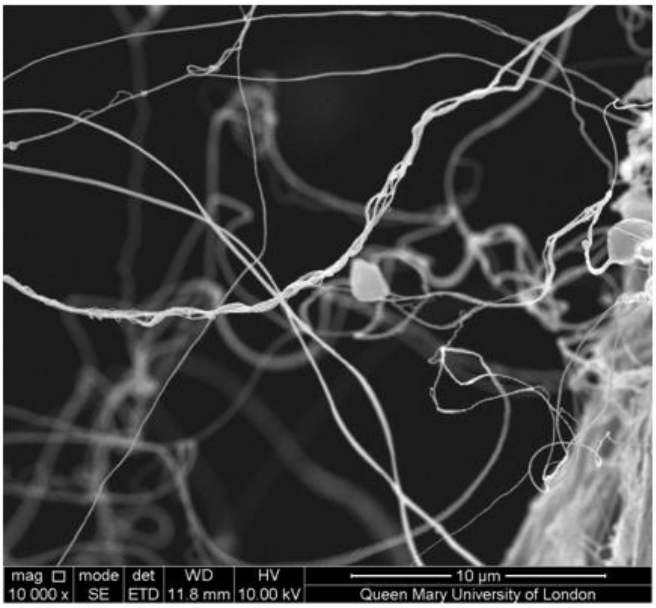

Figure 3.7: SEM image of PTFE fibres.

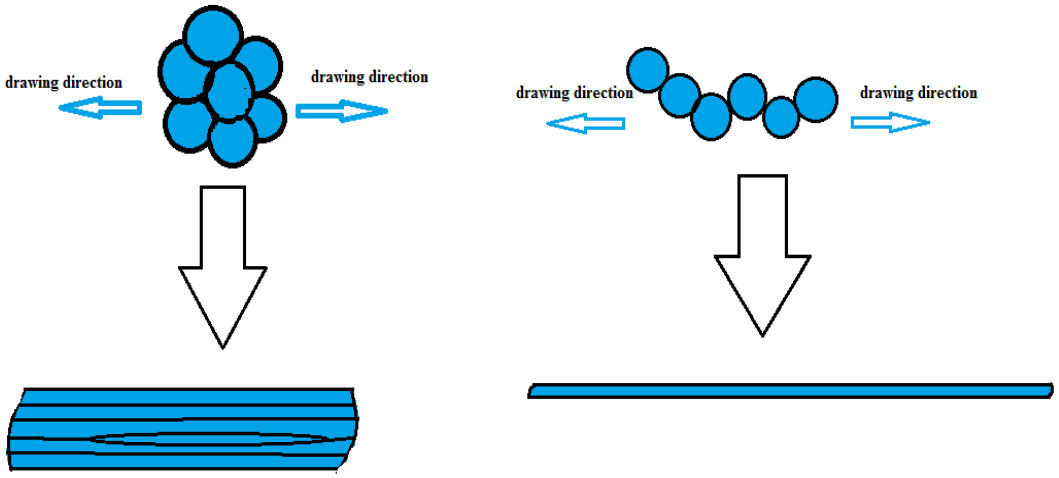

Figure 3.8: Schematic picture of the drawing of PTFE agglomerates.

Most research on PTFE micro- or nanofibres does not mention diameters of individual fibres, as nearly all of these products are (fused) fibre mats rather than individual fibres. In the

work by Sawai and Watanabe [90] on the drawing of fibres from PTFE nascent powders by solid-state co-extrusion, the finest fibre diameter is about 300μm. In the case of PTFE fibres made directly from emulsions, average diameters are as large as 0.35mm. Clearly the single PTFE nanofibers made in the current study are among the finest individual PTFE fibres made so far. Although some other methods like jet-blowing can also produce nanoscale PTFE, the fibrous materials obtained from this method are actually in the form of mats rather than individual fibre [31].

3.3.5 Phase behaviour of PTFE/PVA blends after drawing

Figure 3.9 shows the melting points of PVA and PTFE as a function of PTFE content for drawn PTFE/PVA blend tapes with draw ratio of λ=4. Two clear melting peaks are observed for all compositions, indicating a two-phase system of PTFE and PVA, meaning that the dispersed phase (viz. the fibres) before and after drawing consist of pure PTFE. This has some additional technological advantages since the blending process should not affect matrix removal as this phase consists of pure water soluble PVA. Furthermore, comparing with Figure 3.2, we can see that all melting temperatures have increased a little, because both PVA and PTFE are orientated after drawing. Therefore, Figure 3.9 also indicates towards a fibrillar structure of PTFE/PVA blends after stretching.

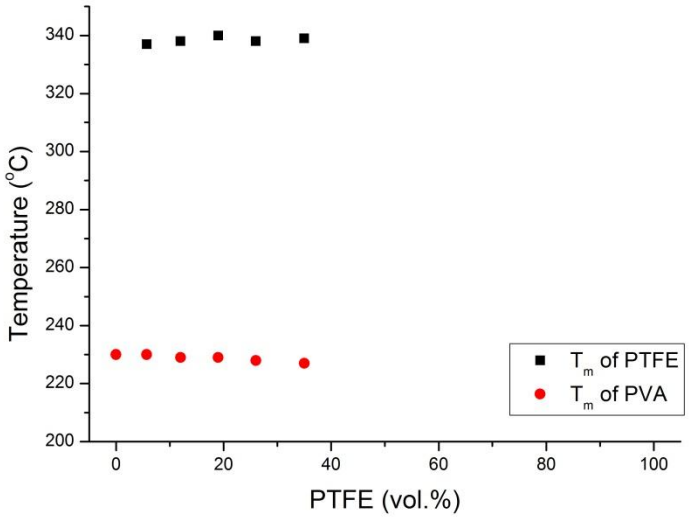

Figure 3.9: Phase diagram of extruded and hot-pressed PTFE/PVA films after solid-state drawing.

3.3.6 Tensile properties of PTFE/PVA blends after drawing

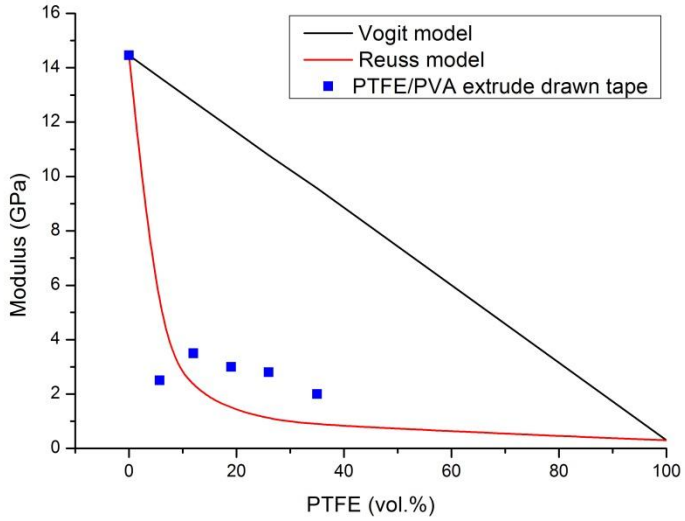

Figure 3.10: Young's modulus of extrusion compounded PTFE/PVA blend tapes with λ = 4 as a function of PTFE content (before removal of PVA) together with theoretical predictions using upper-bound parallel (Voigt) model and lower-bound series (Reuss) model.

Figure 3.10 shows the Young's modulus of the drawn extruded PTFE/PVA tapes with a draw ratio λ = 4together with predictions using the parallel (Voigt) and series (Reuss) model. Similar to the data for casted samples in Figure 2.26, the values of Young's modulus of extruded samples are very close to the properties predicted by the Reuss model, but a little higher than for the cast ones, suggesting that the dispersion morphology is slightly improved. Similar to solution cast samples, the weak adhesion and poor stress transfer between PVA and PTFE are also reasons for this low modulus. For example, the Young's modulus of 5.7 vol.% PTFE is lower than the Reuss model, which is an indication of debonding and the formation of voids during drawing.

3.3.7 Extraction of PTFE nanofibres from drawn blends

As a final processing step, we extracted the PTFE fibres in hot water (80°C) from the blend while magnetic stirring for up to 12 hrs and then filtering. Due to its highly hydrophilic nature, the PVA phase readily dissolved in hot water, leaving behind the PTFE fibres on the filter paper after removal of the PVA/water mixture. Figure 3.11 shows a fibre bundle (Figure 3.11a) together with single PTFE nanofibres (Figure 3.11b). Since the size of the fibre in Figure 3.11a (~1µm) is beyond what is expected for the largest single fibres as predicted by Equation 3.1 (350nm) it is believed that this represents a bundle originating from agglomerated PTFE particles. We could also observe this directly from Figure 3.11a which shows a combination of many tiny fibres. Meanwhile, in Figure 3.11b we can see some thin fibres, one of which has a length up to 10µm, possibly originating from an agglomerate of particles. In the case of agglomeration, the PTFE fibres can have diameters that are similar to single nanofibres but with length of up to 15µm or longer.

All fibres maintained their fibrous structure after removal of the PVA. Although we may expect that the remaining fibres on the filter paper are PTFE nanofibres based on their fibre dimensions and their phase behaviour, we cannot actually identify their composition from the SEM pictures. Therefore, EDS and FTIR were used in an attempt to confirm the composition of these fibres. The former one (EDS) is used to detect the elementary composition of the fibres, while the latter one (FTIR) is used to eliminate the possibility of PVA fibres by comparing its spectrum with filter paper, PVA and PTFE.

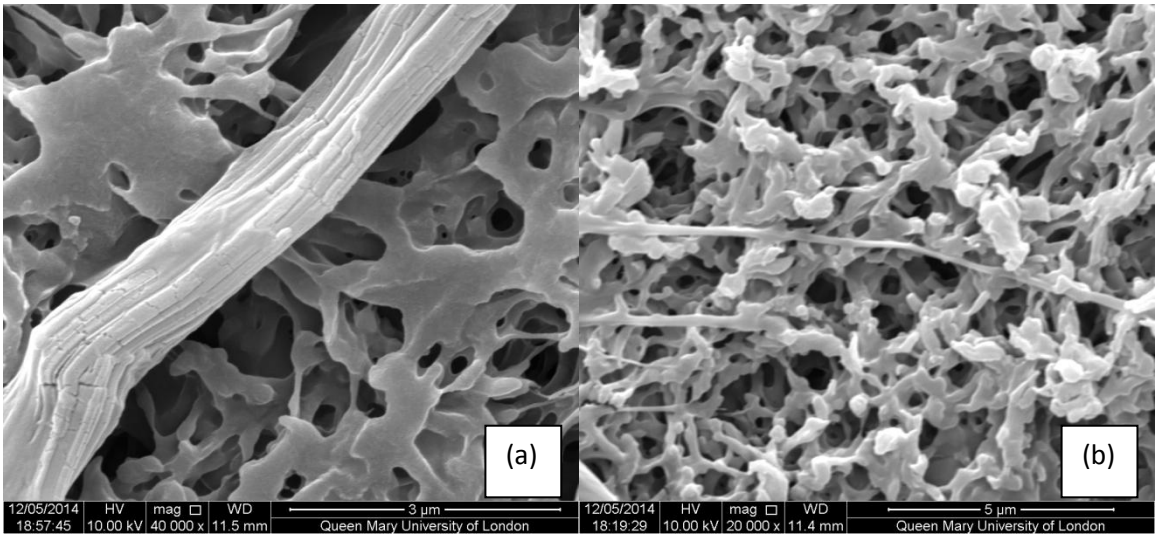

Figure 3.11: SEM images of PTFE nanofibres on cellulose filter paper after of removal of PVA: (a) fibre bundle and (b) single nanofibre.

3.3.8 EDS and FTIR analysis

In order to attempt to identify the composition of these fibres, Energy Dispersive X-ray Spectroscopy (EDS) was applied to the SEM image of Figure 3.12a. The EDS spectrum shown in Figure 3.12 shows a very dramatic F peak, clearly indicating the presence of PTFE. Because of the immiscible properties of PTFE and PVA as proven by the previous DSC tests, the single fibre cannot be a blend fibre of PTFE/PVA; instead, it can only be either a pure PTFE or PVA fibre. With the evidence of the presence of F, we may conclude that those remaining fibres are PTFE nanofibres. Although the atomic ratio of F:C in pure PTFE should be 2:1, the relatively high atomic ratio of C as seen in our experiments is presumably due to the presence of cellulose (filter paper) in the analysed area for EDS. However, although we know that the fibres are not PVA fibres or PTFE/PVA blend fibres, there is still the possibility that dissolved PVA has remained as a coating on the PTFE fibres after the step of removing the matrix. Therefore, FTIR is used to further study this possibility.

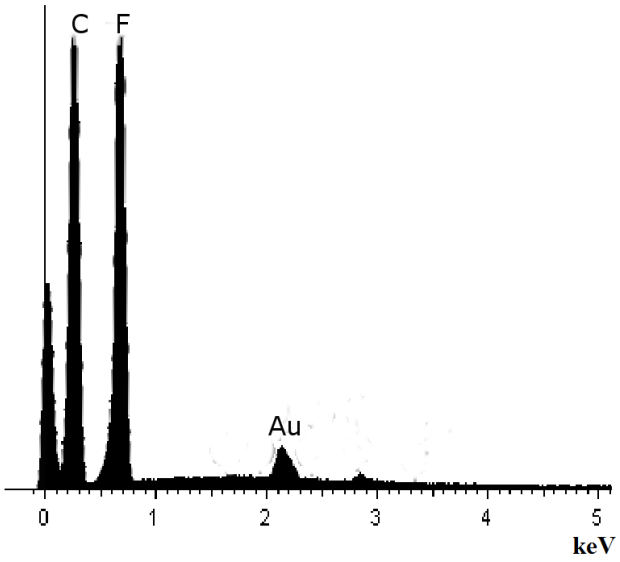

Figure 3.12: EDS spectrum of fibres on filter paper after removal of PVA.

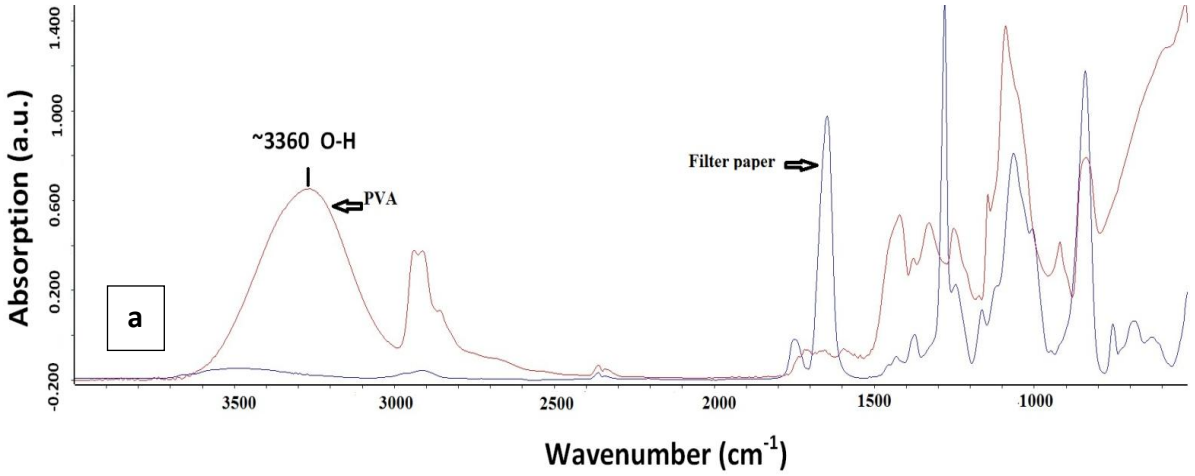

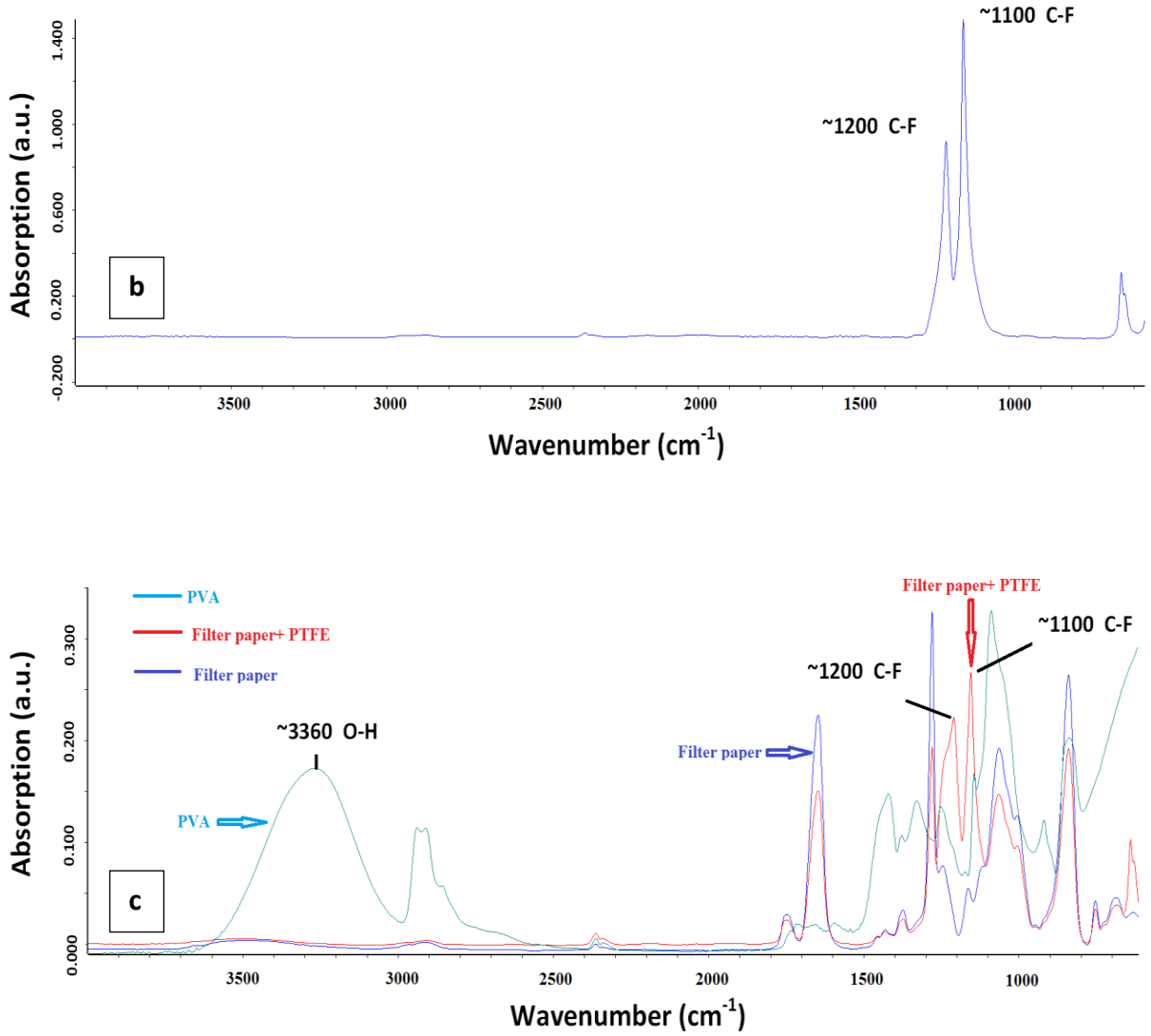

Figure 3.13: FTIR spectra of (a) filter paper and PVA, (b) PTFE, (c) filter paper, PVA and filter paper + PTFE.

In addition to the EDS study, FTIR was performed on fibres deposited on the filter paper Figure 3.13). This filter paper is essentially cellulose, which has hydroxyl groups in its molecular structure, so theoretically there should be a peak at around 3360cm^{-1} representing these hydroxyl groups in cellulose. However, because filter paper is often treated with various coatings, Figure 3.13a shows barely a peak related to the hydroxyl groups at around 3360cm^{-1}, which is assigned to O-H stretching. Comparing the spectra of

filter paper and PVA reveals that the most distinguishable peak of PVA is the O-H peak at around 3360cm^{-1}, which confirms the presence of PVA in the spectra. From this comparison we can see that although filter paper (mostly cellulose) and PVA have both characteristic peaks at 3360cm^{-1}, the intensity of each peak is quite different. Therefore, we could still use this peak to identify the presence of PVA and not confuse it with that of cellulose.

Figure 3.13b shows characteristic peaks of PTFE at 1100cm^{-1} and 1200cm^{-1} as C-F stretching. Clearly, the peaks at these two positions can be used as the characteristic peaks to identify PTFE.

Figure 3.13c shows the spectrum of filter paper + PTFE nanofibres. Comparing this spectrum with the spectra of PVA and filter paper shows the absence of PVA and the presence of the characteristic peaks of PTFE. From this and the EDS data, we can therefore, conclude that the fibres present on the filter paper are indeed pure PTFE nanofibres. Because PVA is high soluble and not compatible with PTFE, it could be fully removed by dissolving and washing.

3.4 Conclusions

From these studies, we could conclude that compared to the processing method based on solution/suspension casting, the dispersion morphology of PTFE particles in PVA is greatly improved after extrusion compounding. The quantity of undrawn PTFE particles after solid-state drawing of the tapes is significantly decreased with this processing method, while the drawing behaviour of the PTFE/PVA blend is also improved. Meanwhile, we could confirm that the PTFE nanofibres produced in this island-in-the-sea method could achieve diameters of 50nm or lower, while lengths can be as high as 10µm due to specific agglomeration of

PTFE particles. Furthermore, through the results of SEM, EDS and FTIR tests and analysis, we could confirm that the nanofibres produced with this method are indeed PTFE nanofibres after dissolution and filtration. However, even with this processing method, we could still not obtain a fully satisfying blend morphology for further fibres formation, while the mechanical properties of the PTFE/PVA blends were also somewhat disappointing although better that that of solution cast blends. Moreover, the process was not stable since a phenomenon of powder compression exists during compounding. In the next chapter, we will further improve the extrusion compounding method with the aim to achieve a better dispersion of PTFE particles in PVA, leading to improved fibre formation and mechanical properties, while at the same time trying to spin the PTFE/PVA blends directly into fibres as a first step towards further industrial scale up.

Chapter 4

Ultrafine PTFE fibres from PTFE/PVA tapes processed by a two-step extrusion compounding process

4.1 Introduction and objective

In the previous chapter, it was shown that extrusion compounding improved the dispersion of PTFE particles in the PVA solution compared to solution cast system, leading to better PTFE fibre formation during subsequent drawing. However, compounding was not always stable and efficient due to a phenomenon called powder compaction, leading to blockage of the extruder.

Powder compression or compaction during extrusion is a phenomenon that occurs during materials processing involving nano- or micro-particles. The phenomenon has been extensively studied in powder technology. General speaking, during powder compression [71-73], densification of the powder happens, including particle rearrangement and plastic deformation. During extrusion compounding, the screws induce a compressive force onto the particles. When the viscosity of the two materials differs greatly as for example in the case of liquid and solid materials, phase separation may occur. Once this happens, the pressure provided by the extruder will start to compact the powder. When this occurs, the

system reaches a state where its dispersion capacity is exhausted because particles are constrained and locked in a fixed position by neighbouring particles [75, 81]. When rearrangement or so-called fragmentation occurs, phase separation becomes even more significant and the pressure in the extrusion chamber increases rapidly. This further increase in pressure can lead either to deformation or to fracture of the particles [74, 76, 77, 78, 79, 80, 82, 84-86]. If the particles are plastic or elastic, they will deform to accommodate the applied force, while alternatively they will break into smaller fragments. During this transitional phase, bonding occurs between contact surfaces of powder particles through an increase in contact surface area between deforming particles, or by an increase in the number of bonding sites in the case of fragmented particles. [83, 87-89] Consequently, powder compression needs to be considered in the case of extrusion of high loadings of particles. The phenomenon can affect product quality, cause an increasing of extrusion chamber pressure, or can even block the chamber and halt the extrusion process.

In this chapter, we aim to improve the stability of the compounding process in order to achieve better fibre formation with a higher efficiency and properties of the blend. Properties, for instance, fibre formation, mechanical properties, molecular orientation, and surface property etc., will be studied and discussed. Furthermore, a first step towards direct spinning of PTFE/PVA blend fibres will be investigated in this chapter as well.

4.2Experimental

4.2.1 Materials

All materials including, grades of poly(vinyl alcohol) (PVA) and poly(tetrafluoroethylene) (PTFE) were the same as described in Chapter 2.

4.2.2Processing and characterization

4.2.2.1 PTFE/PVA blend preparation

PVA powder and PTFE suspension was mixed in beaker at a weight ratio ofPTFE:PVA= 1:9, 2:8, 3:7, 4:6, 5:5 (contents of PTFE in PTFE/PVA are respectively 5.7 vol.%, 12vol.%, 19vol.%, 26vol.% and 35vol.%), with extra water added to make sure the concentration of PVA in water is 25wt.%. Because the PVA has not been completely dissolved in water at this stage, the backpressure created by the spinning die of the mini-extruder causes phase separation of water and PVA powder due to the difference in viscosity, which is also called powder compression. Powder compression creates a situation in which a more solid phase remains near the front of the screw with most of the liquid phase remaining near the back of the screw. This phenomenon will lead to non-uniform mixing, and may even lead to blockage, which dramatically affects the processing efficiency and continuous spinning operations.

Therefore, a two-stage extrusion compounding process was devised, in which in a first mixing step the extruder is fed with the blend mentioned above and processed at temperatures of 80^{o}C, 85^{o}C and 90^{o}C, respectively, at extruder speeds of 10rpm with no recirculation. The extruded blend filament was subsequently pelletized. This pelletized PTFE/PVA blend was then fed again into the mini-extruder at a temperature of 80^{o}C, a

speed of 100rpm, and a circulation or residence time of 5min. Speed was lowered to around 50rpm near the end of compounding. Next, the obtained filament was dried in an oven at about 80^{o}C for 2hrs using thick aluminium foil to ensure the filament stayed straight after drying.

The compression moulding process to make films from this compound is the same as described in Chapter 3. Rectangular samples were cut from these films with the dimensions of 10mm x 50mm for subsequent solid-state drawing.

Drawing procedure, tensile testing, SEM were all the same as described in Chapter 3.

4.2.2.2 XRD

X-ray diffraction was performed using a KAPPA APEX ii DUO diffractometer with a Mo and Cu source at −50kV/40mA (λ=0.154 nm). X-ray scattering patterns were recorded by an APEX ii CCD area detector. Two-dimensional X-ray patterns were transformed into one-dimensional patterns by performing integration of the azimuthal intensity and calibrated with Al_2O_3. The full-width at half-maximum (FWHM) of the obtained intensity distribution pattern was calculated as a normalised measure for the arc length of the reflection. Software Gimp2 was used to convert WAXS 2D images into readable data and Fit2D was used to analysis the WAXS 2D image.

4.2.2.3 PTFE/PVA fibre spinning

Following the same procedure as described in 4.2.2.1, instead of compression moulding the compound into film here we tried to directly spin the blend fibres from the mini-extruder

into as-spun PTFE/PVA fibres. For this, PVA powder and PTFE suspension was pre-mixed in a beaker at a weight ratio of 7:3 (PTFE 19vol.%), adding some extra water to obtain a PVA concentration of 25wt.%. This blend was fed into the mini-extruder with a temperature setting of 80^{o}C, 85^{o}C and 90^{o}C and a speed of 10rpm without re-circulation. The obtained blend filament was pelletized and fed into the mini-extruder again, at a temperature of 80^{o}C, 100rpm, and a circulation time of 5min.

For the direct spinning of the blend fibres from the mini-extruder, we chose a die with a diameter of 1mm. For spinning, the speed was lowered to 10rpm. The blend fibres were subjected to a draw-down of about 4 to obtain a fibre with a diameter of around 0.7mm. Drying of the fibres in an oven at 80^{o}C for 3 hrs completely removed the water from the blend fibres, and the diameter of the fibres decreased to about 0.6mm. These as-extruded fibres were subsequently hot-drawn by hand on a hot plate at 100°C, in the solid-state well below the melting temperature of both PVA and PTFE. At this temperature, the blend fibres could smoothly extend to a draw ratio of 5. The final diameter of these solid-state drawn blend fibres was around 0.3mm.

Subsequent drawing steps, SEM, and XRD test were the same as before.

4.3Results and discussion

4.3.1Dispersion morphology of PTFE/PVA blends by SEM

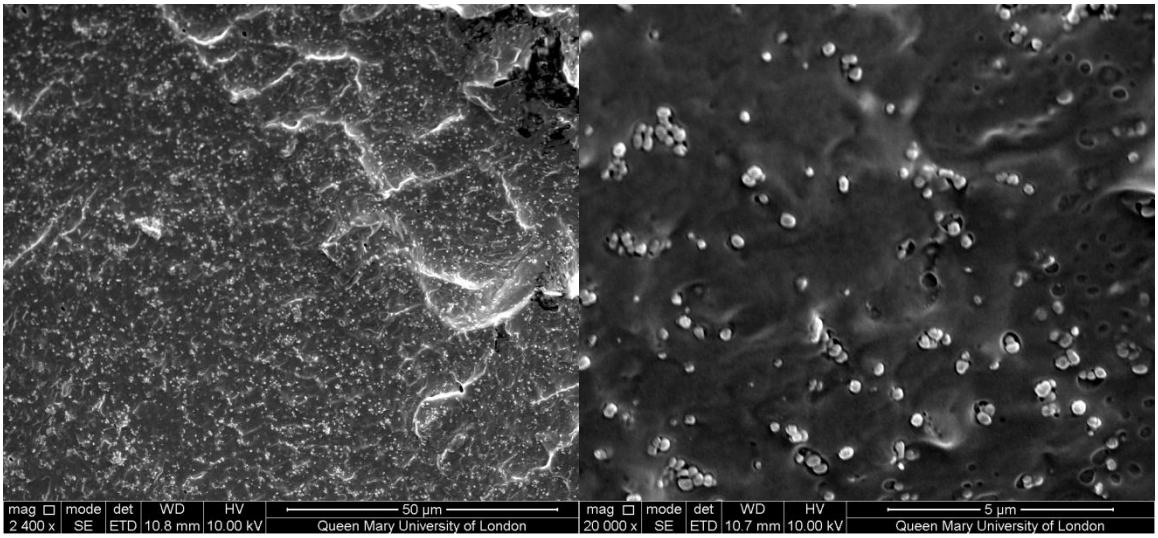

Figure 4.1: SEM images of cold-fractured surfaces of two-steps extrusion compounded film (PTFE 19vol. %).

Figure 4.1 shows the cold-fractured surface of a compounded PTFE/PVA blend (19vol.% PTFE) after hot-pressing. It shows a homogeneous dispersion of the PTFE particles into the PVA matrix with little or no agglomerates, indicating that the high shear forces in the micro-compounding process have led to well dispersed and homogeneous blend morphology. Even at this relatively high PTFE concentration, the individual PTFE particles, with diameters of around 200-300nm, are clearly identified, while also some small agglomerates up to 1µm are present. These agglomerates consisted typically of three to five PTFE particles, which is indicative of the good level of dispersion in these blends. Comparing the SEM pictures of this blend with those of cast and single step extruded specimens, we can clearly see an improved level of dispersion through this two-step method.

4.3.2 Fibre formation after drawing

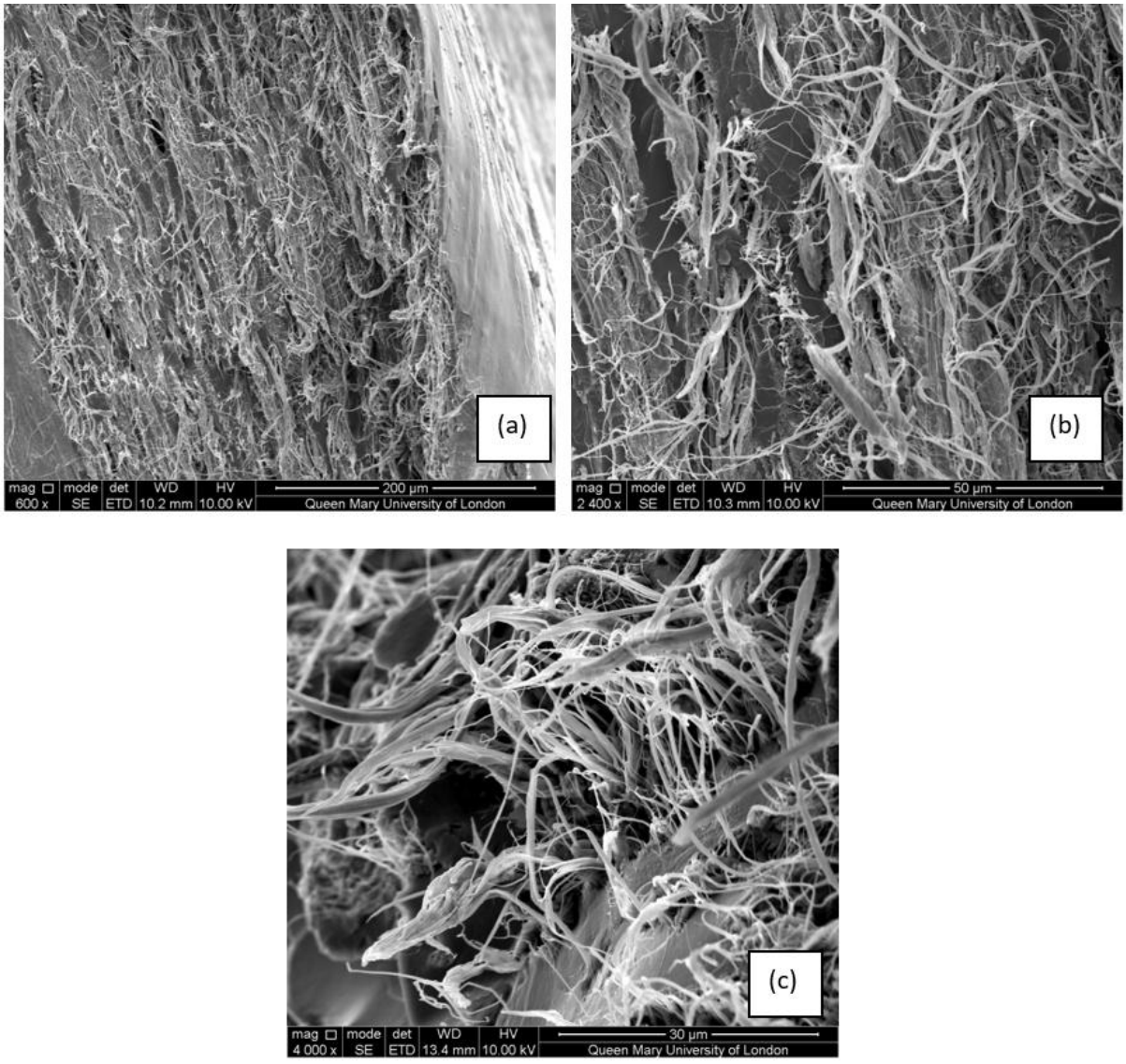

Figure 4.2: SEM images of drawn PTFE/PVA blend tape (a) mag 600x; (b) mag 2400x and (c) mag 4000x.

Figure 4.2 shows that after drawing, there are many fibres present in the PTFE/PVA blend. In addition, in comparison with the single-step extruded samples in Figure 3.4, the length and diameter of the fibres are more uniform in Figure 4.2. These improvements originate from the better dispersion of PTFE particles in the blend. With improved dispersion, the sizes of

the PTFE particle agglomerates are fairly uniform, making the stress distribution more uniform in the blend during stretching. As a result, there are barely any undrawn PTFE particles left in the drawn blend tapes.

4.3.3 Tensile properties after drawing

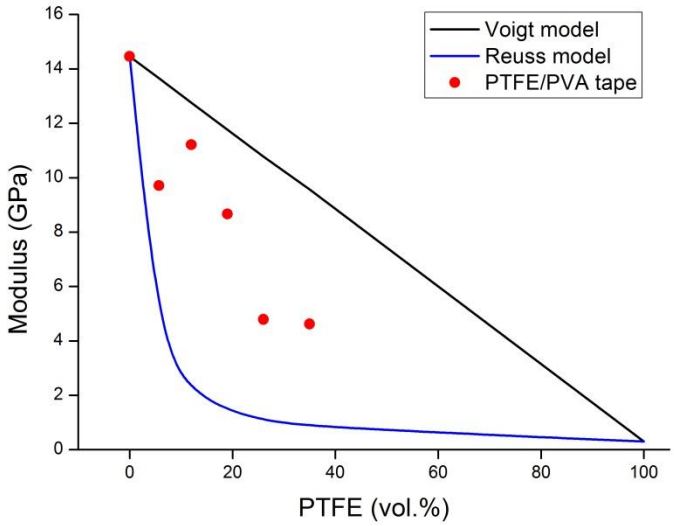

Figure 4.3: Young's modulus of two-step extrusion compounded PTFE/PVA blend tapes as a function of PTFE content (before removal of PVA) together with theoretical predictions using upper-bound parallel (Voigt) model and lower-bound series (Reuss) model.

Figure 4.3 shows the Young's modulus of PTFE/PVA tapes drawn to a draw ratio λ=4 and processed by two-steps extrusion compounding. We can see that the modulus data is positioned in between the parallel model and series model, indicative of a morphology of discontinuous fibres in a polymer matrix. In fact, some compositions (12vol.% and 19vol.%), exhibited a Young's modulus close to that of the parallel model. However, when the content of PTFE reaches 26vol.% or higher, the Young's modulus drops significantly as the PTFE/PVA

blend is no longer able to properly form an optimal island-in-the-sea morphology. Although having said that, the modulus is still better than that of samples prepared by the previous two methods. For the samples of 12vol.% and 19vol.%, the modulus is close to parallel model, suggesting that here the fibres in the blend are well dispersed and are of relatively uniform length and diameter. Figure 4.4, compares the Young's modulus of all three processing methods in the same graph, showing the significant improvements in modulus of the oriented PTFE/PVA blend tapes with changing processing methods from casting to single- and two-step extrusion compounding.

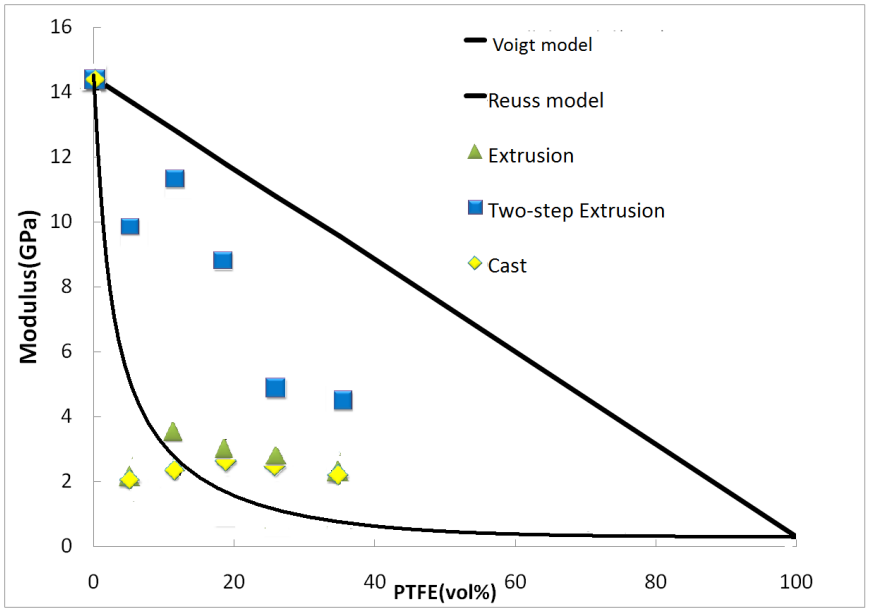

Figure 4.4: Young's modulus of cast, extrusion, and two-step extrusion compounded PTFE/PVA blend tapes as a function of PTFE content (before removal of PVA) together with theoretical predictions using upper-bound parallel (Voigt) model and lower-bound series (Reuss) model.

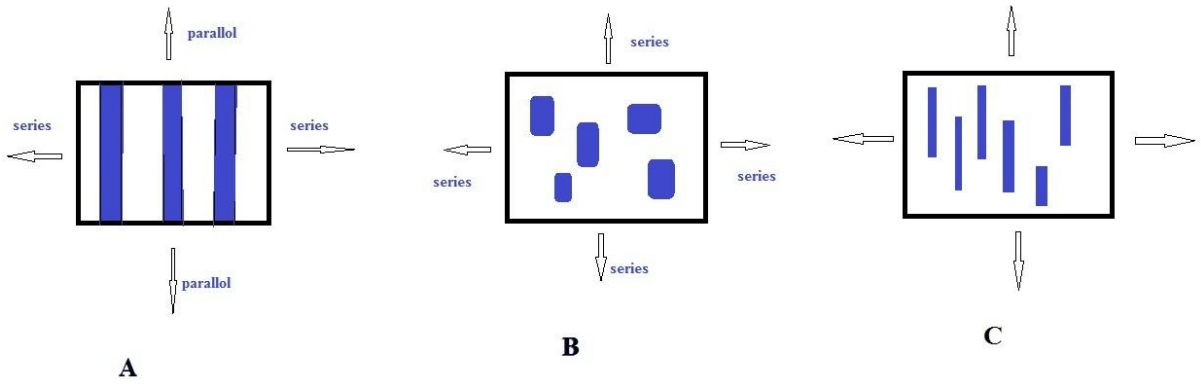

Figure 4.5: Illustration of blend morphology and parallel/series models.

Schematic A in Figure 4.5 shows the theoretical structures of parallel and series model. Previous studies showed that the modulus of the cast and single-step extruded blends were close to the series model. This implies that the microstructure in both these kind of blends are similar to schematic B, with agglomerate sizes being so large that the model is more similar to a series model even after drawing in the parallel direction. However, the modulus of the improved two-steps extruded blends are positioned between the theoretical parallel and series model, and are in some cases even closer to the parallel model. This implies an oriented fibrous microstructure of the blend similar to the one shown in schematic C with less agglomeration and a more homogeneous dispersion.

However, the modulus of even the best blends was still slightly below the parallel model. This is because the PTFE fibres are not continuous and the interfacial interaction between the PTFE and PVA is poor, resulting in weak stress transfer. Meanwhile, compared with the previous two methods, the two-steps extrusion system shows much better mechanical properties. Particularly samples with 12vol.% and 19vol.% PTFE showed high mechanical properties and for this reason we choose 19vol.% PTFE as the model system for direct

spinning of PTFE/PVA blend fibres as a first step towards scaling up the process. In the current work, we only used the Voigt and Reuss models to describe blend properties as they represent upper- and lower bound properties. For a more accurate description of actual blend properties more sophisticated micromechanical models like those proposed by e.g. Kerner, Takayanagi or Halpin-Tsai could be used [91].Typically these models are a combination of parallel and series models and more accurately describe the properties of composites or blends based on discontinuous fibres or particles.

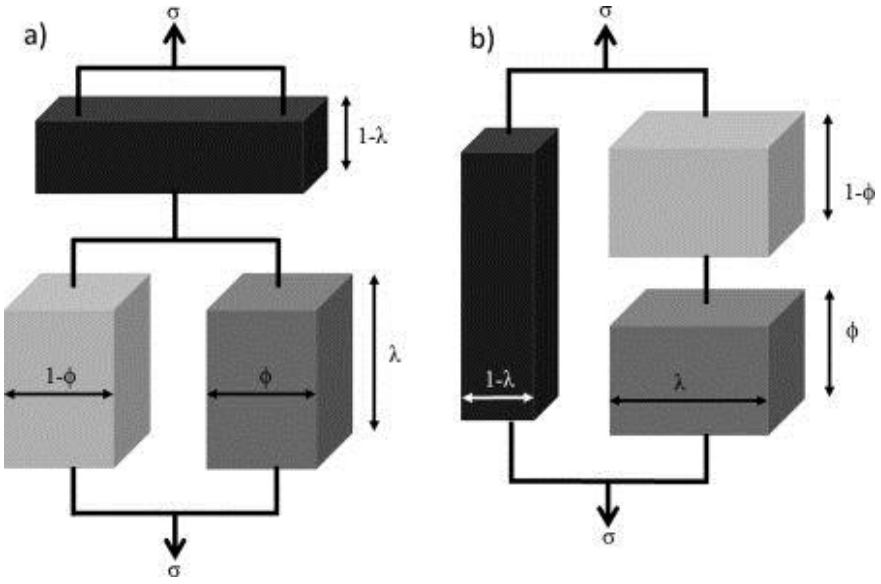

Figure 4.6Schematic representation of Takayanagi Model I (a) and II (b) as an example of combined series and parallel models. v is a function of the volume fraction of the parallel element and λ of the series element. Models I and II are also known as the series-parallel and parallel-series model, respectively.

4.3.4 Fibre formation in directly spun fibres

Figure 4.6 show the cross-sections of an as-extruded PTFE/PVA fibre. In contrast to hot-pressed films here, the PTFE has been partly drawn due to the drawdown of around 4 in the as-extruded fibre.

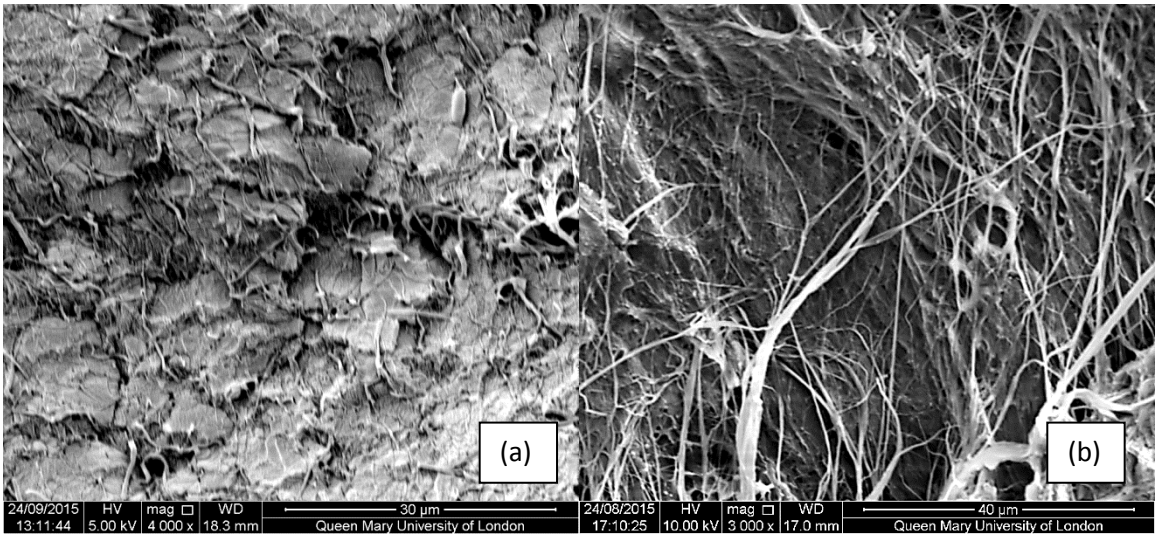

Figure 4.7: SEM images of cold fractured cross-sections of: (a) as-extruded PTFE/PVA fibre (19 vol.% PTFE), and (b) post-drawn PTFE/PVA fibre (λ=5).

The morphologies of the post-drawn PTFE/PVA fibres are very similar to those of the drawn tapes (see Figure 4.2). Length and diameter of the fibres are not only solely determined by draw-ratio but also by initial particle size, dispersion (aggregates) and draw down. Therefore, for the same initial dispersion condition, post-drawn as-extruded fibres and drawn tapes show very similar PTFE fibre formation behaviour. Meanwhile, in Figure 4.7a, we can see some short fibres, showing that fibre formation already starts during the extrusion process of the as-extruded fibre. However, molecular orientation in these fibres is not guaranteed because the high extrusion temperature will most likely lead to chain relaxation and

disorientated. Further XRD will be performed to investigate the chain orientation before and after drawing. Figure 4.7b shows that after drawing of the as-extruded fibres the fibres become longer and thinner than in the case of hot-pressed film and drawn tapes due to the initial draw-down in the as-spun fibre.

4.3.5 XRD analysis

X-ray diffraction (XRD) was performed to study the molecular orientation in the blend tapes and fibres before and after the solid-state drawing. Figures 4.7 show the difference in 2D Wide Angle X-ray Scattering (WAXS) patterns before and after drawing of the pure PVA tapes and the PTFE/PVA blends. The hot-pressed films showed for both systems a diffuse isotropic scattering ring typical of a non-oriented polymer. In the pure WAXS picture of pure PVA before drawing, the ring looks blurred due to two reasons. First, the degree of crystallinity of PVA is not very high, and there is still a large fraction of amorphous phase present in the material. Also the crystallite dimensions of PVA are small, which can also cause this blurring of the WAXS ring. The values of crystallinity were calculated and will be discussed later.

By comparing the 2D WAXS patterns of PVA and PVA/PTFE blends before drawing, we can identify the characteristic rings for each of them. In the case of drawn tapes, there are discrete equatorial reflections with low azimuthal spread typical of a well oriented crystalline phase for PVA and less well-oriented crystalline phase for PTFE.

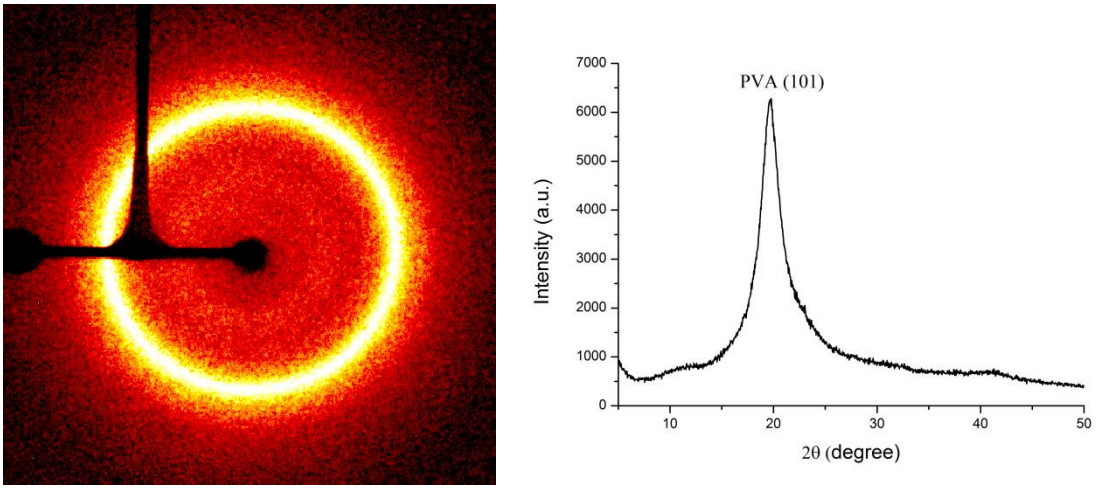
PVA (101)
Intensity (a.u.)
2θ (degree)
0
1000
2000
3000
4000
5000
6000
7000
10
20
30
40
50

(a)

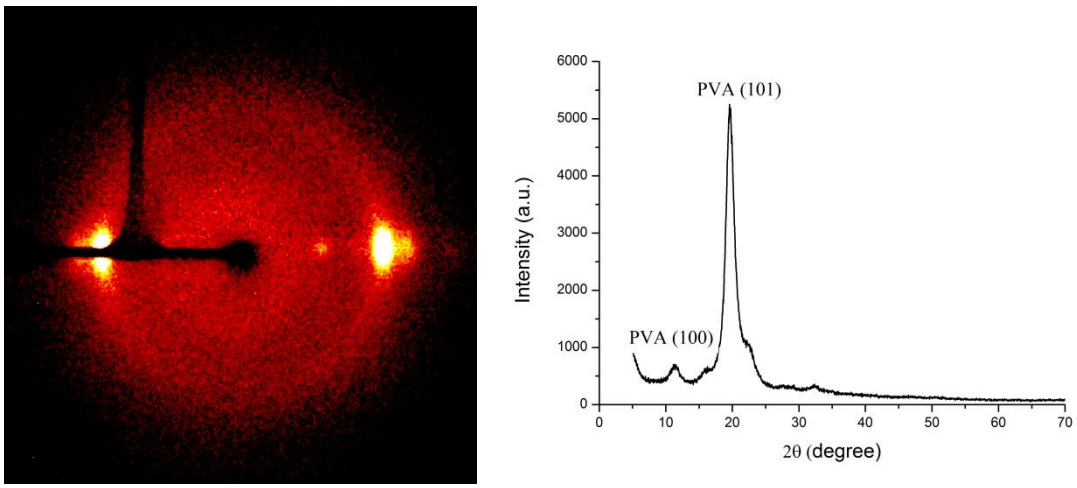
PVA (101)
PVA (100)
Intensity (a.u.)
2θ (degree)
0
1000
2000
3000
4000
5000
6000
0
10
20
30
40
50
60
70

(b)

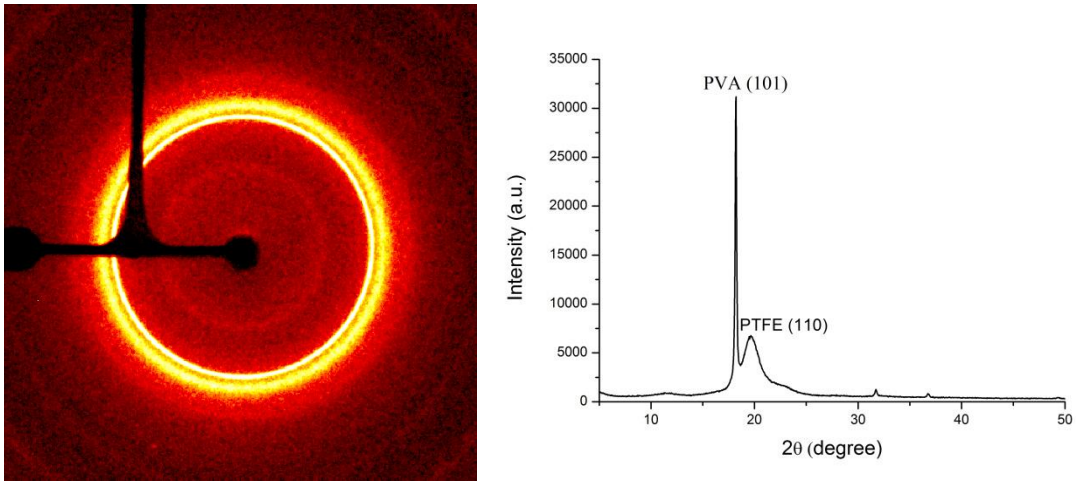

(c)

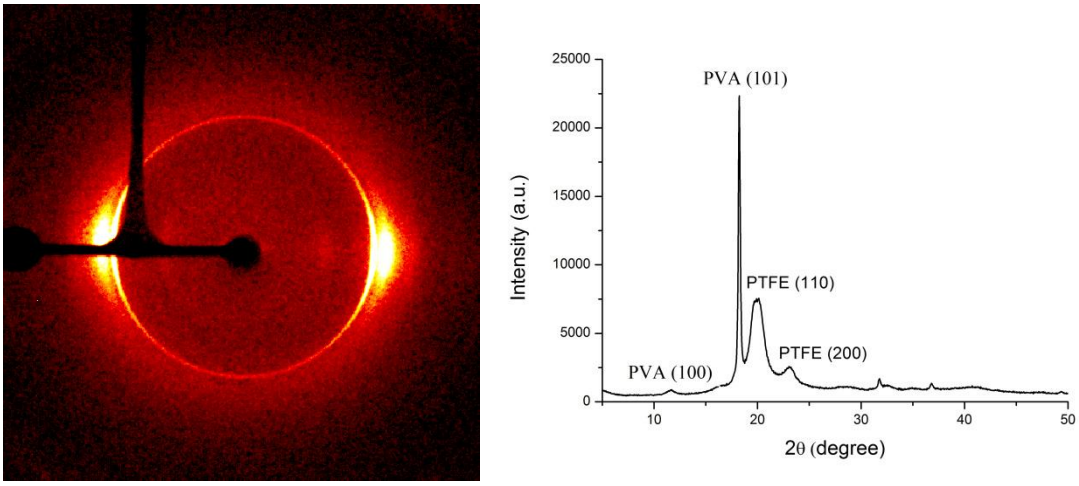

(d)

Figure 4.8:2D WAXS patterns and corresponding 1D patterns of: pure PVA (a) before and (b) after drawing (λ=5), and PTFE/PVA blend tape (PTFE 19 vol.%) (c) before and (d) after drawing (λ=5).

For PVA, two polymer molecules running through each unit cell, and each of the repeating monomers contains two hydroxyl sites, each with 50 % occupancy, thus creating an atactic

structure. In the unit cell of PVA, a = 0.781 nm, b = 0.252 nm, c = 0.551 nm, α = γ = 90 °C ≠ β, so the cell is monoclinic [65]. The crystallographic plane of PVA is calculated with:

$$\frac{1}{d^2} = \frac{1}{(\sin\beta)^2} \cdot \left(\frac{h^2}{a^2} + \frac{k^2 \cdot (\sin\beta)^2}{b^2} + \frac{l^2}{c^2} - \frac{2 \cdot h \cdot l \cdot \cos\beta}{a \cdot c}\right) \qquad \text{Equation 4.1}$$

The cell structure of PTFE changes with temperature and pressure. At 25 °C, the form IV of PTFE it is hexagonal. [66] For hexagonal structure, the crystallographic plane is calculated with:

$$\frac{1}{d^2} = \frac{4}{3} \cdot \frac{h^2 + h \cdot k + k^2}{a^2} + \frac{l^2}{c^2} \qquad \text{Equation 4.2}$$

In which, the d is calculated with Bragg's Law:

$$\lambda = 2d_{hkl} \cdot \sin\theta_{hkl} \qquad \text{Equation 4.3}$$

Here, λ is the wavelength of X-ray used in the test, which is 0.154 nm and θ is the azimuthal angle that can be read from the XRD 1D pattern at the peak of the curve.

The orientation function and crystallinity were calculated from the XRD data, an example of such a calculation is given below for a specimen of drawn blend PTFE/PVA fibres to illustrate the process.

For the determination of the orientation function, we used Fit2D to analysis the WAXS image. All the WAXS images were converted into a readable format for Fit2D software with GIMP2. Initially, we used an Al_2O_3 WAXS image for calibration and to remove background

data. After integrating the WAXS of the reference Al_2O_3 sample, the output parameters are recorded and applied in the further analysis.

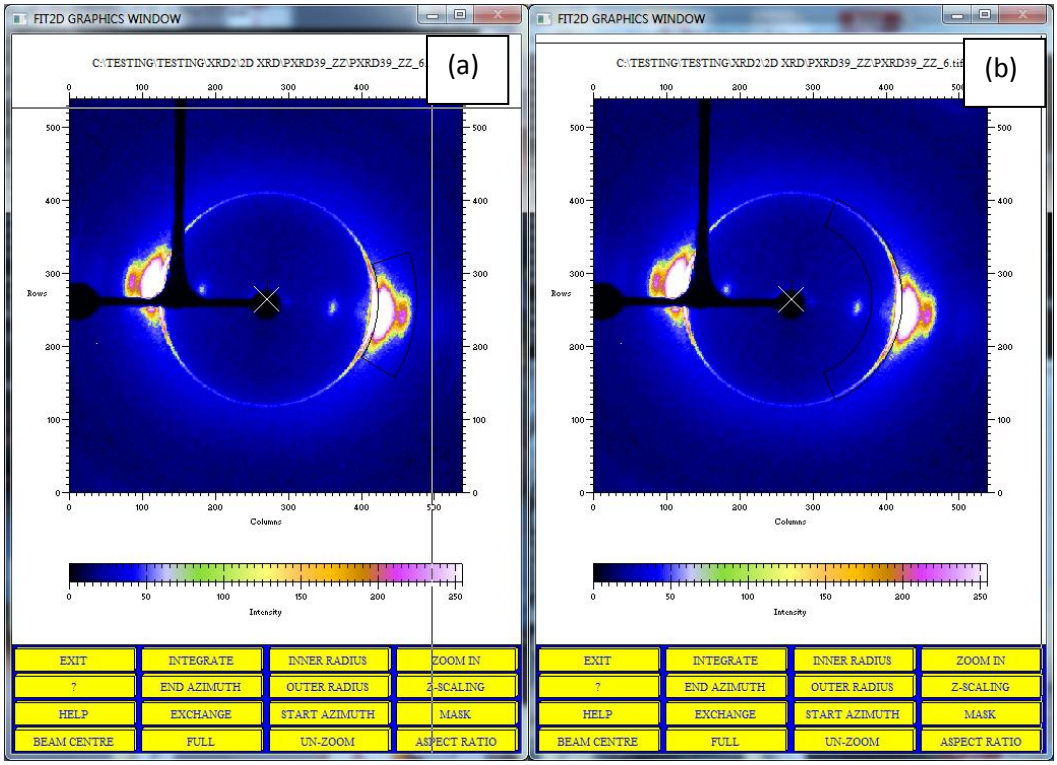

Figure 4.9: Selected areas for (a) PVA and (b) PTFE in the WAXS images.

After calibrating the WAXS image of drawn PTFE/PVA fibres, an area of the arc is selected that needs to be analysed (see the black line). For instance, in Figure 4.9a, the area chosen is the arc present for PVA, while in Figure 4.9b the area chosen is the arc of PTFE. The software will analyse the intensity of each arc in the image and integrates the related curves. For undrawn samples, instead of choosing the arc area, we directly choose the whole ring to detect the intensity. Using the parameters recorded from the reference calibration experiment we can integrate the intensity and obtain the integrated curve as below.

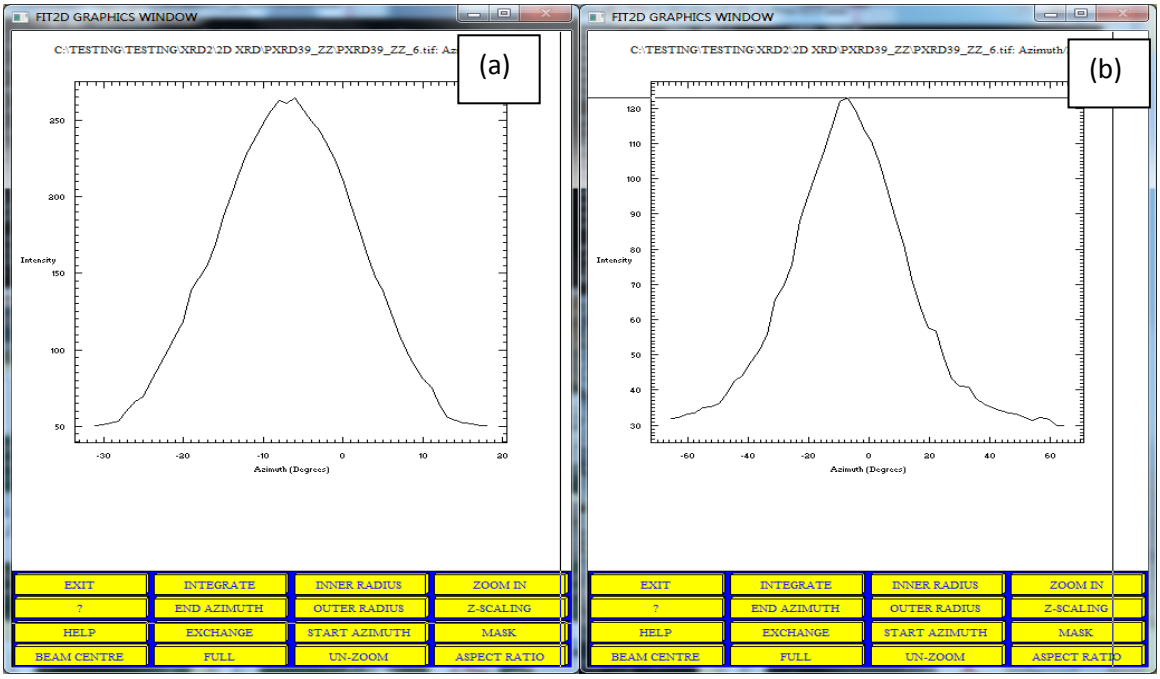

Figure 4.10: Integrated curves of arcs in WAXS images (a) PVA and (b) PTFE.

Figure 4.10 shows the integrated curves for intensity distributions along with the azimuthal angle after the subtraction of the background intensity. Exporting this data into the software Origin 8.0, we can now fit the curve using the GaussFit option as shown below in Figure 4.10.

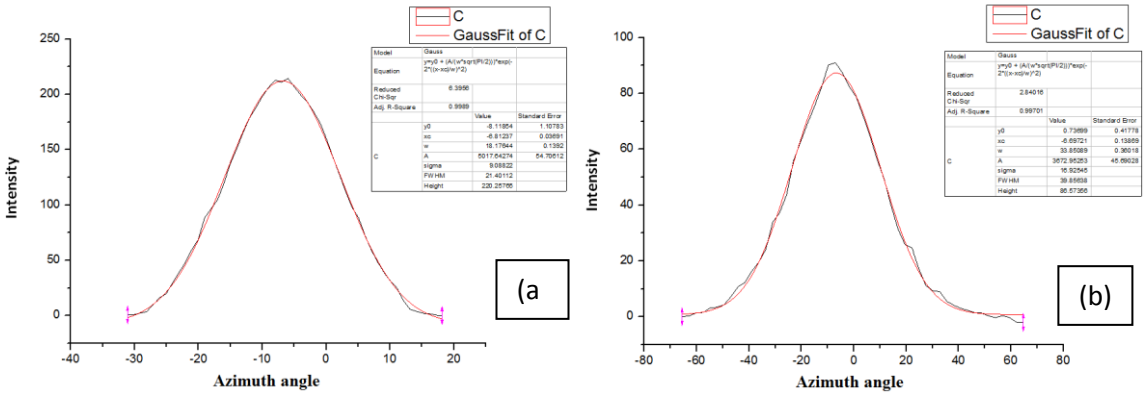

Figure 4.11: GaussFit of intensities distribution along with the azimuthal angle after the subtraction of the background intensity for (a) PVA and (b) PTFE.

Exporting the fitted data into an Excel file together with the equations below can now be used to calculate the orientation function:

$$f_c = \frac{2}{3\cos^2\sigma - 1}\frac{3(\cos^2\phi) - 1}{2} \qquad \text{Equation4.4}$$

$$(\cos^2\phi) = \frac{\int_0^{\pi/2} I(\phi)\cos^2\phi\sin\phi d\phi}{\int_0^{\pi/2} I(\phi)\sin\phi} \qquad \text{Equation4.5}$$

Herman's orientation function (f_c) is the orientation distribution function of the azimuthal angle (ϕ) and is simply a mathematicalconstruction that allows us to describe the degree of orientation of the chain axis relative to some other axis of interest, i.e. the drawing direction. The average ($\cos^2\phi$) between the normal of a givencrystal plane and the drawing direction is calculated by integrating the intensity of the specific 2θ diffraction peak along the ϕ, and I(ϕ) isthe 1D intensity distribution along with the azimuthal angle after subtraction of the background intensity using FIT2D software. When chains are perfectly aligned along the

reference (i.e. drawing) axis, f_c=1, whereas f_c=-½ for chains aligned perpendicular to the reference axis. For random orientation f_c=0.

Importing the fitted data from Origin into Excel, using Equations 4.4 and 4.5 can now be used to calculate the orientation function.

This calculation method is not suitable for WAXS rings. All the WAXS images of undrawn samples are rings, indicating an isotropic crystal structure.

Crystallinity is calculated from the XRD experiments using the equation below:

$$f_c = \frac{\sum A_c}{\sum (A_c + A_a)} \qquad \text{Equation4.6}$$

Here A_c is the integrated area underneath the crystalline peaks and A_a is the integrated area of the amorphous peak. The multiple peak fitting module of Origin is used to fit and integrate the crystalline peak. A simple example is shown below in Figure 4.11 (more specific curves with fitted peaks and hlk will be shown later in Figure 4.14):

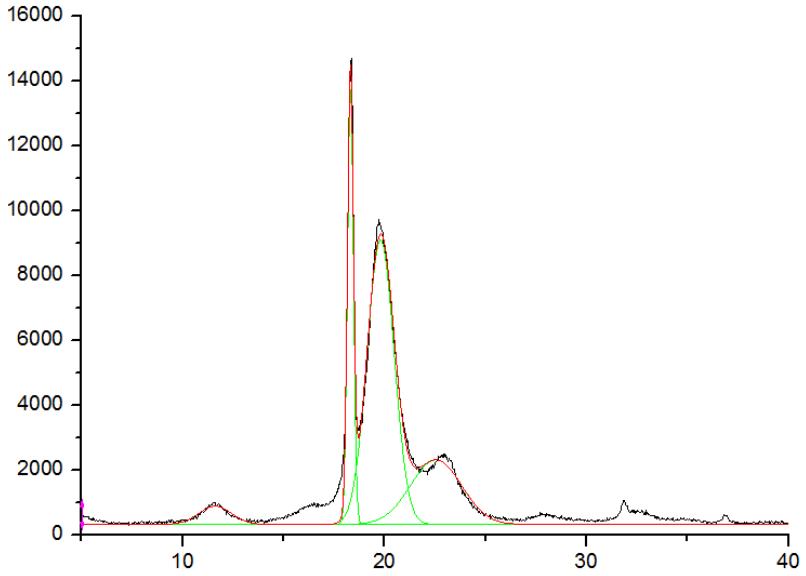

Figure 4.12: Multiple peaks fitting of drawn PTFE/PVA blend fibres.

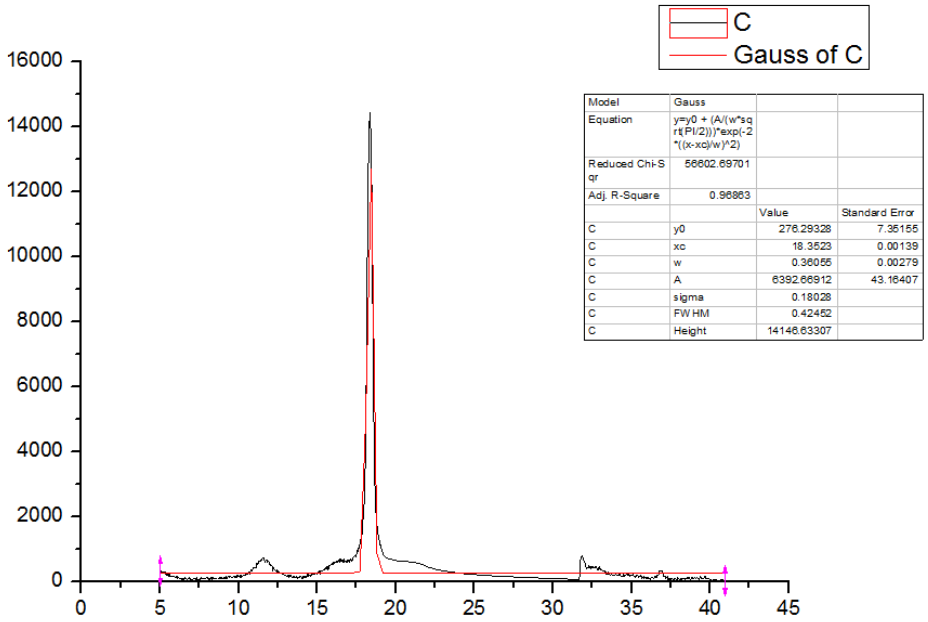

Figure 4.13: Splitting of PVA peak from multiple peaks curve of drawn PTFE/PVA blend fibres.

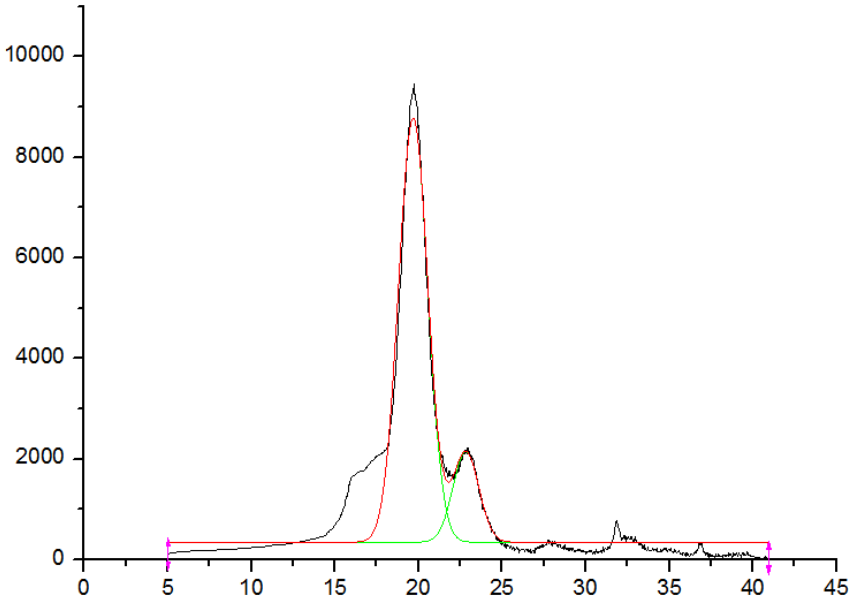

Figure 4.14: Splitting of PTFE peak from multiple peaks curve of drawn PTFE/PVA blend fibres.

Because the area for calculating the degree of crystallinity for each component is only related to the intensity of each neat polymer, we need to split the main curve of each component from the curve for the blend.

After splitting the main curve of each component, we fit this peak in Origin, from which we can get the intensity distribution along with the azimuthal angle of the crystal for each curve. Integration of both the split curve and fitted peak, leads now to the area for the crystallites and the area for crystalline and amorphous phase. Based on these data, we can now calculate the degree of crystallinity.

Table4.1: Orientation function and crystallinity calculation of PVA and PTFE/PVA tape based on the XRD.

Samples		XRD results	
		orientation function	crystallinity degree
Undrawn PVA		(isotropic)	28.7%
Drawn PVA		0.97	43.0%
Undrawn blend tape	PVA	(isotropic)	26.2%
	PTFE	(isotropic)	43.5%
Drawn blend tape	PVA	0.90	45.6%
	PTFE	0.71	54.1%

Table 4.1 shows high values for the Herman's orientation function of PVA in both neat drawn PVA (0.97) as well as the PVA phase in drawn blend tapes (0.90) and fibres (0.92).

The orientation functions for the PTFE phase in the blend tapes and fibres are significantly lower at 0.71 and 0.69, respectively, indicating a lower level of molecular orientation in the PTFE phases presumably due to a non-affine deformation of the dispersed phase during the drawing of the blends as a result of poor adhesion between PTFE and PVA. The peaks are fitted with the multiple peak fitting module of Origin using a Gaussian distribution mode. An example is shown in Figure 4.13 with multiple peaks fitting for each polymer and their hlk peaks, using the methodology described above.

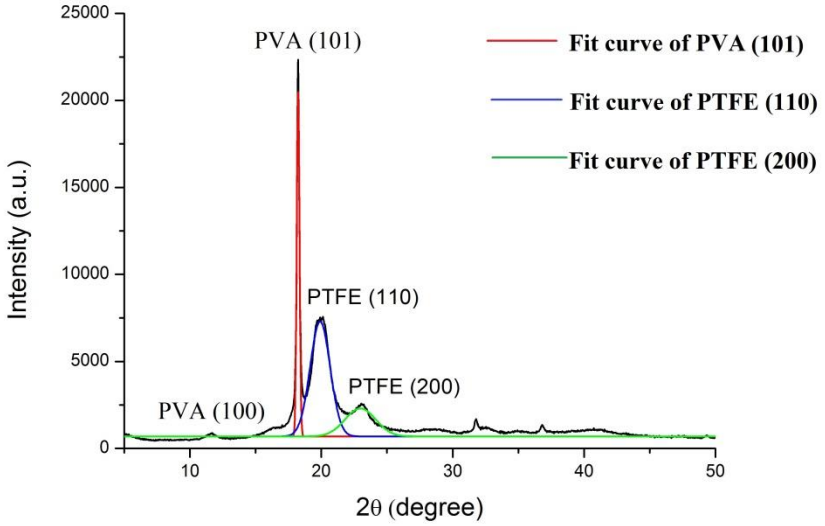

Figure 4.15: Multiple peaks fitting of drawn PTFE/PVA blend tape.

From Table 4.1 we can see that the degree of crystallinity of both PVA and PTFE increased after drawing. The increase in the degree of crystallinity after drawing is smaller for PTFE than for PVA, which is in line with the differences in degree of orientation between the two phases.

Figure 4.16 shows the 2D WAXS patterns for as-extruded PTFE/PVA blend fibres and post-drawn blend fibres. In the case of as-extruded blend fibres (Figure 4.16a) diffuse isotropic scattering is observed typical of a non-oriented polymer, even though there is a draw-down of around 4 by the extrusion process. This suggests that the stretch in the extrusion process does not lead to molecular orientation. However, after drawing (λ=5) by hand on a hot plate at 100°C the as-extruded fibres become highly oriented with discrete equatorial arc reflections, indicating a well-oriented crystalline phase. Based on the width of the arcs and a comparison of the WAXS pictures shown above, we may assume that the degree of

orientation in the as-extruded post-drawn fibres is similar to that of the hot-pressed post-drawn tapes. This is confirmed by the calculated orientation function of the tape and fibre.

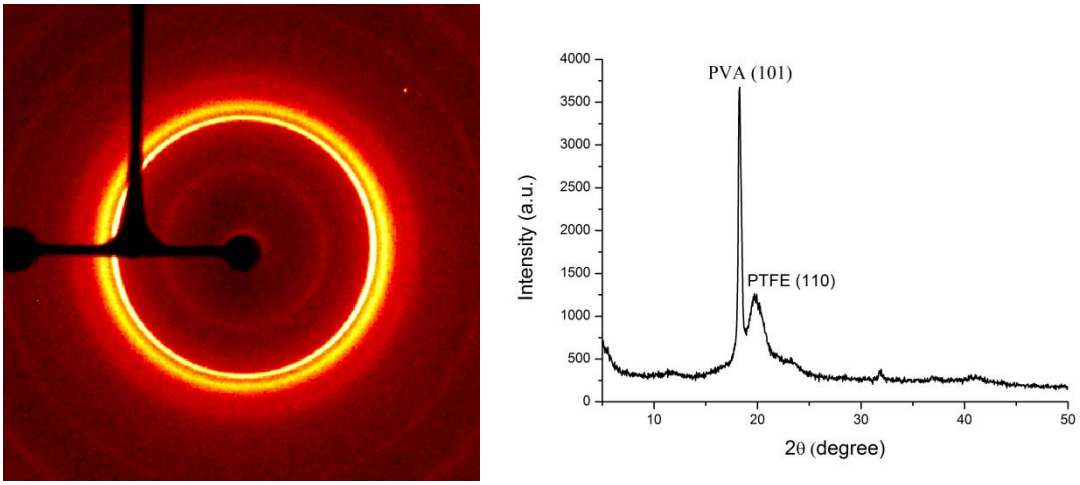

(a)

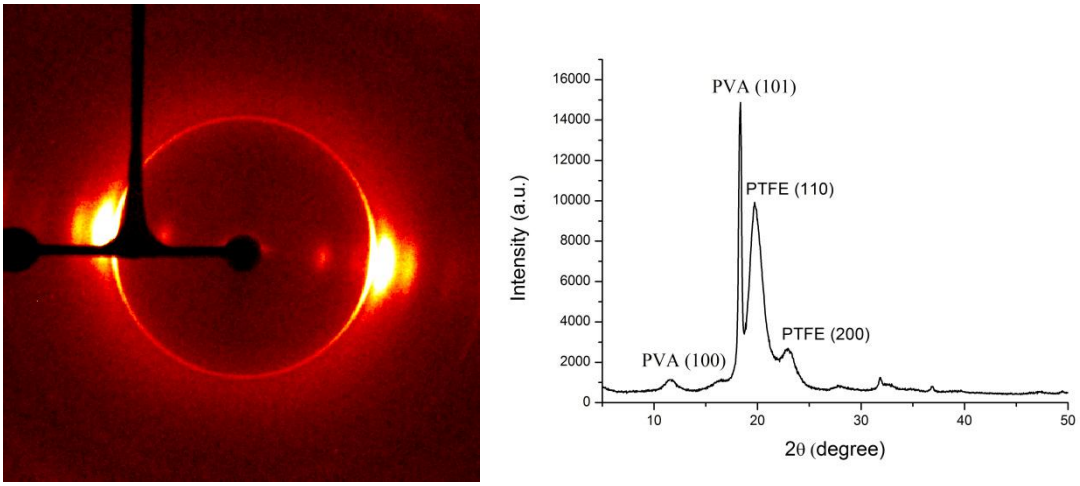

(b)

Figure 4.16: 2D WAXS patterns of blend fibres (PTFE 19vol.%) and corresponding 1D patterns: (a) as-extruded, (b) post-drawn blend fibres (PTFE 19vol.%) (λ=5).

Using the same analysis method as mentioned above, we also calculated the orientation function, crystallinity and crystal size of drawn and undrawn PTFE/PVA composite fibres (see Table 4.2).

Table 4.2: Orientation function, crystallinity and crystallite size calculated for PVA and PTFE/PVA fibres based on XRD data.

Samples		XRD results	
		Herman's orientation function	crystallinity
Blend fibres	PVA	(isotropic)	25.9%
	PTFE	(isotropic)	50.5%
Drawn blend fibres	PVA	0.92	39.2%
	PTFE	0.69	64.2%

From Table 4.2 we can see that the crystallinity of the blend fibres is rather similar to the blend tape as discussed in the previous part of this chapter. Both PVA and PTFE have nice levels of molecular orientation, while the degree of crystallinity and crystal size also increased after stretching. This is an indication that the properties of PVA/PTFE blends are similar for both fibre or tape form. Since both have similar draw ratios, orientation functions, degree of crystallinity and crystal sizes, the mechanical properties are also expected to be similar.

Previous studies on melt-spun PTFE fibres [28], showed that the crystallinity of ultrahigh molecular weight PTFE can reach values as high as 80% before processing. However, the crystallinity of melt crystalized samples is typically around 40%, while medium or lower

molar mass PTFE grades can reach crystallinities of 60% from melt. In the case of superdrawing of PTFE virgin powders[29], the crystallinity could reach a maximum of 87% while an orientation function was reported as high as 0.997. Similar to virgin powders, in the case of superdrawing of PTFE nascent powders by solid-state coextrusion[89],the crystallinity was 96% and the orientation function was 0.998. The reason for this high crystallinity and orientation function was probably because of the high draw ratio of these fibres, with some of them even reaching a maximum draw ratio of 400. For PTFE fibres directly made from emulsion, crystallinity is around 70% and the orientation function about 0.92 [14].

4.3.6 Tensile properties of PTFE/PVA fibres

For blend fibres (PTFE 19vol %), the draw down in the extrusion process is about 4 while the solid-state draw ratio is about 5. The final diameter of the drawn blend fibres is around 0.35mm. From tensile testing, the average Young's modulus was calculated at approximately 5GPa. Compared with the data in Figure 4.4 we can see that the modulus is a bit lower than for the two steps extrusion process but higher than for both the solution/suspension casting and single-step extrusion.

4.3.7 Water content and degradation

For stable mixing, we set the ratio of PVA: water at a constant 3:7 w/w (water 74vol.%), and only changed the ratio of PTFE/PVA to ensure that the blends had similar fluidity and viscosity. However, during the process of extrusion and pelletization, the amount of water in the blend dropped.

Table4.3: Weight loss of TGA for PTFE/PVA blend

	PVA	PTFE	Water
Weight percentage	27 %	11 %	62 %
Volume percentage	25 %	6 %	69 %

	Total weight	Water wt.%	Water weight	Polymer weight
Before process	M1	62 wt.%	0.62*M1	0.38*M1
After process	M2	X	x*M2	(1-x)*M2
After TGA	M3	0	0	M3

In order to investigate this issue, we took a specimen of PTFE/PVA (PTFE 19 vol.%) and measured the water content before and after processing. The details are listed in Table 4.3.

$$\begin{cases} 0.38 \times M1 = (1-x) \times M2 = M3 \\ M3 = 0.38 \times M1 \\ M3 = 0.57 \times M2 \end{cases}$$

According to the calculation above, we obtain x = 0.43.

Hence, the water loss = 0.62 - 0.43 = 0.19.

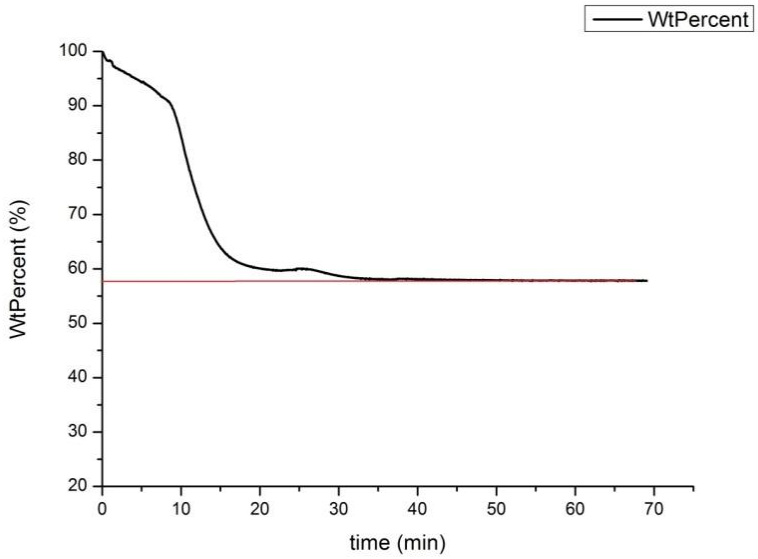

Figure 4.17: Low-temperature TGA of PTFE/PVA for the determination of water content.

Compared with the TGA data shown in Figure 4.17, we can see that after heating there is 57 wt.% of PTFE/PVA content remaining, so the weight loss (W_{loss}= W_{before}- W_{after}) is 43 wt.% (100 wt.% - 57 wt.%) of the total weight. Therefore, after extrusion, pelletization and storing in sealed sample bags, the content of water in the blends is about 43 wt.% and the water loss is 19 wt.% (62 wt.% - 43 wt.%). This water loss should be considered if the process is transferred to other systems as it may have great implications on processability.

4.3.8 Surface properties of blend fibres

PVA is a hydrophilic material and PTFE is super-hydrophobic. Therefore, it is interesting to investigate the surface properties of the blend fibres as this may open up interesting applications on its own.

Since water is the most common liquid in life and the many applications including textiles interact with water, the following experiments are based on the interaction of these tapes with water. The average values of different contact angles are shown in Table 4.4 to Table 4.8. Each value was the average of four specimens.

Table 4.4: Static contact angles of PVA, drawn PVA, as-extruded blend fibres and drawn blend fibres.

Sample	PVA film	Drawn PVA	As-extruded blend fibres	Drawn blend fibres
Static contact angle	38^{o}	30^{o}	26^{o}	39^{o}

From Table 4.4 we can see that the static contact angles do not change all that much with or without the addition of PTFE, while they are also quite similar before or after drawing.

Table 4.5: Advancing and receding contact angle of PVA.

Sample inclined angle	Advancing angle	Receding angle
27^{o}	41^{o}	31^{o}
34^{o}	41^{o}	23^{o}
53^{o}	45^{o}	20^{o}
94^{o}	45^{o}	19^{o}

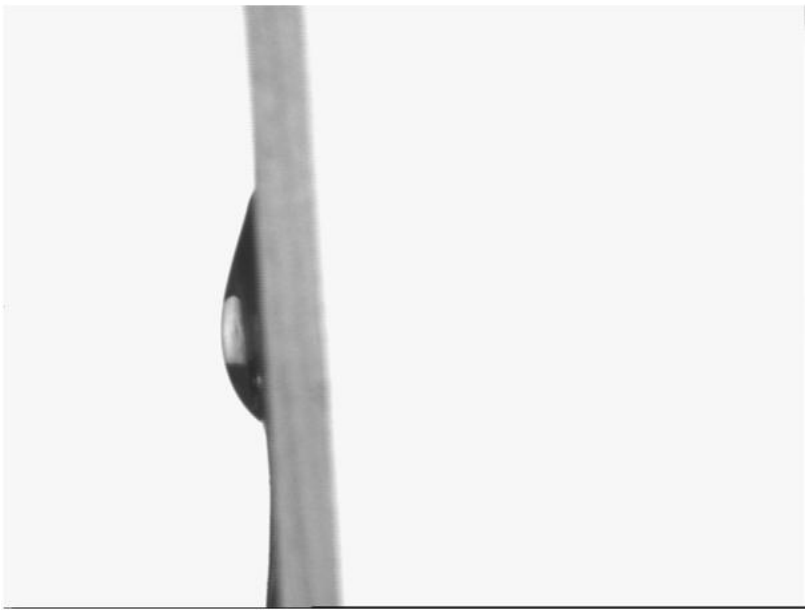

Figure 4.18: Water droplet attaches to PVA substrate even when positioned vertically.

From Table 4.5 and Figure 4.18, we can see that undrawn PVA is highly hydrophilic, meaning that a water droplet does not move even when the substrate is placed vertical. However, after drawing, the water drop slides much easier of the PVA tape as droplet motion starts already at an inclined substrate angle of 32^{o} (Table 4.6).

Table4.6: Advancing and receding angles of drawn PVA.

Sample inclined angle	Advancing angle	Receding angle
32 ^{o}	41 ^{o}	20 ^{o}

Table4.7: Advancing and receding angles of blend fibres (PTFE 12 vol%).

Sample inclined angle	Advancing angle	Receding angle
18 ^{o}	31 ^{o}	20 ^{o}
30 ^{o}	40 ^{o}	11 ^{o}
39 ^{o}	40 ^{o}	11 ^{o}

Table 4.8: Advancing and receding angles of drawn blend fibres (PTFE 12vol %).

Sample inclined angle	Advancing angle	Receding angle
28 ^{o}	37 ^{o}	24 ^{o}
35 ^{o}	39 ^{o}	21 ^{o}
43 ^{o}	36 ^{o}	13 ^{o}
65 ^{o}	36 ^{o}	8 ^{o}

In Table 4.7 and 4.8, we can see that water droplet motion is similar for both drawn and undrawn samples, but for undrawn specimen the advancing and receding angle does not change while flowing. On the drawn one, the advancing angle does not change but the receding angle decreases significantly during droplet motion. This suggests that the surface free energy is less for the drawn tapes and that droplet motion is more sensitive to the inclined angle.

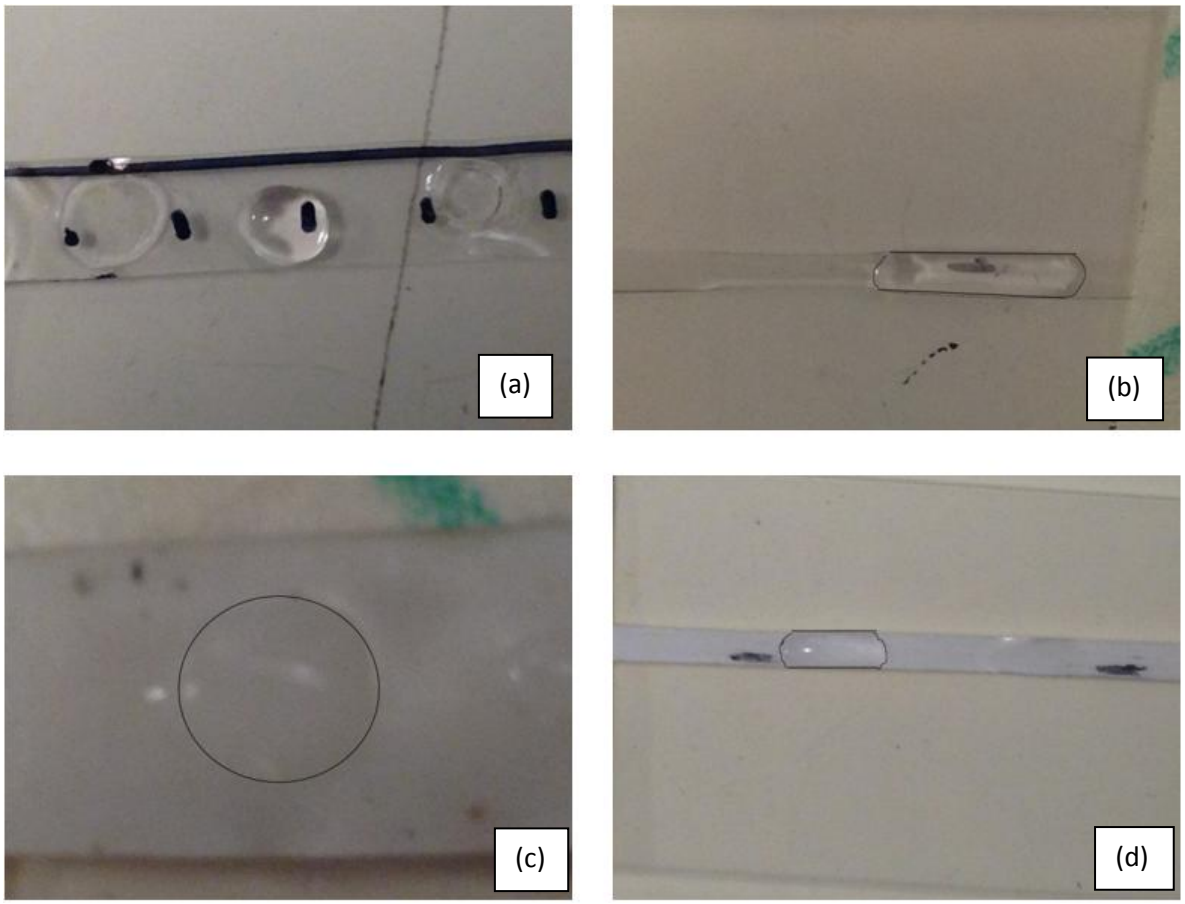

Figure 4.19: Water droplet on (a) PVA, (b) drawn PVA, (c) as-extruded blend tape and (c) drawn blend tape.

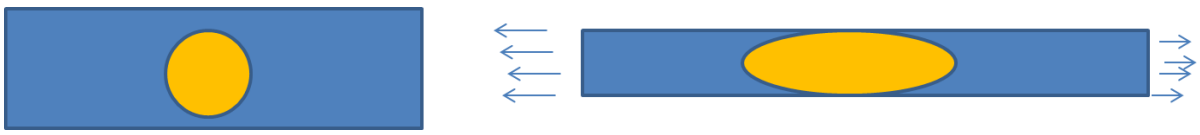

Figure 4.20: Illustration of water droplet shape on drawn and undrawn tapes.

Figure 4.19 and 4.20 indicate that a water droplet extends in the drawing direction. From these, we can conclude that the drawn blend fibres have a hydrophilic surface with water droplets showing a high mobility on this surface.

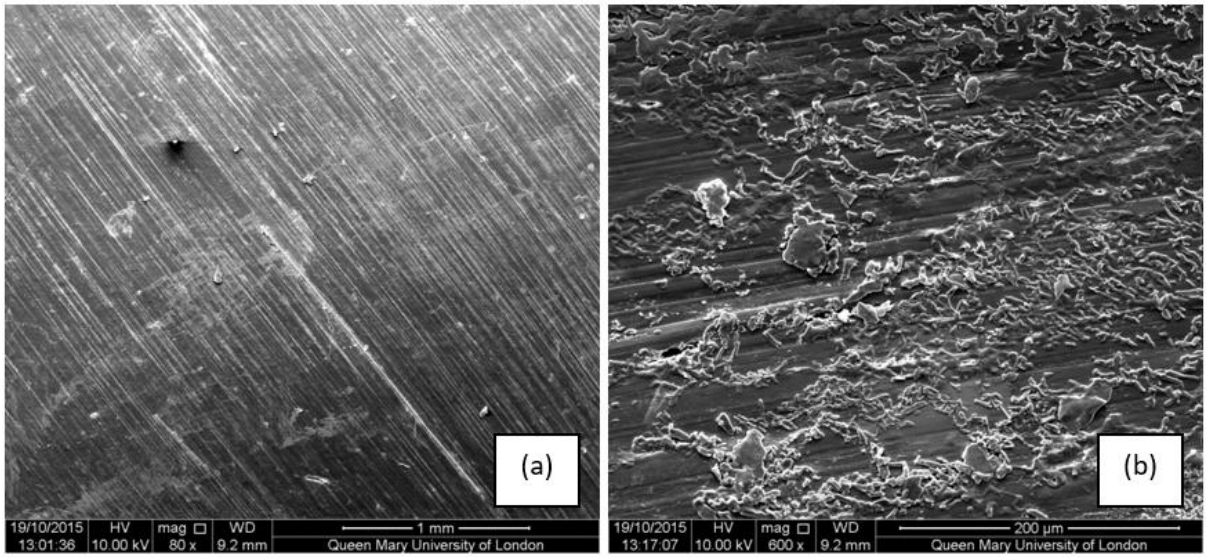

Figure 4.21: Drawn blend tape surface (a) before and (b) after the application of water droplet.

Figure 4.21 shows that after placing a water droplet onto the surface of a PTFE/PVA tape at room temperature, some of the PVA is extracted from the blend. This can be important for applications as one can imagine that dirt on the surface could be removed by water droplet motion, however, this will be at the expense of the removal of a small amount of PVA.

From all of this it can be concluded that blend fibres of super-hydrophilic and super-hydrophobic polymers with an island-in-the-sea morphology in where the super-hydrophilic material is the sea phase and the super-hydrophobic material the island phase, the blend fibre surface becomes super-hydrophilic. This opens up possibilities for some interesting applications.

4.4 Conclusions

The current two-steps extrusion compounding method solved most of the compounding issues of mixing powders and liquids, while at the same time improved the dispersion of PTFE particles in PVA solution. Blends prepared by this method showed good levels of PTFE particle dispersion, which resulted in very few remaining undrawn PTFE particles after drawing. Meanwhile, also the tensile properties of the PTFE/PVA blend tapes and fibres were significantly improved. Furthermore, XRD results confirmed that the drawn blend does not only show fibre formation but also exhibits true molecular orientation after drawing. However, although some initial experiments showed that these PTFE/PVA blends can be directly spun into fibres, we still need to establish the potential of this method on a pilot-scale extrusion line. In addition, some interesting surface properties were reported for the PTFE/PVA blend fibres.

Chapter 5

Ultrafine PTFE fibres by twin-screw extrusion compounding and spinning using plasticized PVA, and water/ethylene glycol as a solvent

5.1 Introduction and objective

In the previous chapters, it was shown that the modified island-in-the-sea method has great potential for the processing of ultrafine PTFE fibres. Proof-of-principle was shown using lab-scale mixing methods such as solution stirring and compounding using a mini-extruder. Here we will try to transfer this technology to a more industrially relevant processing technology based on twin-screw extrusion for compounding and fibre spinning.

Twin-screw extrusion is a very common method used in the plastics industry for compounding, extrusion and fibre spinning. Twin-screw extruders are widely used for mixing, compounding or reactive polymer processing. They can be co-rotating or counter-rotating, intermeshing or non-intermeshing [92].With similar screw design, cross-sections and rotational speed, co-rotating extruders have a better mixing efficiency and axial velocity, while counter-rotating extruder show greater pressure build up. The velocity of the flow reaches its maximum value at the screw tip in co-rotating extruders and in the intermeshing

zone in counter-rotating extruders [93].In combination with a feeding pump and melt pump, it is easy to control the amount of material in the machine, ensuring stable spinning.

In contrast to the mini-extruder used in previous chapters, the twin-screw extruder has no recycling design. Hence, the residence time is very different and we will significantly need to adjust the various processing parameters when moving the material system from mini-extruder to twin-screw extruder. In fact, we may even have to consider replacing water for another solvent or plasticizer in order to enlarge the processing temperature window and create a more suitable material system for twin-screw extrusion and spinning.

5.2Experimental

5.2.1 Materials

Grades of poly(vinyl alcohol) (PVA) and poly(tetrafluoroethylene) (PTFE) were the same as described in Chapter 2. Ethylene glycol (EG), was purchased from Sigma-Aldrich Co Ltd.

Plasticized PVA1799 (plasticizer is glycerol, which is confirmed in further tests), with a melt-flow index (MFI) of 1.2 - 5 g/10min at 190°C, a melting temperature of 180°C, tensile strength ≥ 20 MPa, and density 1.20 - 1.28 g/cm^3 was purchased from Weifang HuaWei New Materials Technology Co., Ltd (China).

5.2.2Processing and characterization

5.2.2.1 TGA of plasticized PVA1799

Because plasticized PVA1799 has a different melting temperature and decomposition temperature than pure PVA, thermogravimetric analysis (TGA) tests were performed using a TA Instruments Q500 to get an indication of the processing temperature window of this material. TGA involved the heating of a polymer sample from 20^{o}C (room temperature)to 1000^{o}C at a heating rate of 20^{o}C in a nitrogen atmosphere.

TGA testing of polymer stability involved also isothermal heating for 10min and then increasing the temperature to 60^{o}C with a dwell time of 30min to remove remaining water absorbed from the air. This is followed by heating to 200^{o}C at a rate of 10^{o}C followed by a dwell period of 30min to see if the sample would decompose or remain stable at a temperature close to the decomposition temperature from the TGA test. Then, similar to before, samples were heated to 1000^{o}C followed by switching to air feed for the final burning step to clean the sample holder.

5.2.2.2 DSC of plasticized PVA1799

Differential scanning calorimetry (DSC) was performed using a Mettler-Toledo 822e. The sample was heated from room temperature to 50^{o}C and held at this temperature for 90min to remove the water absorbed from the air in the PVA. Cooled down to 20^{o}C, and then started the test by heating up to 150^{o}C, followed by1 min temperature holding. Repeating the process three times but now by respectively heating up to 175^{o}C, 200^{o}C and 215^{o}C. The

heating rate was 10^{o}C/min. The heating was limited to 215^{o}C to prevent degradation of the PVA.

5.2.2.3Plasticized PVA1799/PTFE/water system processed by twin-screw extruder

First, some initial sets of experiments were carried out in the mini-extruder to confirm the optimal processing temperature for PVA1799. Trails were performed at 120 ^{o}C, 140 ^{o}C, 160 ^{o}C, 170 ^{o}C and 180 ^{o}C. From these extrusion trials, it was found that the extrudate was hard and rigid at low temperatures and plastic at increasing temperatures, while light yellowing started to occur on extrudate above 170 ^{o}C. Therefore, for further processing 170 ^{o}C was selected.

For the PTFE/PVA1799 blend composition, we followed our previous experiments and selected a PTFE: PVA1799 = 3:7 w/w (19vol.% PTFE). PVA particles were again pre-mixed with PTFE suspension (65wt.%). Part of this mixture was dried in an oven at 80^{o}C for 24 hrs to remove water, while another part was not subjected to this drying cycle. The mini-extruder temperature was set temperature at 140^{o}C while extruder speeds evaluated were 10rpm, 25rpm, 50rpm, 75rpm and 100rpm, respectively with a re-circulation or residence time of 30sec, 1min, 2min, 3min, 4min and 5min. Meanwhile, the purge speed was set as 10rpm, 20rpm, 30rpm, 40rpm and 50rpm. From these extrusion experiments, we could see that the compound was not completely dry when at short residence times, had better melt strengths during extrusion, while mixing was better at high speeds. However, extrusion speed and purge speed had to be kept low to obtain good quality strands. Therefore, at this stage, we could confirm that the good quality strands could be extruded from PVA1799 using the following process parameters: no pre-drying, two steps mixing at high speed (100

rpm) for 30-45sec followed by low speed mixing (20rpm) for 45-60sec and finally purging at low speed (10-20rpm).

The next step involved direct spinning from the mini-extruder using a fibre die with a diameter of 1.5mm. Due to the high viscosity and low fluidity, some parameters need to adjust to avoid to high pressure. After some initial experiments, the parameter setting for the direct spinning from the mini-extruder were: first stage mixing step at 90^{o}C for 3min and 100rpm, followed by a second mixing step at 140^{o}C for 1min and 100rpm, finally followed by spinning at 20-30rpm.

Based on the processing experience for PVA1799 using the mini-extruder, we now aim to transfer this technology to a twin-screw extruder (Dr. Collin Twin-Screw Kneader ZK 25 x 42 L/D, with melt pump) (see photograph below).

Photograph 5.1: Dr. Collin Twin-Screw Kneader ZK 25 x 42 L/D.

First, we pre-mixed the PVA1799 with PTFE suspension and added a little extra water. Left the blend overnight until the PVA had fully absorbed the water with no liquid water presenting. In this case, the water, as a plasticiser, has completely interacted with the PVA molecules forming hydroxyl bonds with PVA, while at the same time lowering the melting temperature and viscosity of the PVA. The water content was measured by TGA. Because processing is performed below the melting temperature of PVA1799, the viscosity is high, which creates high pressures in the twin-screw extruder. Temperatures were respectively set at 90^{o}C, 100^{o}C, 110^{o}C, 120^{o}C, 130^{o}C and 140^{o}C together with a residence time of about 2min. Because the processing window of PVA1799in water is narrow, only 90^{o}C was acceptable. The fibre die used was a three-hole die with a diameter of 3mm. As-spun filaments were collected directly without pelletizing because the compound was too soft for pelletizing as a result of the presence of water. Filaments were therefore first dried in an oven at 70^{o}C for 3hrs until fully dry and subsequently pelletized.

Compression moulding for film, post-drawing for tape and tensile testing were as the same as described in Chapter 3.

5.2.2.4 Removal of ethylene glycol

For this the blend fibres were immersed in methanol for 24hrs, removed from the methanol and left to dry at room temperature for 48hrs to evaporate the methanol that remained on the fibres.

5.2.2.5 Hot drawing of blend tapes

The drawing steps are basically the same as for blend tape described previously, except we drew fibres both before and after removing the plasticizer. The maximum draw ratios of the fibres before and after the removal of the plasticizer were quite different and much lower after the removal of plasticizer.

5.2.2.6 Plasticized PVA1799/PTFE/EG processed by twin-screw extruder

Because the processing window of PTFE/PVA1799 with water as a solvent is narrow and water evaporates during compounding, here ethylene glycol (EG) was used instead of water. Before moving to the twin-screw extruder, again some initial experiments were performed to evaluate the processability of this EG based system in the mini-extruder. After trying different temperatures and concentrations, we were able to spin pure PVA1799 fibres from solutions of 50wt.% EG, at 170^{o}C and a residence time of 3min at 50rpm. The diameter of the fibres was 1.20mm before draw down, while the final as-spun fibres had a diameter of 0.28mm, hence a drawdown of 18.

Next, the processability of the PTFE/PVA1799/EG was investigated in the mini-extruder. Blends of PVA1799 and PTFE suspension were mixed with EG. In this blend system, EG: PVA was 1:1 w/w, while the PTFE: PVA ratio was set at 3:7 w/w. After some trials, the extrusion temperature was set at 170^{o}C, the residence time at 5min, with a screw speed of 100rpm. The diameter of the fibres was 1.6mm before draw down in spinning and the diameter of the as-spun fibres was around 0.75mm, leaving a draw down ratio of around 5. From these

initial experiments in the mini-extruder, it was concluded that good quality PVA1799 and PTFE/PVA1799 filaments could be spun using this plasticized PVA system together with EG.

After these successful initial trials in the mini-extruder, we now aimed to transfer this technology to the twin-screw extruder. Again, first, pre-mixed PVA1799 pellets with PTFE suspension and then dried it in an oven at 80°C for 2 days.

A metering pump was used to feed the ethylene glycol into the twin-screw extruder. Before processing, the ethylene glycol flow was measured as a function of pump rate (Figure 5.1)

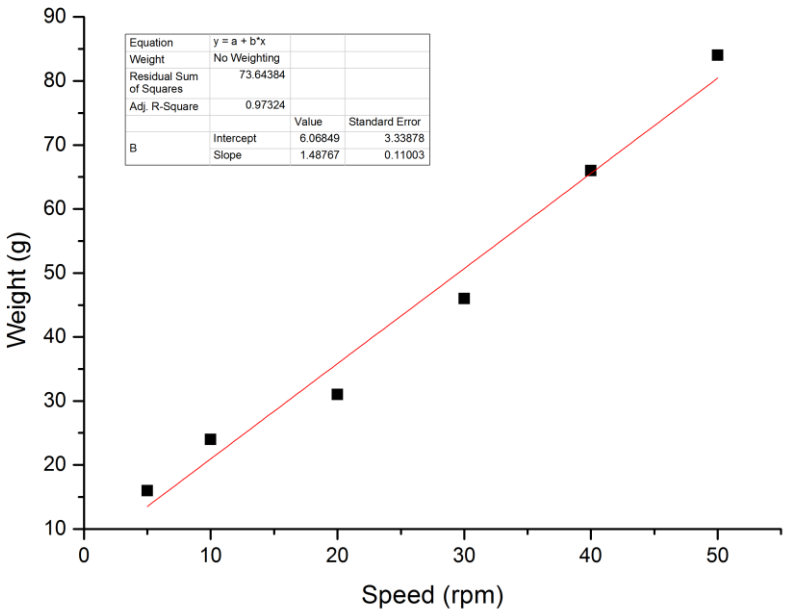

Figure 5.1: Pumped weight of EG as a function of pump speed and fitted linear function equation.

Using the linear fit function of Origin, we could obtain the feeding rate for ethylene glycol as:

$$y = 1.48x + 6.1$$

After a few sets of experiments and adjustments, eventually, the PVA was spun at 175 ^{o}C using a PVA: EG ratio of 5:5.

For the processing of the PTFE/PVA1799/EG system, the temperature was set at 175^{o}C for a composition of (PVA+PTFE): EG = 3:7. Although the spinning line ran smoothly in general, there was a minor problem in that the spinning line was not stable enough to continuously spin for at least 10min because of bubble formation in the filaments. Although the materials were dried for days, we still believe this was due to some residual water. TGA tests were therefore used to study this phenomenon and solve the problem.

In TGA, two sets of samples were tested: sample 1, PTFE/PVA1799 dried at 80^{o}C for 2 days; sample 2, PTFE/PVA1799 dried at 120^{o}C for 2 days. Both blends were tested from room temperature to 120^{o}C at a heating rate of 5^{o}C/min, followed by an isothermal dwell for 30min and then again heating to 400^{o}C at 5^{o}C/min in N_2, followed by a burning up step by heating at 50^{o}C/min until 1000^{o}C in air.

After many experiments, the temperature settings for the spinning of PTFE/PVA/EG in the twin-screw extruder was: zone 01 - 170^{o}C, zone 02 - 175^{o}C, zone 03 - 175^{o}C, zone 04 - 169^{o}C, zone 05 - 169^{o}C, zone 06 - 175^{o}C, zone 07 - 177^{o}C, zone 08 - 170^{o}C; n = 200rpm; and MF=2.71kg/h.

5.3 Results and discussions

5.3.1 Thermal behaviour of plasticized PVA1799

Figure 5.2 shows a TGA scan for PVA1799. Weight drops only slowly up to a temperature of about 210°C, after which it drops faster until about 450°C. The first stage of weight reduction is associated with water loss, while the second stage is associated with polymer degradation. To confirm this assumption, we held the temperature constant at 60°C for 30min to specifically study the water loss and at 200°C for 30min.

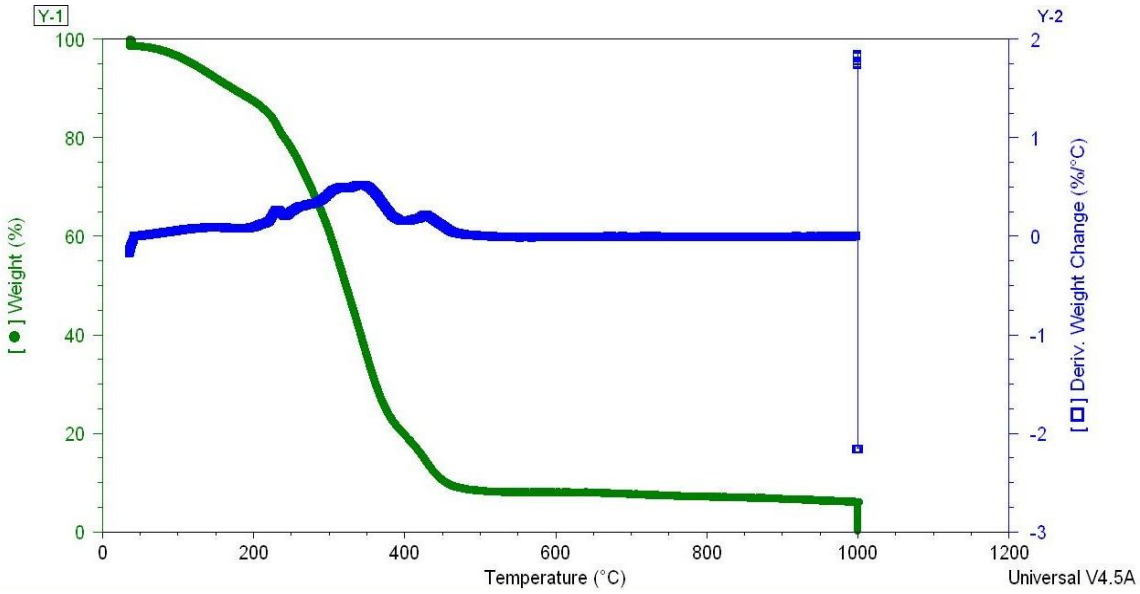

Figure 5.2: TGA scan of PVA1799 when heating at a rate of 5°C/min, showing the decomposition temperature of PVA1799.

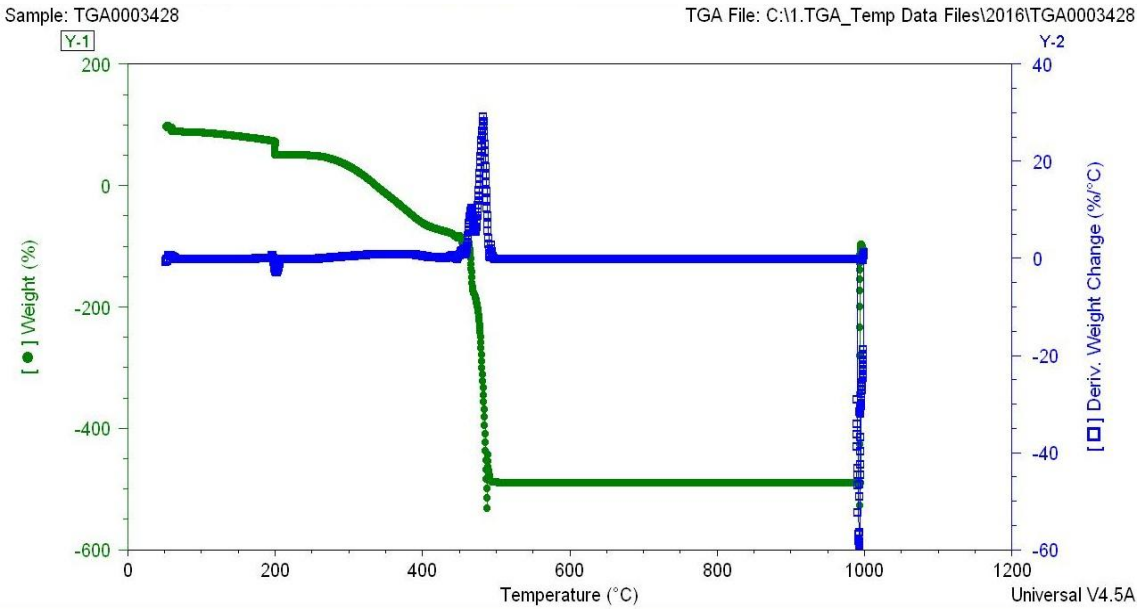

Figure 5.3: Isothermal TGA scan at 60°C and 200°C of PVA1799.

From the isothermal TGA scan in Figure 5.3, we can see that weight loss is limited until 200°C, confirming that the weight loss observed during continuous heating in Figure 5.2 is the result of water evaporation. There is a small weight loss at 200°C, which we could consider as the start of decomposition. After holding for 30min, the weight loss is still minor until weight starts to drop at around 270°C, indicating that here significant degradation occurs. The final sharp weight drops at around 500°C relates to carbonisation.

From these TGA experiments, we could conclude that the blend is processable for temperatures below 200°C. Considering the possible oxidisation without nitrogen protection, a processing temperature below 180°C seems to be more realistic. This actually had already been confirmed in our spinning experiments, which showed discolouration of PVA at temperatures of around 175°C.

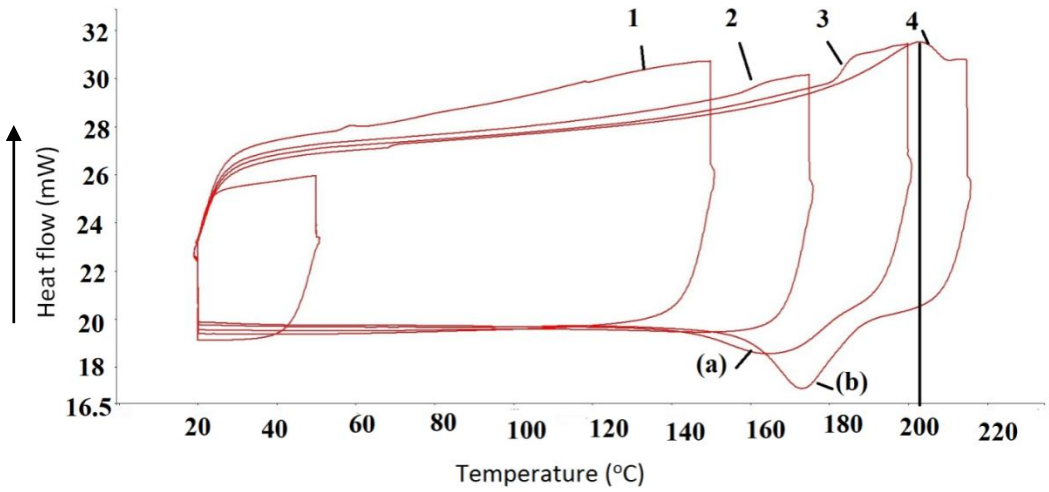

Figure 5.4: DSC scan for PVA1799 with four heating and cooling cycles.

Cyclic DSC experiments were performed to investigate the change in melting temperature and crystallinity with heating as a result of a reduction in plasticizer content. From the DSC experiment in Figure 5.4, we can see that PVA1799 starts to melt at 180 ^{o}C, with a melting point at about 205^{o}C. Comparing peak (a) and peak (b), we can also observe that the crystallization temperature and crystallinity of PVA1799 increased in the 4th cycle, indicating that now the plasticiser is partly extracted from the PVA at this high temperature. In cycle 3 and cycle 4 we can see that melting starts at around 180 ^{o}C in cycle 3 while it does not even start to melt in cycle 4 at that temperature. Along with the loss of plasticiser, the melting temperature shown in cycle 4 is almost the same as for pure PVA. The melting temperature of PVA1799 is shown below.

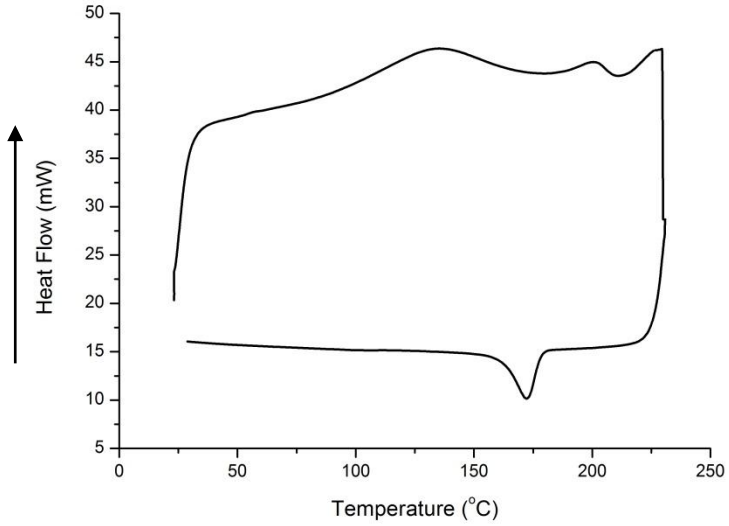

Figure 5.5: DSC scan for PVA1799 (one cycle).

Figure 5.5 shows an increase of heat flow, reaching its peak at around 135°C, which is related to the evaporation of water. Meanwhile, another peak starts at 175°C and reaches its peak at about 200°C. This is the melting peak of PVA1799. The next peak starts at around 220°C and keeps increasing but does not reach a peak at the maximum heating temperature, which is related to polymer degradation. Therefore, we can see that PVA1799 starts to melt at a lower temperature than pure PVA and has a melting peak slightly below that of pure PVA at around 200°C. This shows that the extent of plasticization in PVA1799 is not sufficient. From TGA and DSC tests, we can learn that the melting temperature of PVA1799 is fine for low-temperature solution spinning; but for melt-spinning process, additional plasticization is required. Otherwise, melt spinning is not possible because the melting temperature is higher than the decomposition temperature meaning that the polymer will decompose before melting.

5.3.2 Plasticizer of PVA1799

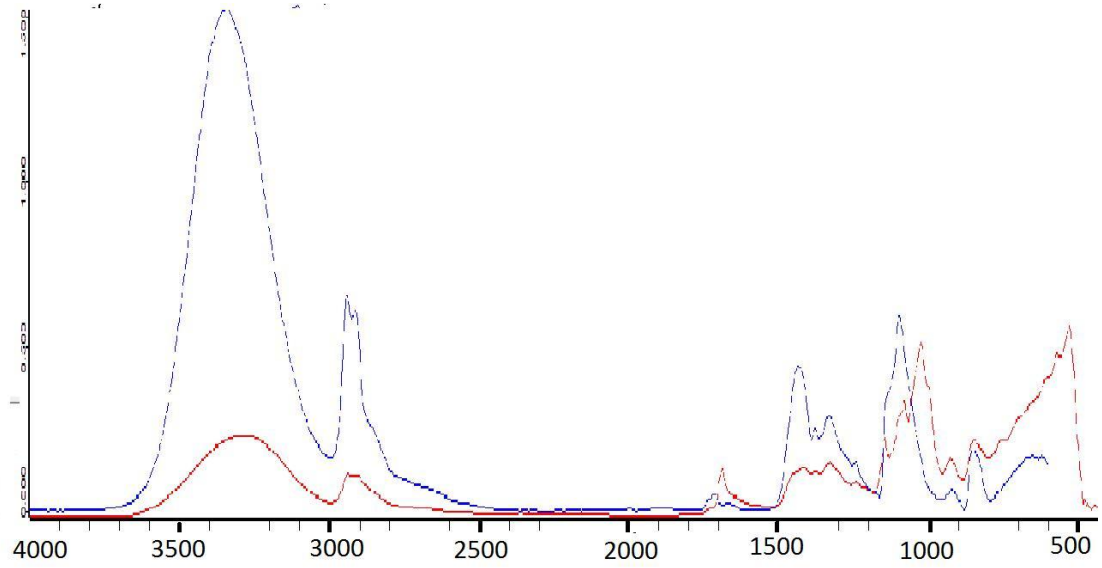

3 Hits	Hit Quality	Compound name	Entry No.	Molecular formula	Molecular weight	CAS number
1	300	Poly(Vinyl alcohol)	348	C2H4O1		9002-89-5
2	296	Glycerol	106	C3H8O3	92.1	56-81-5
3	208	Glycerol	106			

Figure 5.6: FTIR spectrum of PVA1799.

Although the information on the plasticiser used in PVA1799 is not clear, we mentioned in the literary review already that the most common plasticiser for PVA is glycerol [68] [69] [70]. FTIR data of PVA1799 shown in Figure 5.6 revealed that indeed the components of PVA1799 are PVA and glycerol.

5.3.3 Fibre formation before and after drawing of films made by twin-screw compounding

5.3.3.1 PTFE/PVA1799/water system

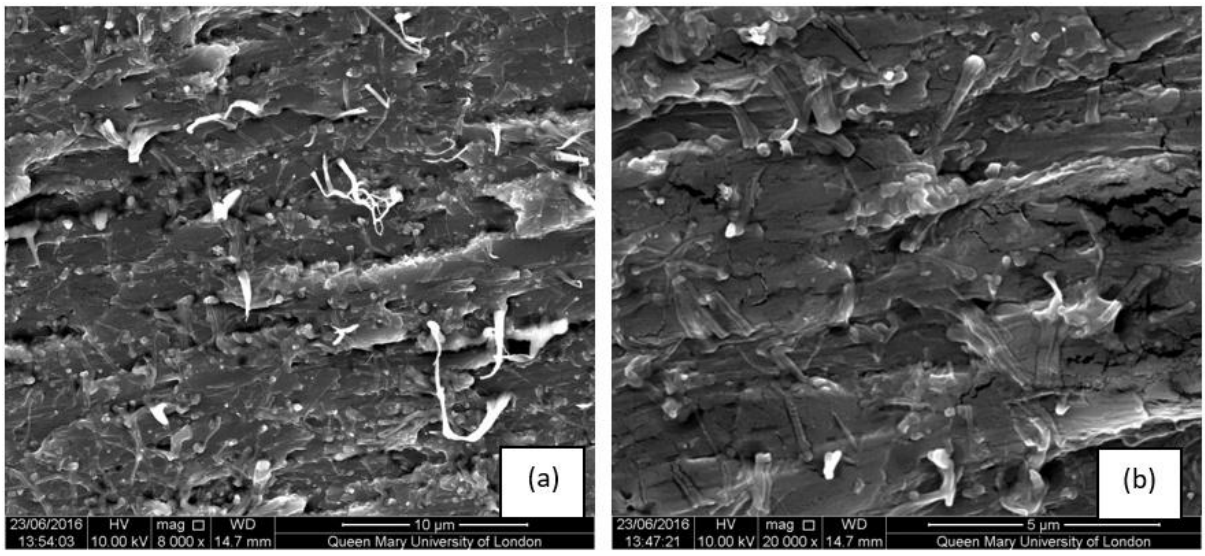

Figure 5.7: SEM images of cold fractured cross-sections of PTFE/PVA1799 tape made from compression moulded film of PTFE/PVA1799/water compounded in a twin-screw extruder.

Figure 5.7a shows the morphology of a post-drawn tape made from a compression moulded film of PTFE/PVA1799 compounded using water as a plasticizer in a twin-screw extruder. In this sample, even after compression moulding there are many short fibres still present in the matrix. These fibres were formed as result of the drawdown during extrusion. After compression moulding the dispersion of PTFE fibres is still homogeneous but now isotropic. In Figure 5.7b, we can see that the length of the fibres in this sample is around 1-2µm, and that the diameter is at least below 200nm with the exception of some agglomerated fibres.

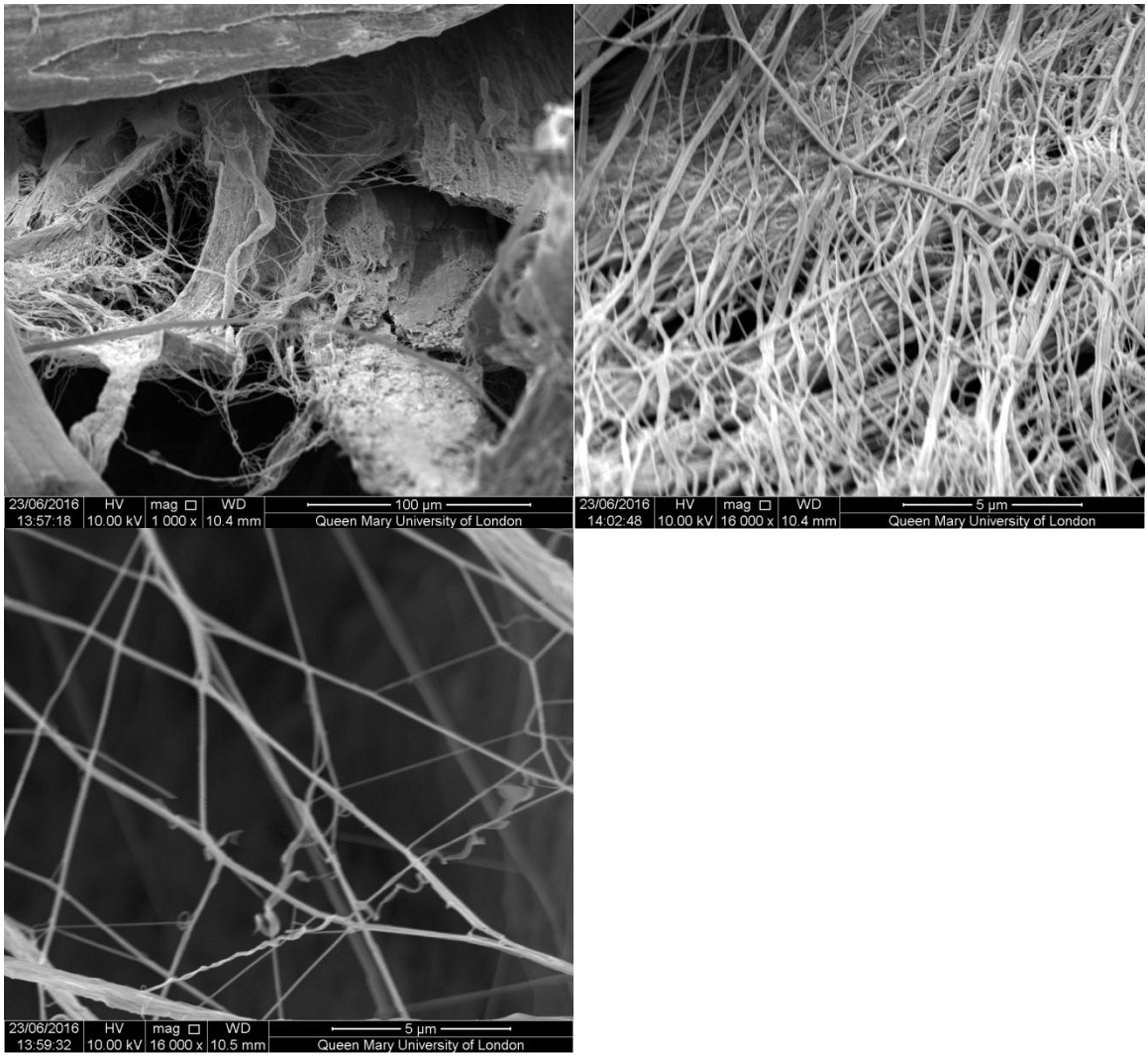

Figure 5.8: SEM images of cold fractured cross-sections of drawn PTFE/PVA tapes from compression-moulded films from PTFE/PVA1799/water system processed using a twin-screw extruder.

Figure 5.8 shows the morphology of the tapes after post-drawing of the PTFE/PVA1799 film. It can be seen that these isotropic films after post-drawing have almost completely been converted into a highly fibrillar structure. Because of the uniform dispersion of PTFE particles in the twin-screw extruder followed by a drawdown during spinning, there are no undrawn PTFE particles left in the blend after solid-state drawing according to these SEM observations. Moreover, Figure 5.9 shows clearly two separated phases in these samples, a

PVA matrix phase and the PTFE fibre phase. From this, we can conclude that PTFE fibre formation is highly effective in this PTFE/PVA1799/water system as processed by twin-screw extrusion. Therefore, from a PTFE nanofibres fabrication point of view, this methodology seems very interesting for industrial scale up.

5.3.3.2 PTFE/PVA1799/EG system

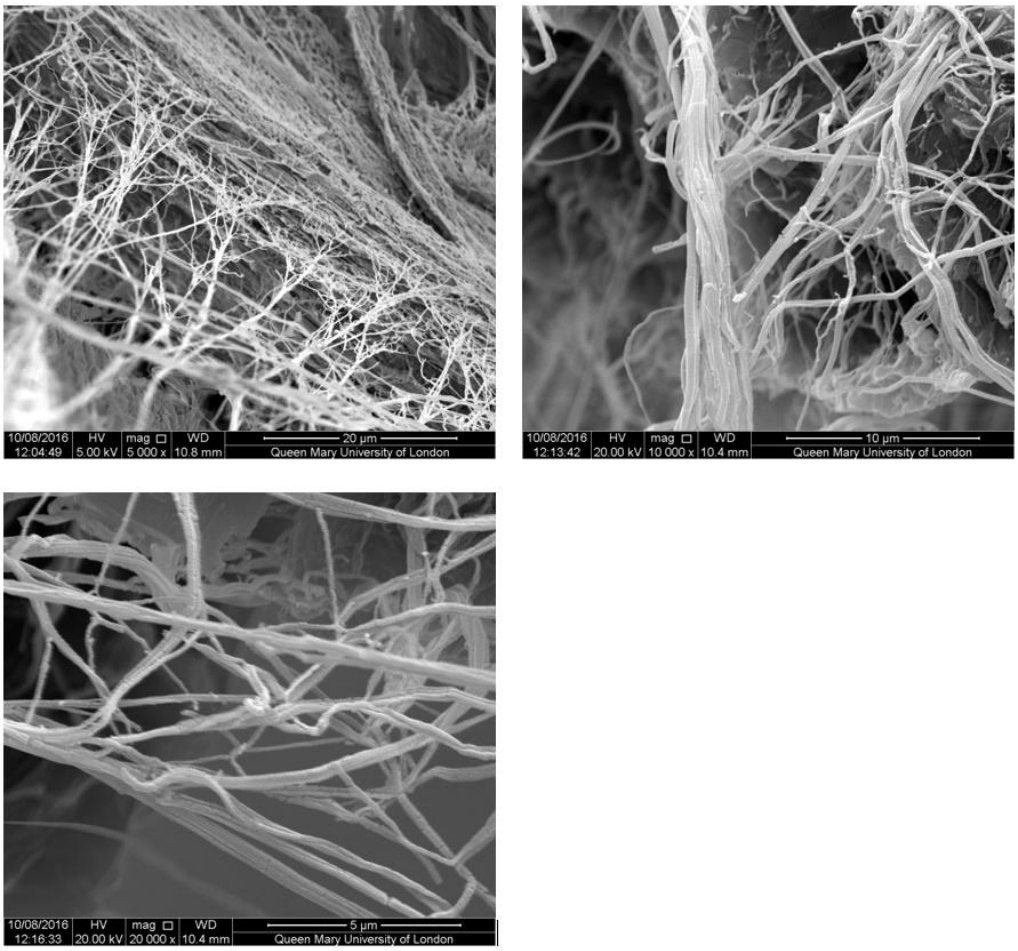

Figure 5.9: SEM images of cold fractured cross-section of drawn PTFE/PVA tapes processed from compression moulded PTFE/PVA1799/EG films processed using a twin-screw extruder (λ=4).

Figure 5.9 shows a highly fibrillar structure of PTFE/PVA tapes after extraction of EG and drawing the compression moulded films. PTFE fibres in these tapes are fairly uniform in size and highly elongated without any remaining undrawn particles.

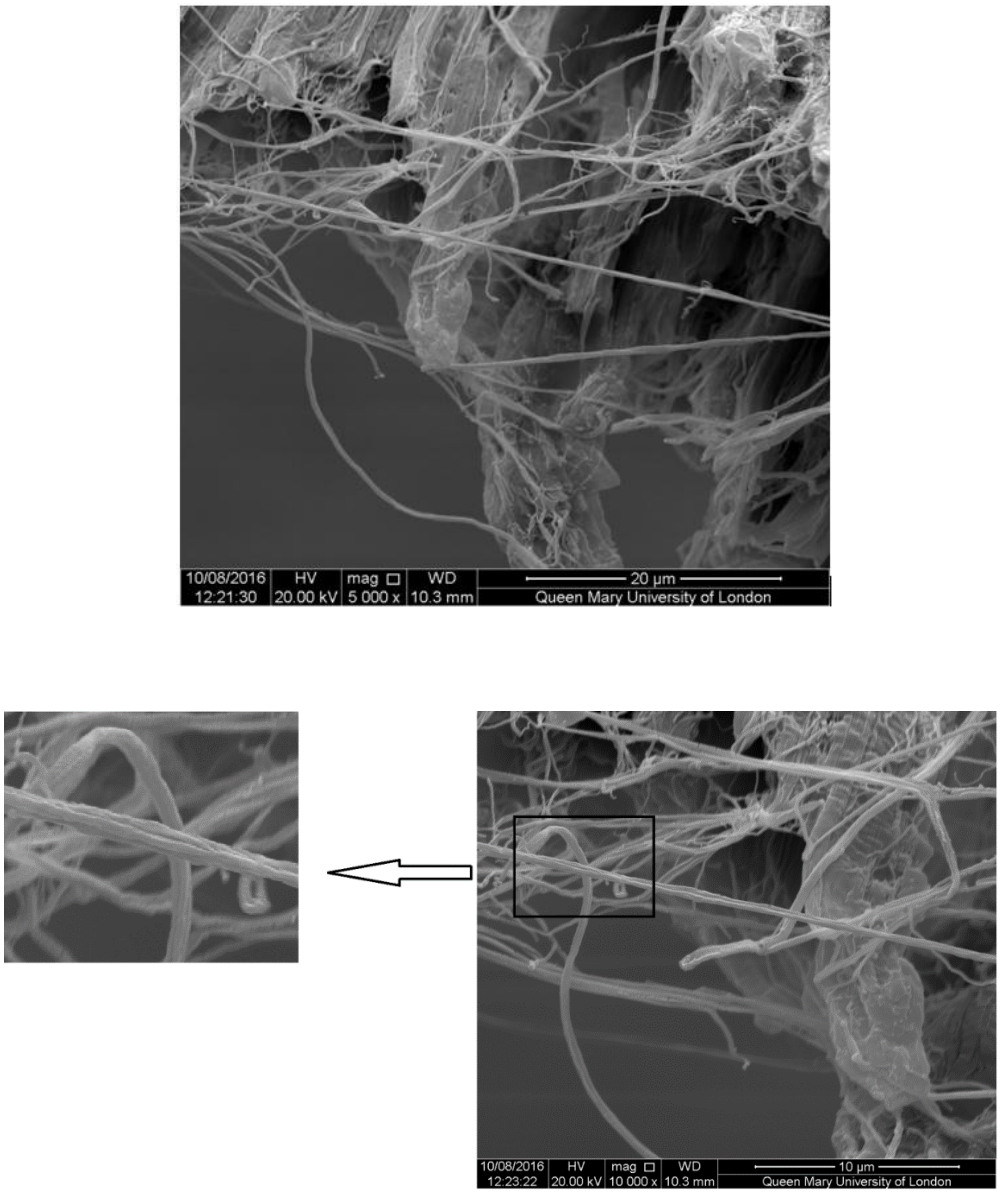

Figure 5.10: SEM images of cold fractured cross-section of drawn PTFE/PVA tapes from compression moulded PTFE/PVA1799/EG film processed using a twin-screw extruder (λ=4)

Figure 5.10 illustrates the fibre formation of long fibres after drawing of the films with the EG extracted. From the zoomed in area of these long fibres, we can see that the PTFE fibres are actually fibre bundles of aggregates of single fibres. These PTFE fibres can reach lengths over 30µm while the diameter is still sub-micron at about 500nm.

In the previous experiment the EG was removed from the compression moulded films before drawing. Here, we report on the effect of the presence of EG on fibre formation behaviour in the blends. Figure 5.11 shows that the structure of a drawn blend tapes with EG still present in the sample.

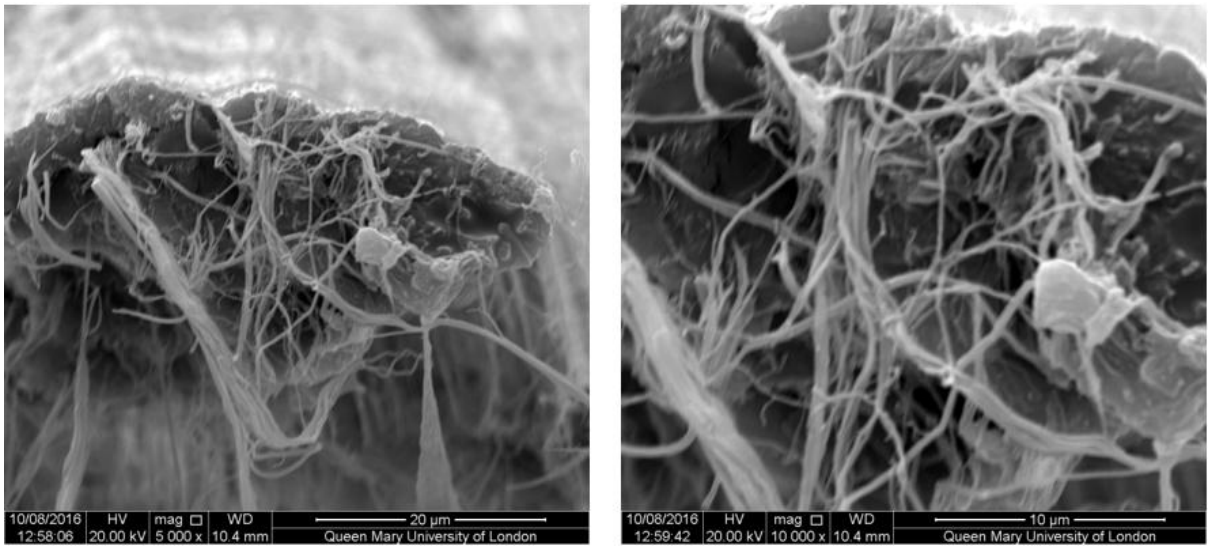

Figure 5.11: SEM images of cold fractured cross-section of drawn PTFE/PVA/EG tape processed from compression moulded PTFE/PVA1799/EG film using twin-screw extrusion (λ=4) (before EG extraction).

The fibre formation behaviour with EG present is clearly different from the structure shown in Figure 5.9 where EG was removed prior to drawing. Before removing the EG from the

blend fibres, most of the PTFE was drawn into fibres while the PVA basically remains as an isotropic matrix. The presence of ethylene glycol prevents the PVA from becoming fibrillar. Instead, it remains as an isotropic matrix, with PTFE fibres embedded in this matrix. Some of these fibres could even reach lengths of 50µm. However, we also notice that the number of fibres is much lower, indicating the presence of undrawn particles. This is also shown in Figure 5.12, where we can see some long fibres together with many undrawn PTFE particles.

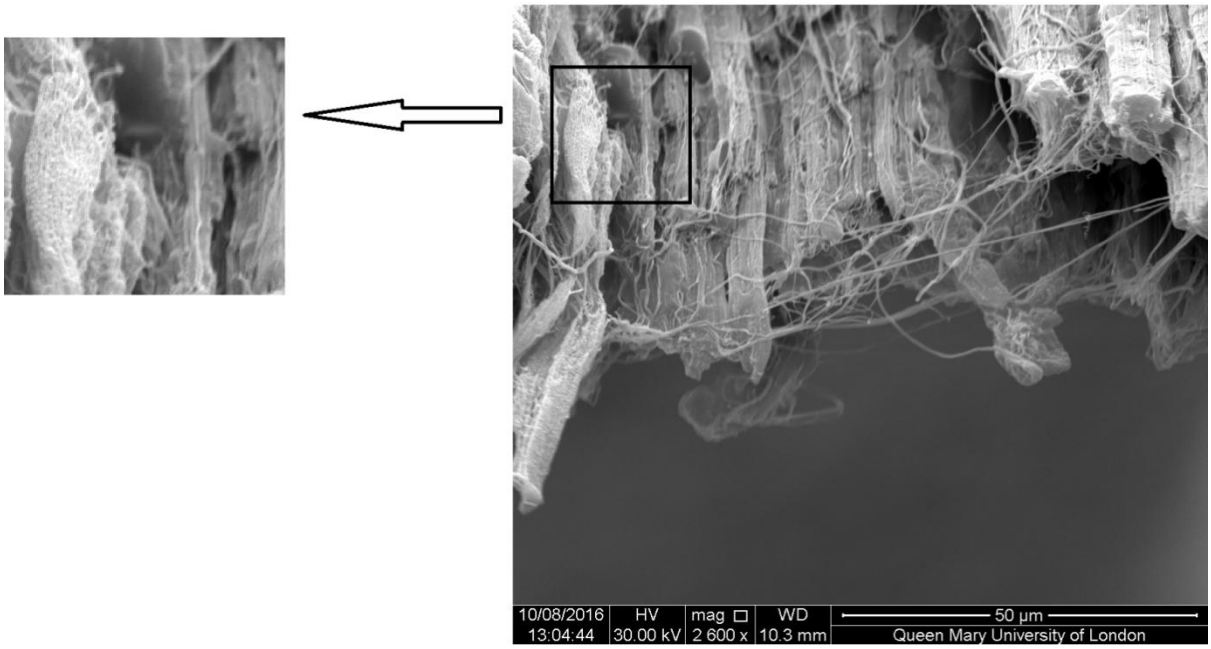

Figure 5.12: SEM images of cold fractured cross-section of drawn PTFE/PVA/EG tape processed from compression moulded PTFE/PVA1799/EG film using twin-screw extrusion (λ=4) (before EG extraction).

These experiments show that it may be beneficial to extract the EG prior to drawing, although extraction will also affect the draw ratio, while fibre formation may actually be better. Unless there is some special requirement for long PTFE nanofibres, we can still process using solid-state drawing with the EG present, but the fibre yield might be low.

5.3.4 Summary of solid-state drawing and draw ratio

Figure 5.13 shows and overview of the maximum draw ratio achieved for all the systems investigated. Sample 1 shows excellent drawability, presumably because of the remaining ethylene glycol, which reduces the molecular interactions between PVA chains. However, because of the presence of ethylene glycol, there is a concern that the plasticizer may affect the interaction between PVA and PTFE, leading to poor stress transfer and a higher fraction of undrawn PTFE particles. This was indeed confirmed by SEM in Figure 5.12, which showed a large number of undrawn PTFE particles in the system with the EG still present.

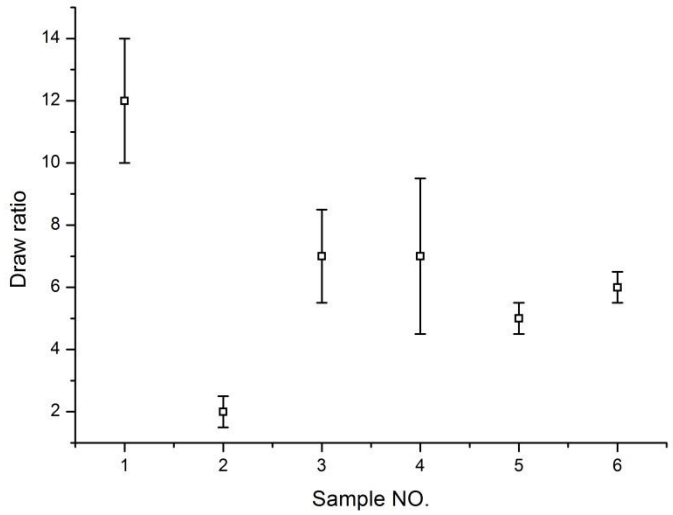

Figure 5.13: The maximum draw ratio of: 1. PTFE/PVA1799/EG fibres before extraction (mini-extruder); 2. PTFE/PVA1799/EG fibres extracted with methanol and dried in an oven at 80^{o}C (mini-extruder); 3. PTFE/PVA1799/EG fibres extracted with methanol and dried at room temperature (mini-extruder); 4. PTFE/PVA1799/water filament (without compression moulding) dried in an oven (twin-screw extruder); 5. PTFE/PVA/water tape (solution casting); 6. PTFE/PVA/water tape (mini-extruder)

For sample 2, we can see that the drawability is very poor. This is because of the drying process in the oven. When the samples are dried in an oven at 80^{o}C for 24hrs, not only methanol and possibly ethylene glycol is evaporated, but also annealing occurs, leading to crystal growth and an increase in crystal size and crystallinity. As a result, this sample becomes brittle and the draw ratio drops. Compared to sample 2, sample 3, which was dried at room temperature, exhibits a much better drawability. Sample 4 has a similar draw ratio to sample 3, however, because the filament diameter of sample 4 is much bigger than for sample 3, sample 4 may potentially exhibit the higher draw ratio. This is because the drawability of PTFE/PVA blend is not only dependent on the intrinsic drawability of the PVA but also affected by the size of the PTFE agglomerates. When the diameter of the fibre becomes smaller, the value of $d_{agglomerate}/d_{fibre}$ increases.Since the size of the PTFE agglomerates is affected by dispersion, the value of $d_{agglomerate}/d_{fibre}$ basically only varies with fibre diameter. Therefore, although the average draw ratios of sample 3 and sample 4 are very close, sample 4 still exhibits the highest maximum draw ratio.

Figure 5.14 compares the draw ratio of all samples, showing that the draw ratio of samples with ethylene glycol is somewhat higher than that of samples with only water. Interestingly, even with the plasticisers removed from the blend, the effects on crystallinity still remains. With the addition of ethylene glycol, the drawability of the blend could be doubled.

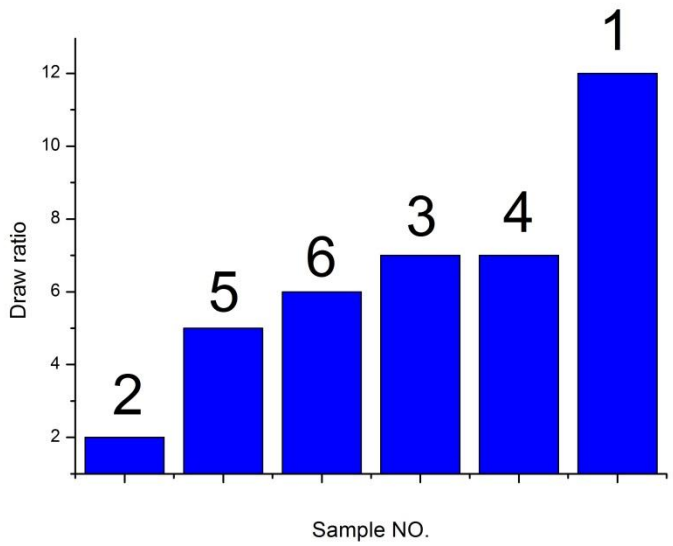

Figure 5.14: Comparison of maximum draw ratios of all samples (the sample numbers are similar to those mentioned in Figure 5.13).

5.3.5Tensile properties

Table 5.1 shows that the PTFE/PVA1799/EG fibre sample has a much higher Young's modulus than all other samples and that its value almost reaches the theoretical Young's modulus calculated by the parallel (Voigt) model (see Figure 3.6), indicating that this sample exhibits both an excellent dispersion morphology as well as highly oriented and long PTFE fibres.

Table 5.1: Young's modulus of all samples (λ = 4).

Sample details	Sample No.	Modulus (GPa)
PTFE/PVA1799/water fibres via twin-screw extruder	1	0.22
PTFE/PVA1799/EG fibres via mini-extruder	2	10.24
PTFE/PVA/water tapes via casting	3	2.63
PTFE/PVA/water tapes via mini-extrusion	4	3.06
PTFE/PVA/water tapes via two-step mini-extrusion	5	8.67
PTFE/PVA/water fibres via two-step mini-extrusion and spinning	6	5.00

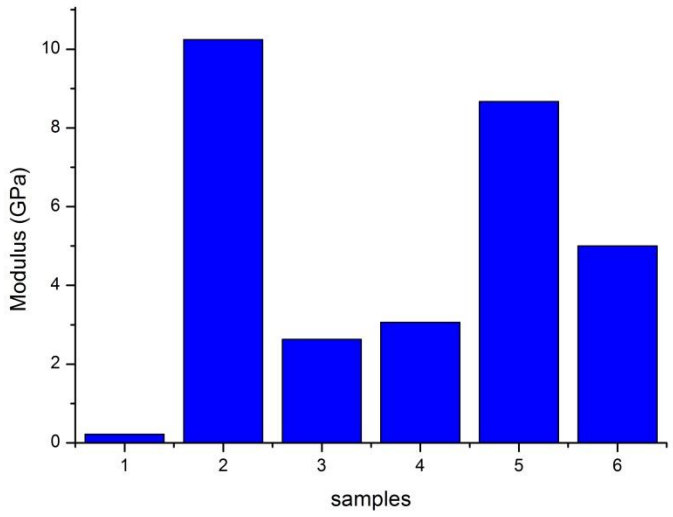

Figure 5.15: Comparison of the Young's modulus of all samples (λ=4).

Generally speaking, sample2 processed with ethylene glycol (EG) shows the highest modulus value. This is because hydrogen bonds exist in the crystal lattice of PVA, resisting shear

deformation and intermolecular chain slippage. Therefore, the unfolding of lamellae is restricted during the solid-state drawing. Moreover, the presence of EG increase the number of hydrogen bonds compared to samples processed in water. The increasing values of modulus for samples 3, 4 and 5 are the result of improved dispersion situation and mixing morphology, as was discussed in previous chapters. The lowest modulus was obtained for the PVA/PTFE/water sample processed by twin-screw extrusion, probably due to void formation in the blend fibres as a result of the evaporation of water. In contrast to the mini-extruder, there is no degassing zone present in our twin-screw extruder machine to remove the steam from water evaporation.

5.3.6 Water content in PTFE/PVA1799 blends

Figure 5.16 shows the TGA scan for the PTFE/PVA1799/water blends, while Figure 5.17 shows a scan for a system with EG. As mentioned before we believe that the weight loss below 200^{o}C originates from the evaporation of water, indicating that a significant amount of water is present in the blend (4wt.%). When the temperature reaches around 190^{o}C, the weight loss rapidly increases. Since at that temperature there should be little remaining water in the sample, further weight loss should be the result of PVA degradation. When the samples are heated isothermally at 120^{o}C, can also see a dramatic weight loss. Considering the temperature involved, this is obviously the result of water evaporation. Therefore, from these TGA tests we can conclude that both samples 1 and 2 contain about 4wt.% of water, even after the samples were pre-dried for 2 days. Residual water is detrimental to the fibre spinning operation since steam and bubble formation will affect the continuous spinning process.

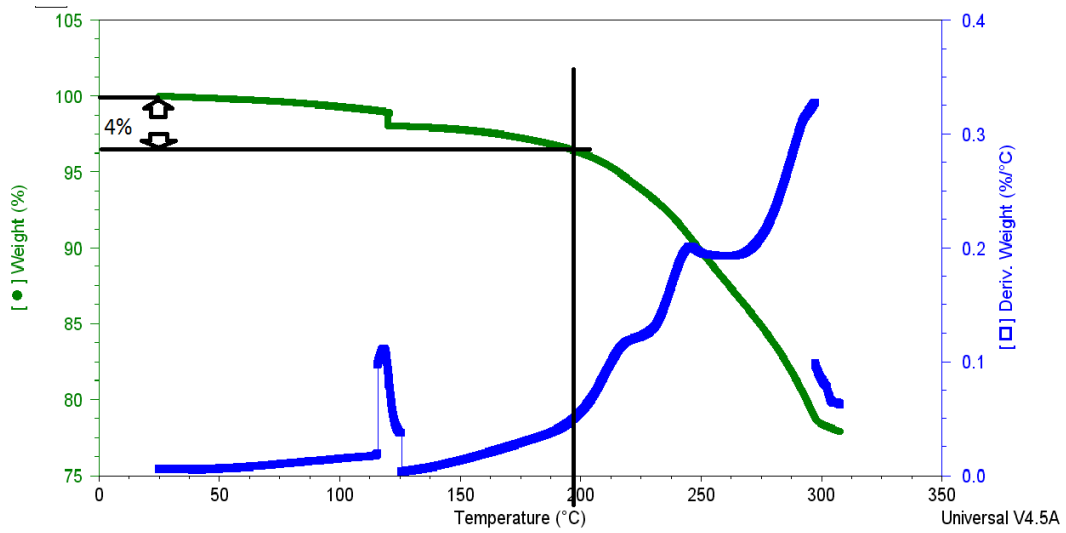

Figure 5.16: TGA scan of sample 1 dried at 80 °C for 2 days, showing significant weight loss as a result of residual water.

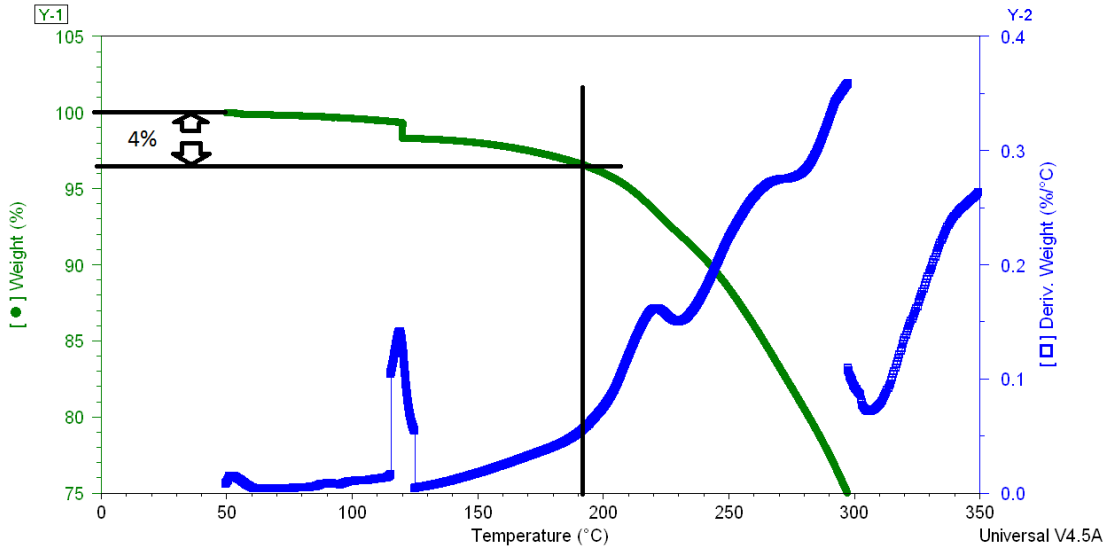

Figure 5.17: TGA scan of sample2 dried at 120 °C for 2 days, showing significant weight loss as a result of residual water.

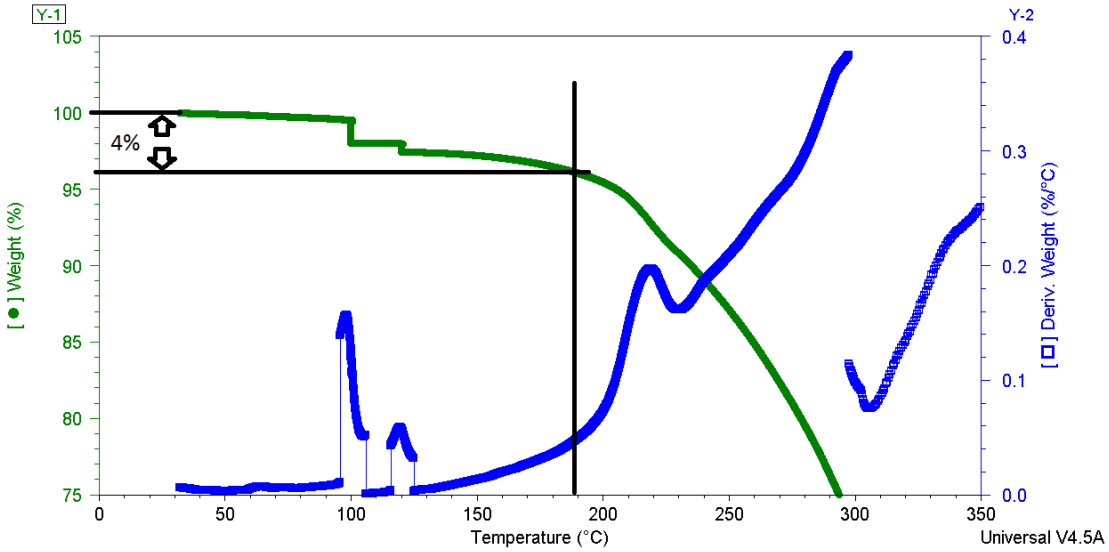

Figure 5.18: Isothermal TGA scan for sample 2 dried at 120 °C tested at 100 °C for 2hrs to remove water in the TGA furnace.

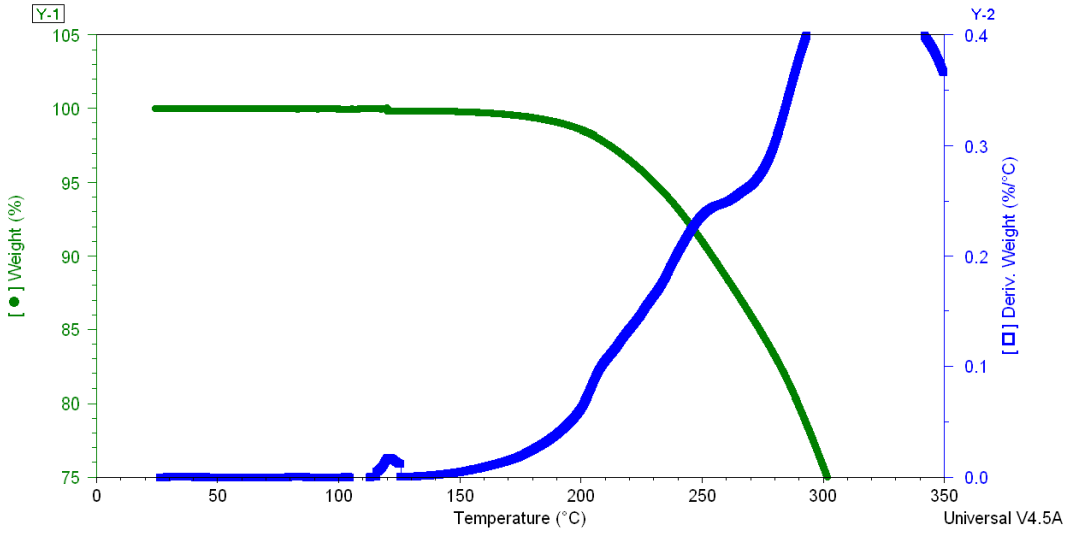

Figure 5.19: TGA scan of sample 2 dried at 120 °C for 2 days and tested immediately after drying, showing no weight loss up to 190 °C.

From the TGA scan shown in Figure 5.18 we can see that the main water loss happens in the isothermal stage at a temperature of 100^{o}C. Compared with the previous two TGA results (Figure 5.16, 5.17), the weight loss at 120^{o}C and between 120^{o}C and 190^{o}C is much smaller.

Figure 5.19 shows a TGA scan that is run immediately after drying, leaving no time for water uptake from the air. In this case, no weight loss is observed which indicates that all the water is removed by drying. Thus, when the drying is performed around/above 100^{o}C, the drying process itself is efficient. However, it is the water uptake from the air in the sample after drying that subsequently affects the spinning process.

5.4 Conclusions

This chapter describes some of the issues involved with the scale up of the island-in-the-sea PTFE nanofibre spinning process. Both PTFE/PVA/water and PTFE/PVA/EG systems could be scaled up to twin-screw extrusion machinery, while fibre formations after post-drawing was excellent with PTFE fibres having uniform dimension and high lengths.

The advantage of the PTFE/PVA/water system is that the processing temperature is low, avoiding potential degradation of PVA, Moreover, these blend fibres showed excellent fibre formation after drawing, while the use of water as a plasticizer is very environmentally friendly, low cost with easy post-processing treatment to remove and recover the water. However, it was found that this system was not very stable and that the processing window was narrow because of water evaporation during processing.

The system of PTFE/PVA/EG showed much better stability as a result of a wider processing temperature window, while at the same time the blends showed better drawing behaviour

and tensile properties. However, the disadvantage of the PTFE/PVA/EG system is that the presence of even small amounts of water in the PVA may lead to processing issues at elevated temperatures, occasionally causing phenomena like bubble and steam formation. Moreover, the additional step of ethylene glycol (EG) extraction with methanol is less convenient and less environmentally friendly than a system based only on water.

Chapter 6

Conclusions and future work

6.1 Conclusions

According to the studies and results described in this thesis, we believe that it is possible to fabricate PTFE nanofibres using a modified island-in-the-sea method. In this method, PTFE particles from suspension are dispersed in a PVA/water solution. After mixing a morphology of PTFE particles in a PVA matrix is obtained, which after solid-state drawing at elevated temperatures but below the melting temperature of PVA and PTFE results in a highly fibrillar structure of ultrathin PTFE fibres in a PVA matrix. After removal of the PVA matrix in water, the ultrathin PTFE nanofibres could be obtained.

The thesis reports on the optimization of a number of material and processing parameters for this method, including the evaluation of different methodologies to obtain homogeneous dispersions of PTFE particles in PVA/water solutions, the selection of optimal PTFE/PVA blend compositions, the optimization of spinning and post-drawing conditions, and the use of plasticizers to increase processing windows etc. Results showed that the optimal blend composition for homogeneous dispersions lies between 12vol.% and 19vol.% PTFE in PVA, while the optimal drawing temperature was around 100^{o}C.

PTFE nanofibres produced through this method had diameters of 50 nm or lower, while their length could be up to 10µm in the case of agglomerated PTFE particles. After dissolving the PVA and filtration, the remaining nanofibres were confirmed as neat PTFE nanofibres by EDS and FTIR. Meanwhile, XRD showed that these nanofibres were also highly orientated at a molecular level.

PTFE/PVA blends could be directly spun using a lab-scale mini-extruder into as-spun fibres with a draw-down of around 4. After subsequent solid-state drawing at elevated temperatures, the final PTFE/PVA blend fibres had a diameter of around 0.3mm. These PTFE/PVA blend fibres could also be produced at a larger pilot-scale using twin-screw extrusion, with these fibres showing excellent PTFE nanofibre formation.

Besides extrusion compounding, the process of dispersion casting was also investigated. Here the dispersion state of PTFE particles in the PVA was rather poor, with this poor state of dispersion affecting further PTFE nanofibre formation and tensile properties of the PTFE/PVA blend fibres or tapes. Poor dispersion not only lead to the formation of PTFE fibres bundles rather than individual PTFE nanofibres but also was responsible for plenty of undrawn PTFE particles after solid-state drawing.

The dispersion morphology of PTFE particles in PVA could be greatly improved with extrusion compounding, resulting in a significant reduction of undrawn PTFE particles after post-drawing. Also the drawing behaviour of the PTFE/PVA blend processed by extrusion compounding was improved. However, blend morphology and subsequent fibre formation together with the mechanical properties of the PTFE/PVA blend fibres were still not optimal for this single-step compounding based process.

Therefore, a two-step compounding method was developed that lead to significantly improved dispersions of PTFE particles in PVA and very few undrawn PTFE particles after solid-state drawing. Moreover, also the tensile properties of the PTFE/PVA blend tapes and fibres were significantly increased. For example, the Young's modulus of the PTFE/PVA blends with 12vol.% and 19vol.% PTFE got very close to the upper-bound values predicted by the parallel Voigt model.

In order to increase the processing window in twin-screw extrusion the use of ethylene glycol (EG) as a plasticizer was investigated. The advantage of water as a plasticizer is that it is very environmentally friendly, while the water can also be removed and recovered very easily. However, the disadvantage of water is that the processing window of such a PVA solution becomes very narrow since water evaporates fast during processing at high temperatures.

The advantage of EG over water is its much larger processing window, resulting in more stable extrusion and spinning operations. Moreover, PTFE/PVA blends processed with EG could be post-drawn to higher draw ratios and exhibited better mechanical properties. However, the EG system showed to be very sensitive to residual water in the blend with even the tiniest amount of water absorbed from the air in the PVA leading to bubble formation and fibre breakage during spinning. Hence, careful drying is here essential. An additional extraction step is also necessary for this system, as the EG needs to be extracted from the blend fibre by methanol.

6.2 Future work

In future work, we could focus on three main parts. First, more research is needed for improving and optimizing the large-scale production of PTFE nanofibres using twin-screw extrusion. Secondly, the properties of the PTFE nanofibres need to be further characterized as well as the ability to make non-woven mats from these fibres. Thirdly, the properties of the PTFE/PVA blend fibres should be further studied for potential applications in textiles.

The first research task should focus on the manufacturing of PTFE nanofibres using the island-in-the-sea method in a twin-screw extrusion and spinning line. The PTFE/PVA/EG system seems most suitable for this work. In the case of PTFE/PVA/EG, materials pre-drying and PTFE/PVA premixing are two important factors that need to be addressed before spinning, as remaining water and PTFE particle agglomeration affects the continuous spinning operation. In order to improve the large-scale production of PTFE nanofibres, we could optimize the process through some modifications on the twin-screw extruder, for example, through the addition of a vacuum degassing system that removes possible steam, or by adjusting screw designs. Moreover, we could also try to adjust and modify the extraction step to match the material quantity for large-scale processing. For example, the method of filtration may yield a too low efficiency for industrial scale processes. Because of the significant differences in density of PTFE and PVA/water solution (respectively 2.2 g/cm^3 and 1g/ml), we could try some centrifugal or precipitation driven separation to remove the solution phase directly to increase efficiency.

Once sufficient amounts of ultrafine PTFE fibres have become available, these staple fibres need to be processed into a non-woven mats for applications such as filter membranes, super-hydrophobic textiles etc. By controlling the length of the PTFE nanofibres, they could

also be used in coatings or other systems as an additional fibrous materials to improve some specific properties of polymers. It is expected that future research will be particularly directed towards potential application areas of such PTFE nanofibres and its textiles.

On the other hand, the properties of the PTFE/PVA blend fibres are also worth studying in more detail. Potentially some unique characteristics may arise through combining superhydrophobic and superhydrophilic materials, with both of them having excellent chemical resistance and biocompatibility. Therefore, a study into how these superhydrophobic and superhydrophilic properties can affect each other and how they can be used to control the surface properties of blend fibres is of great interest. Altering the blend morphology could potentially lead to some interesting surface properties of PTFE/PVA blend fibres or films for practical applications in e.g. biomedical products, specialty textiles, biodegradable films and soon.

References

[1] Carlson D, Walter S. Fluoropolymers, organic. Ullmann's encyclopedia of industrial chemistry. VCH, Weinheim. 1988; 393–429

[2] Dishart K T, Creazzo J A, Ascough M R. The DuPont Program on Fluorocarbon Alternative Blowing Agents for Polyurethane Foams. Journal of Building Physics, 1988, 12(2):89-107.

[3] Roy P, Britt P, DuPont, Fluorofinishes. 1938.

[4] Arthur M, American Heritage's Invention & Technology, Schlesinger's syllabus. 2010, 25(3), 42.

[5] Hacker B C. richard rhodes. The Making of the Atomic Bomb. New York: Simon and Schuster. 1988: 886.

[6] Becmeur F, Geiss S, Laustriat S, et al. History of Teflon. European Urology, 1990, 17(4):299-300.

[7] Andrews, David, and Bill W. "Ten years later, chemical safety and justice for Dupont's Teflon victims remain elusive." (2015)

[8] Chmielewski A G, Haji-Saeid M, Ahmed S. Progress in radiation processing of polymers. Nuclear Instruments & Methods in Physics Research, 2005, 236(1–4):44-54.

[9] Sun J, Zhang Y, Zhong X, et al. Modification of polytetrafluoroethylene by radiation—1. Improvement in high temperature properties and radiation stability. Radiation Physics & Chemistry, 1994, 44(6):655-659.

[10] Anonymous. Fluoropolymer Comparison - Typical Properties. Dupont Company,2006[79]

[11] DuPont Teflon PTFE fluoropolymer resin: Properties Handbook [Online] http://www2.dupont.com/Teflon_Industrial/en_US/assets/downloads/h96518.pdf

[12] Lee H, Lee B P, Messersmith P B. A reversible wet/dry adhesive inspired by mussels and geckos. Nature, 2007, 448(7151):338-41.

[13] Klaus H, Tilman Z, Peter C D, et al. Fluoropolymers, Organic.Ullmann's encyclopedia of industrial chemistry.2014.

[14] Takagi Y, Lee J C, Yagi S I, et al. Fiber making directly from poly(tetrafluoroethylene) emulsion. Polymer, 2011, 52(18):4099-4105.

[15] Perepelkin K E, Carbochain Synthetic Fibres. Khimiya, Moscow. 1973: 165-354.

[16] Kabanov V A, Akutin M S, and Bakeev N F. Encyclopedia of polymers. SovetskayaEntsiklopediya, Moscow. 1977

[17] Dorutina T S, Perepelkin K E. Fibres from Fluorine-Containing Polymers. NIITEKhim, Moscow. 1980.

[18] Dorutina T S, Perepelkin V M, et al., Maunfacture and use of fibres with specific properties, VNIIVProekt, Mytishchi. 1980: 3-7.

[19] Ryauzov A N, Gruzdev V A, et al., Chemical Fibre Manufacturing Technology, Khimiya, Moscow. 1980.

[20] Dreizenshtok G S, Loffe A Z, and Gluz M D, Polytetrafluoroethylene Fibres, NIITEKhim, Moscow. 1989.

[21] Perepelkin K E. Fluoropolymer Fibres: Physicochemical Nature and Structural Dependence of their Unique Properties, Fabrication, and Use. A Review. Fibre Chemistry, 2004, 36(1):43-58.

[22] Perepelkin K E. Physicochemical Nature and Structural Dependence of the Unique Properties of Polyester Fibres. Fibre Chemistry, 2001, 33(5):340-352.

[23] Perepelkin K E. Principles and Methods of Modification of Fibres and Fibre Materials. A Review. Fibre Chemistry, 2005, 37(2):123-140.

[24] Horrocks A R, Mcintosh B. 8–Chemically resistant fibres. High-Performance Fibres, 2001:259-280.

[25] Dreizenshtok G S, Gal A É, Sorokin E Y, et al. Destruction of cellulose during the process of sintering fibres from dispersions of polytetrafluoroethylene. Fibre Chemistry, 1984, 15(3):202-204.

[26] Lenz J, Krassig H, et al., EineneuartigeMethodezurHerstellung von Polytetrafluoräthylen-Fasern und -Filamenten, LenzingerBer., 44, 52-58 (1978).

[27] Pugachev A K, Roslyakov O A, Making Fluoroplastic into Articles. Technology and Equipment, Khimiya, Leningrad. 1987.

[28] Goessi M, Tervoort T, Smith P. Melt-spun poly(tetrafluoroethylene) fibers. Journal of Materials Science, 2007, 42(19):7983-7990.

[29] Endo R, Kanamoto T. Superdrawing of polytetrafluoroethylene virgin powder above the static melting temperature. Journal of Polymer Science Part B Polymer Physics, 2001, 39(39):1995-2004.

[30] Takagi Y, Lee J C, Yagi S I, et al. Fiber making directly from poly(tetrafluoroethylene) emulsion. Polymer, 2011, 52(18):4099-4105.

[31] Borkar S, Gu B, Dirmyer M, et al. Polytetrafluoroethylene nano/microfibers by jet blowing. Polymer, 2006, 47(25):8337-8343.

[32] Dasdemir M, Maze B, Anantharamaiah N, et al. Influence of polymer type, composition, and interface on the structural and mechanical properties of core/sheath

type bicomponent nonwoven fibers. Journal of Materials Science, 2012, 47(16):5955-5969.

[33] Ndaro M S, Jin X, Chen T, et al. Splitting of Islands-in-the-Sea Fibers (PA6/COPET) During Hydroentangling of Nonwovens. Journal of Engineered Fibers & Fabrics, 2007, 2(4):1-9.

[34] Kamiyama M, Numata M. Islands-in-sea type composite fiber and process for producing the same: US, US7622188[P]. 2009.

[35] Goda H, Numata M, Kamiyama M, et al. Method of producing islands-in-sea type composite spun fiber: US, US8128850[P]. 2012.

[36] Hwang Y N, Kim W J, Park J H. Island-in-sea fiber, artificial leather and methods for producing the same: US, US20120135653[P]. 2012.

[37] Baker M I, Walsh S P, Schwartz Z, et al. A review of polyvinyl alcohol and its uses in cartilage and orthopedic applications. Journal of Biomedical Materials Research Part B Applied Biomaterials, 2012, 100(5):1451.

[38] Hassan C M, Peppas N A. Structure and Applications of Poly(vinyl alcohol) Hydrogels Produced by Conventional Crosslinking or by Freezing/Thawing Methods[M]// Biopolymers · PVA Hydrogels, Anionic Polymerisation Nanocomposites. Springer Berlin Heidelberg, 2000:247-254.

[39] Kamiya R, Asakura S. Gel-spinning of partially saponificated poly(vinyl alcohol). Journal of Applied Polymer Science, 2015, 77(13):2872-2876.

[40] Cha W I, Hyon S H, Ikada Y. Gel spinning of poly(vinyl alcohol) from dimethyl sulfoxide/water mixture. Journal of Polymer Science Part B Polymer Physics, 1994, 32(2):297-304.

[41] Yang E, Qin X, Wang S. Electrospun crosslinked polyvinyl alcohol membrane. Materials Letters, 2008, 62(20):3555-3557.

[42] Schellekens R, Bastiaansen C. The drawing behavior of polyvinylalcohol fibers. Journal of Applied Polymer Science, 1991, 43(12):2311-2315.

[43] Chen N, Li L, Wang Q. New technology for thermal processing of poly(vinyl alcohol). Gaofenzi Cailiao Kexue Yu Gongcheng/polymeric Materials Science & Engineering, 2014, 30(2):192-197.

[44] Nishino T, Kani S, Gotoh K, et al. Melt processing of poly(vinyl alcohol) through blending with sugar pendant polymer. Polymer, 2002, 43(9):2869-2873.

[45] Famili A, Marten F L, Nangeroni J F. Packaging, molding materials, films, containers: US, US 5206278 A[P]. 1993.

[46] Diaz T C C, Meyer J P G, Cruz C A. Melt-processed blends containing poly(vinyl alcohol): US, US 5744546 A[P]. 1998.

[47] Nishimura H, Donkai N, Miyamoto T. Preparation and thermal properties of thermoplastic poly(vinyl alcohol) complexes with boronic acids. Journal of Polymer Science Part A Polymer Chemistry, 2015, 36(17):3045-3050.

[48] Liu Y L, Chiu Y C. Novel approach to the chemical modification of poly(vinyl alcohol): Phosphorylation. Journal of Polymer Science Part A Polymer Chemistry, 2003, 41(8):1107-1113.

[49] Haralabakopoulos A A, Tsiourvas D, Paleos C M. Modification of poly(vinyl alcohol) polymers by aliphatic carboxylic acids via reactive blending. Journal of Applied Polymer Science, 2015, 69(9):1885-1890.

[50] Barlow A, Campbell R C. Nitric acid digestion and crystallinity of ethylene–vinyl acetate copolymers. Journal of Applied Polymer Science, 1967, 11(10):2001-2006.

[51] Zhang Q Q, Lei S H, Wang X L, et al. Research on Discrimination of 3D Fluorescence Spectra of Phytoplanktons. Spectroscopy & Spectral Analysis, 2004, 24(10):1227-1229.

[52] Wu Q, Chen N, Wang Q. Crystallization behavior of melt-spun poly(vinyl alcohol) fibers during drawing process. Journal of Polymer Research, 2010, 17(6):903-909.

[53] Jang J, Dong K L. Plasticizer effect on the melting and crystallization behavior of polyvinyl alcohol. Polymer, 2003, 44(26):8139-8146.

[54] Ru W, Qi W, Li L. Evaporation behaviour of water and its plasticizing effect in modified poly(vinyl alcohol) systems. Polymer International, 2003, 52(52):1820-1826.

[55] Li L, Wang Q, Wang R. Enhancing mechanical properties of poly(vinyl alcohol) blown films by drawing and surface crosslinking. Journal of Applied Polymer Science, 2010, 98(2):774-779.

[56] Liu Z, Feng Y, Yi X. Thermoplastic starch/PVAl compounds: Preparation, processing, and properties. Journal of Applied Polymer Science, 2015, 74(11):2667-2673.

[57] Ku T H, Lin C A. Shear Flow Properties and Melt Spinning of Thermoplastic Polyvinyl Alcohol Melts. Textile Research Journal, 2005, 75(9):681-688.

[58] Alexy P, Káchová D, Kršiak M, et al. Poly(vinyl alcohol) stabilisation in thermoplastic processing. Polymer Degradation & Stability, 2002, 78(3):413-421.

[59] Alexy P, LacíK I, Šimková B, et al. Effect of melt processing on thermo-mechanical degradation of poly(vinyl alcohol)s. Polymer Degradation & Stability, 2004, 85(2):823-830.

[60] Hodge R M, Bastow T, Edward G H et al. Free Volume and the Mechanism of Plasticization in Water-Swollen Poly(vinyl alcohol). Macromolecules, 1996, 29(25):8137-8143.

[61] Voigt W. Voight, W.: Über die Beziehung zwischen den beiden Elastizitätskonstanten isotroper Körper. Annalen Der Physik, 2006, 274(12):573-587.

[62] Reuss A. Berechnung der Fließgrenze von Mischkristallen auf Grund der Plastizitätsbedingung für Einkristalle. ZAMM - Journal of Applied Mathematics and Mechanics / Zeitschrift für Angewandte Mathematik und Mechanik, 1929, 9(1):49–58.

[63] Hull D. An Introduction to Composite Materials[M]. Cambridge University Pre, 1981.

[64] Aboudi J. Mechanics of composite materials - A unified micromechanical approach. Nasa Sti/recon Technical Report A, 1991, 93(11):987-1002.

[65] Assender H E, Windle A H. Crystallinity in poly(vinyl alcohol). 1. An X-ray diffraction study of atactic PVOH. Polymer, 1998, 39(18):4295-4302.

[66] Rae P J, Dattelbaum D M. The properties of poly(tetrafluoroethylene) (PTFE) in compression. Polymer, 2004, 45(22):7615-7625.

[67] Wu W, Tian H, Xiang A. Influence of Polyol Plasticizers on the Properties of Polyvinyl Alcohol Films Fabricated by Melt Processing. Journal of Polymers and the Environment, 2012, 20(1):63-69.

[68] Lin H M, Wang W C, Pen H C. Polyvinyl alcohol film composition, and polarizing plate employing the same: US, US8168091[P]. 2012.

[69] Aliberti V A, Monaghan L J, Sullivan D M. Polyvinyl alcohol films plasticized with monophenyl ether of polyoxyethylene[D]. US, 1968.

[70] DuPont™ Teflon Product Information.PTFE TE-3893, Fluoropolymer resin.

[71] Fischmeister H F, Arzt E. Densification of Powders by Particle Deformation. Powder Metallurgy, 1983, 26(2):82-88.

[72] Chandler H W, Sands C M, Song J H, et al. A plasticity model for powder compaction processes incorporating particle deformation and rearrangement. International Journal of Solids & Structures, 2008, 45(7–8):2056-2076.

[73] Degarmo E P, Black J T, Kohser R A. Materials and processes in manufacturing. The Macmillan Company, 1957.

[74] Johansson B, Wikberg M, Ek R, et al. Compression behaviour and compactability of microcrystalline cellulose pellets in relationship to their pore structure and mechanical properties. International Journal of Pharmaceutics, 1995, 117(1):57-73.

[75] Aulton M E. Aulton's pharmaceutics : the design and manufacture of medicines. Available Online on Www.ijpsr.com Journal of Pharmaceutical Sciences & Research Issn, 2007, 4(11):1488-1502.

[76] Berggren J, Frenning G, Alderborn G. Compression behaviour and tablet-forming ability of spray-dried amorphous composite particles. European Journal of Pharmaceutical Sciences, 2004, 22(2–3):191-200.

[77] Roberts R J, Rowe R C. The compaction of pharmaceutical and other model materials - a pragmatic approach. Chemical Engineering Science, 1987, 42(4):903-911.

[78] Rowe CR and Roberts RJ. Mechanical properties. In: Alderborn G and Nyström C, editors. Pharmaceutical powder compaction technology, vol. 71. New York, Basel: Marcel Dekker Inc, 1996. pp. 283-322.

[79] Roberts RJ, Rowe RC, and Kendall K. Brittle--ductile transitions in die compaction of sodium chloride. Chemical Engineering Science. 1989;44(8): 1647-1651.

[80] Johansson B, Alderborn G. Degree of pellet deformation during compaction and its relationship to the tensile strength of tablets formed of microcrystalline cellulose pellets. International Journal of Pharmaceutics, 1996, 132(1–2):207-220.

[81] Duberg M, Nyström C. Studies on direct compression of tablets XVII. Porosity—pressure curves for the characterization of volume reduction mechanisms in powder compression. Powder Technology, 1986, 46(1):67-75.

[82] Alderborn G, Pasanen K, Nyström C. Studies on direct compression of tablets. XL Characterization of particle fragmentation during compaction by permeametry measurements of tablets. International Journal of Pharmaceutics, 1985, 23(1):79-86.

[83] Nyström C and Karehill PG. The importance of intermolecular bonding forces and the concept of bonding surface area. Pharmaceutical powder compaction technology. 1996(71): 17-53.

[84] Nicklasson F, Alderborn G. Modulation of the tabletting behaviour of microcrystalline cellulose pellets by the incorporation of polyethylene glycol. European Journal of Pharmaceutical Sciences, 1999, 9(1):57.

[85] Nicklasson F, Alderborn G. Compression shear strength and tableting behavior of microcrystalline cellulose agglomerates modulated by a solution binder (polyethylene glycol). Pharmaceutical Research, 2001, 18(6):873-877.

[86] Nicklasson F, Johansson B, Alderborn G. Occurrence of fragmentation during compression of pellets prepared from a 4 to 1 mixture of dicalcium phosphate dihydrate and microcrystalline cellulose. European Journal of Pharmaceutical Sciences, 1999, 7(3):221.

[87] Nyström C, Alderborn G, Duberg M, et al. Bonding Surface area and Bonding Mechanism-Two Important Factors fir the Understanding of Powder Comparability. Drug Development and Industrial Pharmacy, 1993, 19(17-18):2143-2196.

[88] Stanley-Wood N G, Shubair M S. The variation of the surface topography of granules under compression with degree of binder addition. Powder Technology, 1980, 25(1):57-64.

[89] Eriksson M, Alderborn G. The effect of particle fragmentation and deformation on the interparticulate bond formation process during powder compaction. Pharmaceutical research, 1995, 12(7):1031-9.

[90] Sawai D, Watanabe D, Morooka N, et al. Superdrawing of polytetrafluoroethylene nascent powder by solid-state coextrusion. Journal of Polymer Science Part B Polymer Physics, 2010, 44(23):3369-3377.

[91]Joseph S, Thomas S. Modeling of tensile moduli in polystyrene/polybutadiene blends. Journal of Polymer Science Part B: Polymer Physics. 2002; 40(8): 755-64.

[92] White J L, Kim E K. Twin Screw Extrusion Technology and Principles. 2010. 295

[93] Shah A, Gupta M. Comparison of the flow in co-rotating and counter-rotating twin-screw extruder. ANTEC. 2004:447